NASA Contractor Report 175035

Influence of Large-Scale Motion on Turbulent Transport for Confined Coaxial Jets

Volume I—Analytical Analysis of the Experimental Data Using Conditional Sampling

(NASA-CR-175035) INFLUENCE OF LARGE-SCALE MOTION ON TURBULENT TRANSPORT FOR CONFINED COAXIAL JETS. VOLUME 1: ANALYTICAL ANALYSIS OF THE EXPERIMENTAL DATA USING CONDITIONAL SAMPLING Final (Connecticut

N86-20395

Unclas

G3/07 05601

David C. Brondum and John C. Bennett

The University of Connecticut
Storrs, Connecticut

January 1986

Prepared for
Lewis Research Center
Under Grant NAG 3-350

National Aeronautics and
Space Administration

TABLE OF CONTENTS

NOMENCLATURE

f = local fraction of inner jet fluid (ie., concentration)

k = turbulence energy [m^2/s^2]

m = mass flow rate [kg/s]

r = radius (mm)

R_0 = radius of sudden expansion (mm)

u = axial velocity (m/s)

v = radial velocity (m/s)

w = azimuthal velocity (m/s)

z = streamwise coordinate (mm)

= dissipation rate of turbulence [m^2/s^3]

$_m$ = eddy diffusivity

<u>Superscripts</u>

$-$ = mean quantity

' = fluctuating quantity

PRECEDING PAGE BLANK NOT FILMED

PAGE ii INTENTIONALLY BLANK

INTRODUCTION

The outlet flow for a combustion chamber is determined by the complex pattern of the flow field through it. In order to perform parametric studies on the flow, it is necessary to have an accurate simulation program for prediction of the combustion process. Since combustors of practical interest are highly turbulent, understanding turbulent transport in this type of flow is critical to the development of computational procedures to be used in these simulations.

Modern combustion chambers typically have an annular configuration with fuel in a fine spray form being mixed into the airstream. This mixture is achieved with an array of fuel nozzles which ensure uniform fuel spray distribution. these nozzles may be of the swirl or non-swirl type, although the swirl type is usually used to promote rapid burning. The fuel-air mixture is burned in the combustion chamber and the resulting gases are delivered to the turbine inlet. A stabilized flame in the combustion process is necessary to achieve uniform burning, resulting in a desirable temperature profile at the turbine inlet (pattern factor). Other important parameters in the combustion process include burning length (flameout), noise production, pollutant emissions (reactant products), and engine performance (combustion efficiency).

Computational procedures for predicting the combustion process are being developed and improved by numerous researchers (1,2,3,). These procedures predict the velocity, species, temperature, and reaction rate distribution within the combustors which in turn are used to calculate the previously named parameters. Because of the turbulent nature of the flow, mathematical models are used for the turbulent transport of mass (species), momentum, and heat. The data used to develop and verify these models have in the past been restricted to velocity and momentum transport measurements. Methods used prior to the mid-nineteen seventies for acquiring turbulent mass and momentum transport data have been indirect, requiring compromising assumptions or probes unsuitable for recirculating flows. Bennett & Johnson (4) have used new optical techniques to simultaneously measure a scalar quantity (mass) and velocity, and therefore mass transport.

Morganthaler (5) performed an

> "assessment of the relative importance of turbulent mass, momentum, and energy transport, so that emphasis for the future could be directed to modeling the critical processes rather than merely continuing the historical trend of modelling turbulent momentum transport."

His results point out a critical need for the future in that

> "turbulent transport of mass was demonstrated to be far more significant than the transport of either energy or momentum for a coaxial hydrogen jet reacting with an external high temperature air stream."

In order to provide an adequate data base for verifying computational procedures used for modeling mass transport, Bennett & Johnson (6) used laser velocimetry (LV) to obtain velocity measurements while simultaneously using laser-induced flourescence

(LIF) to obtain concentration data for a coaxial jet geometry. In a companion paper, Syed & Sturgess (7) used the data of Bennett & Johnson for comparison with computational methods currently in use. While finding qualitative agreement of all variables, there were some significant quantitative discrepancies. Among their conclusions was that "prediction of mean quantities alone is not a sufficiently strict criterion" for evaluating the success of a turbulence model, but that "it is necessary to examine also the agreement obtained for fluctuating quantities and their cross correlations" (i.e., mass flux).

It should be pointed out that some of the difficulty encountered in accurately predicting the flow can be attributed to the lack of a set of good initial conditions. Another limiting factor - possibly the dominant one in certain situations - is the incomplete understanding of the mechanisms involved in the flow. One such mechanism is the influence of the large-scale motion on the turbulent transport. The understanding of this influence is the main thrust of this research effort.

Other comparison studies of turbulent flow in a coaxial jet have been done by Habib & Whitelaw, including experimental data obtained using hot wires (8) and using LV (9). In each study, the largest discrepencies were in the upstream region where the flow is developing and recirculation zones occur. They concluded that these errors were "associated with the inadequacy of the eddy-viscosity hypothesis." Again it is seen that a better understanding of the mechanisms involved is needed to improve the computational procedures currently in use.

The experimental efforts of Bennett & Johnson have also continued and produced some interesting results (10) which in some cases are contradictory to traditional thinking. Complete details of the experiments and data are found in the final NASA contractor reports of Bennett & Johnson (11) for a non-swirling flow and Roback & Johnson (12) for a swirling flow. These works were done on a coaxial jet configuration using water in both jets and fluorescin dye as a trace element. Bennett & Johnson show two distinct shear regions for the non-swirling flow (fig. 1a); one between the inner and annular jets and one between the annular jet and the recirculation region. The innermost shear layer develops as the annular fluid gradually fills the center jet, resulting in what has been called counter-gradient transport. Computational procedures for evaluating scalar (concentration) gradient and a transport diffusion coefficient, ε_m defined by

$$m = - \varepsilon_m \left(\frac{\partial f}{\partial x}\right)$$

In many turbulent flows the scalar transport does not follow such a simple dimensional model and the traditional approach does not work.

The swirling flow results of Roback & Johnson (12) show a flow field (Fig. 1b) similar to that for the non-swirling case. they found a large eddy shear region between the inner and annular jets and one between the annular jet and outer recirculation zone. Unlike the non-swirling flow however, they found a large recirculation region on the centerline which gave the flow some different characteristics.

The multiple scale results of Bennett & Johnson are an example of a situation for which this simple gradient model is inadequate. Figure 2 shows regions of the flow field where this is the case. This region is qualitatively similar to the region where the inner jet fluid is being accelerated by the annular jet, although it is somewhat more extensive. Bennett & Johnson hypothesized that this was due to "response time or distance required to change the character of the turbulent structure". Another interesting finding was that the peak absolute values of the axial mass transport rates were higher than the values for the radial transport even though the peak radial concentration gradients were more than ten times the axial concentration gradients.

Observation of the concentration signal during the experiments showed much large-scale flow intermittency with the developing portion of the flow field. At axial locations within the upstream region (where the flow is developing), there were large-scale fluctuations in the signal: they were either negative (indicating a slug of annular jet fluid) or positive (suggesting a slug of inner jet fluid). No immediately recognizable periodicity in the occurrence of these fluctuations was found and no local peaks in the concentration autocorrelations were identified. It was believed that these excursions did identify the presence of a large-scale motion within the region.

This later work of Bennett & Johnson gives some justification for studying the influence of the large-scale motion on the turbulent transport. The comparisons of Syed & Sturgess, as well as Habib & Whitelaw, also support this in that, for both studies, the region of greatest discrepancy is the upstream region where the flow is developing. Since this region is known to include large-scale motion, it seems reasonable to investigate the effects of that motion on the flow.

In addition, Schetz (13) has reviewed the mixing flows in terms of both experimental results and the implications for turbulence modeling. One of his basic conclusions was that large-scale structures are an essential aspect of future experimental and modeling studies for a wide variety of flows. Mathiew & Jeandel (14) point out that the large interacting eddies can have a time scale quite differenct from the dissipative time scale associated with the fine structure portion of the flow. Launder (15) has introduced multiple time scale models, chosen to give the best predictions. These scales could be chosen more appropriately from experimental data directly if the role of the large scale were identified. Finally Borghi (16) questions the importance of large coherent structures in combusting flow. His conclusion is that, for the upstream region, the numerical predictions are not close to observed data because either large structures or the redistribution of kinetic energy is badly calculated.

In summary, for the confined coaxial jet, the presence of large-scale structures has been identified in the region where computational predictions have shown to be least effective. Several researchers have hypothesized that the large-scale structures may be the source of these discrepancies. With this in mind, this study was undertaken to identify a way of detecting these structures and to determine the influence they have on the turbulent transport of the flow.

BACKGROUND

The notion of large-scale coherent structures in turbulent flow is not a new one. Several authors - including Roshko (17), Cantwell (18), and Davies & Yule (19) - have summarized many of the developments in this area. A starting point in any discussion must be a clear definition of the subject. Yule (20) defines coherent structures as large eddies which, (i) are repetitive in structure, (ii) remain coherent for distances downstream very much greater than their length scales, and (iii) contribute greatly to the properties of turbulence, in particular, turbulent energy and shear stress, entrainment and mixing.

The experimental work of Brown & Roshko (21) is considered classic in the study of large-scale motion in turbulent mixing layers. Their efforts (fig. 3) revealed the "presence of well-defined large structures", with the Reynolds number varying from a low value with no visible fine-scale turbulence to a higher value where it does exist. The significant point is that in each case "the measured mean properties of the flow, the velocity and density profiles, spreading rate, etc. are the same". They concluded that the "mean flow is controlled by the large organized structures which, it may be seen, are not affected by the small-scale turbulence appearing at the higher values of Reynolds number."

By observing the movement of the structures, Brown & Roshko (21) found that their spacing and diameter increased with increasing downstream distance. The large-scale structures move at nearly constant streamwise velocity (equal to the mean flow velocity) which is independent of their size and location. Brown & Roshko conclude that they amalgamate into larger structures as they convect downstream. Winant & Browand (22) observed fluid rolling up into "discrete two-dimensional vortical structures" which periodically "interact by rolling around each other" eventually forming one larger vortex. Finally, Dimotakis & Brown (23) found similar large-scale coherent structures at a high Reynolds number ($3x10^6$). Their flow visualization study showed that these structures did exist and "appear to dominate in determining the overall characteristics of such flows".

Blackwelder & Kaplan (24) studied bursting in a turbulent boundary layer. They observed, using flow visualization, "a high degree of coherence over a considerable area in the direction normal to the wall", and found that bursts were associated with a high degree of velocity fluctuation. Their conditional averaging process showed the coherent structures to have turbulent transport properties an order of magnitude greater than the overall flow. This is in agreement with the work of Lu & Willmarth (25) who found large contributions to the turbulent transport from the coherent structures. Boundary layer flows have been studied more than any other type and are probably the best understood in terms of coherent structures. It is useful to apply this knowledge in developing a better understanding of other flows.

The experimental work of Bennett & Johnson (11) for non-swirling flow and Roback & Johnson (12) for swirling flow is the basis for the present study. The configuration they chose was a confined coaxial jet with a sudden expansion, a meaningful yet geometrically simple case. It simulates the two-stream inlet and the diffuser (sudden expansion) similar to flow in combustors. Water was chosen for the experiments; the resultant capability for injecting dye into either stream was utilized for flow visualization and mass transport studies. The use of water limits the simulation in that it eliminates combustion and multiple species as variables to be considered. Water also reduces the effect of molecular diffusion to a negligible level. These limitations still resulted in a set of results useful in evaluating combustor design calculation codes; before the addition of combustion, the codes should be expected to accurately predict this more limited flow. To create this data base for comparison with models, the emphasis was on statistically repeatable data collection. As the emphasis was not on large-scale structures (i.e., conditional sampling), this limits the data's usefullness in studying large-scale structures somewhat. For example, it is not possible to trace the flow of a particular structure past a measurement location since the data collection rates needed for statistically steady data limit the number of samples within any one structure.

Bennett & Johnson (4, 11) and Roback & Johnson (12) documented the flow fields shown in figure 1a and 1b respectively. The ratios of jet diameters are approximately 0.25 for the inner jet and 0.50 for the annular jet (compared to the pipe diameter). The flow chosen for documentation has Reynolds numbers of 15,900 and 47,500 for the inner and annular streams respectively. These values are within the turbulent flow range and are typical of gas turbine combustors. The data base resulting from these experiments consists of simultaneous two-component velocity data (u-v, u-w, v-w) and simultaneous concentration-velocity data (u-f, v-f, w-f) at numerous axial and radial locations on the flow field.

The comparison work of Syed & Sturgess (7), which utilized Bennett & Johnson's data base, was done with a two-dimensional k-ϵ model employed in the TEACH computer program. The largest of the discrepancies between experiment and predictions occurred in the upstream region where the flow was developing and included recirculation zones. For fluctuating velocity components, agreement was good qualitatively, but only fair quantitatively. Mean axial velocity profiles were found to be in better agreement. The centerline concentration growth is predicted to occur sooner than experiments indicated, while the subsequent decay is predicted later than found experimentally. Mass flux predictions exhibited similar discrepancies, as did limited momentum transport comparisons.

In the two Habib & Whitelaw studies (8, 9), their data is compared with predictions, again using the two-equation turbulence model in the TEACH code. Using hot-wire data, predictions of mean velocity distributions agreed well with the experimental data in the downstream regions. Shear stress distributions showed good agreement downstream but again had some trouble in the upstream flow developing region. Although the LV measurements in the second study were an improvement over the hot-wire data, errors were still found in the recirculation zone, reinforcing the need for modeling improvements in the prediction of turbulent transport.

In summary then, large-scale structures have been shown to contribute significantly to turbulent transport (at least in boundary layers). In addition, flow regions for which numerical predictions and experimental results differ the most are known to contain large-scale structures. It seems apparent that a better understanding of large-scale structures will be necessary for continued development of prediction methods. The present investigation represents an initial effort in this area for axisymmetric shear layers.

ANALYSIS

This study involved looking at the effects of the large-scale structures on the data collected by Johnson & Bennett (11) and Roback & Johnson (12). These data were used previously to study the overall flow characteristics. The present effort verified the overall properties; but the main thrust was on the large-scale structure properties and their influence on the overall flow.

In order to identify the role of large-scale structures in influencing turbulent transport, it is first necessary to separate these structures from the small-scale turbulent portion of the flow. A detector or trigger for the structure must be selected. Several potential detectors were identified based on other studies, including several done on turbulent boundary layers (24, 26). One possible detector is large velocity fluctuation compared to turbulence intensity, the rationale being that large-scale structures will involve blobs with larger velocity changes than for the overall flow. Another possible detector is concentration fluctuation. The entrainment and vortex pairing phenomena previously discussed led to this idea. Roshko (17) showed data from a concentration probe in a mixing layer where fluid from one stream penetrates deeply into the other stream, resulting in large concentration fluctuations. He states that information about the mixing can be obtained by measuring a scalar property such as temperature, density, or species concentration. The experiments of Bennett & Johnson and Roback & Johnson, previously discussed, also showed these large concentration fluctuations in regions where the large-scale structures are known to exist. Concentration fluctuation was chosen as the detector for this study.

The ultimate test of any detector is the completeness of the emerging pattern. Completeness refers in this case to a well-defined pattern, since a detector which yields randomly varying results cannot be a true detector. One way of testing a detector is to plot the relative frequency of each individual detection as a function of position. Relative frequency is the number of occurrences at each location ratioed by the complete set of data at that location. This can help identify the approximate size and most probable location of the large-scale region. These plots were done and will be discussed later.

Another useful plot is the scatter plot where the velocity fluctuation is plotted as a function of the concentration fluctuation or where fluctuation of one velocity component is plotted against the fluctuation of another velocity component. These types of plots help establish the existence of the large scale in the flow and assist in separating these structures from the general low level turbulence. They are also beneficial in determining if the large-scale correlation is significant.

An example of a plot with a zero correlation, shown in Figure 4, has almost all of the data concentrated uniformly near the center. A small amount of data has fairly large negative concentration fluctuations, but are equally distributed among positive and negative velocity fluctuations, yielding a zero correlation. Figure 5 shows data with much more scatter in both directions and a zero correlation. A situation where there is very little concentration fluctuation and very large positive and negative velocity fluctuations in the flow can be seen in Figure 6. This data is taken in the recirculation zone where flow reversal occurs, but no large-scale motion is apparent. Data taken within the shear layer between the two jets is shown in Figure 7. Here there is much scatter in the data and a strongly negative correlation.

Once the detector was selected, a conditional sampling technique was used to determine the large-scale influence on the mass transport. Conditional sampling is a technique used to extract that portion of the data associated with the large-scale structures (as identified by the detector). One of the earliest uses of this experimental technique wass that of Kovasznay, et al (27) in 1970 on a turbulent boundary layer. Mathieu & Charnay (28) have reviewed this sampling method and much of the work done utilizing it. They point out that the difficulties of conditional sampling "are not due to the detection of signals", but are "consequences of the delicate choice of an adequate criterion". Blackwelder & Kaplan (24) used conditional averaging to examine the effect of coherent structures on the Reynolds stress for a turbulent boundary layer. The idea of conditional sampling or averaging, again from Mathieu & Charnay, is simply "the observation of a property only when some criterion is satisfied". This basic idea has been adapted to an analytical technique, rather than an experimental one, for this study.

A computer program was written to perform conditional sampling on the simultaneous concentration-velocity data using concentration fluctuation as a trigger. A flow chart of this program is shown in Figure 8 and a program listing is included in

Appendix A. This program made it possible to quantitatively separate the effect of the large-scale motion from the overall turbulent motion on the mass transport. Figures 9, 10, and 11 show sample results from this program for the non-swirling flow. The section under DATA OUTPUT....includes various statistical parameters calculated using all of the data at that point (these results are those reported in Ref. 11, 12). The lower section under CONDITIONAL SAMPLING RESULTS contains statistical parameters based on conditional sampling of the data according to concentration fluctuation. The information shown includes the concentration fluctuation range and the number of data samples in the range. Also included are mean velocity, relative mean velocity, root mean square velocity fluctuation, mass transport coefficient, and transport ratio, all calculated using only the data in the range. The relative mean velocity is defined as the mean velocity for a given concentration fluctuation range minus the mean velocity for all the data samples at that point. The transport ratio is defined as the mass transport coefficient:

$$\frac{\overline{f'u'}}{f_{rms}\,u_{rms}}$$

for the data in a given concentration fluctuation range divided by the overall mass transport coefficient. The local fraction of inner jet fluid is used for concentration (f) and $\overline{f} = 1.0$ by definition at the sudden expansion (Fig. 1).

An example of data taken at a point on the inner edge of the shear layer is shown in Figure 9. The first interesting item is the negative overall mass transport coefficient. This combined with the fact that $\frac{\partial f}{\partial x} < 0$ leads to the following: $\frac{\overline{f'u'}}{\frac{\partial f}{\partial x}} > 0$

which is inconsistent with normal gradient transport models already discussed. Moving to the conditional sampling results, it is seen that the majority of the large concentration fluctuations are negative. This is to be expected here since the inner jet fluid contains the dye (Fig. 1) and thus has $\bar{f} \approx 1.0$. Any fluid swept into the region due to the large-scale motion will be outer jet fluid, with $\bar{f} \approx 0.$, and will result in a negative concentration fluctuation. An examination of the conditional sampling results shows two distinct flow characteristics among the data. The first is for the the data with $|f'| < .2$, where the gradient transport model seems to fit. This data has a positive (or slightly negative) mass transport coefficient and very small relative mean velocity, indicating this well-mixed fluid is moving almost uniformly in the axial direction. The second flow characteristic is for the data with large concentration fluctuations (in this case $|f'| \geq .2$). This data is seen to have orders of magnitude, larger relative mean velocities and transport coefficients than the other data. the larger relative mean velocity indicates this fluid is not well-mixed with the rest of the flow and is moving at a considerably different, in this case higher, velocity than the mean flow due to the large-scale motion. The much larger mass transport coefficient indicates that even though the number of data samples is small, this data is responsible for the majority of the axial mass transport at this point. This data has a negative transport coefficient which, as already shown, is contrary to gradient transport. These data appear to be part of large-scale structures not well mixed with the overall flow and exhibit characteristics inconsistent with gradient transport.

Figure 10 shows data from a point well inside the shear layer under the strong influence of the large-scale motion. Once again the overall transport coefficient is negative, indicating that this is not a gradient transport situation. Since this location is inside the shear layer it is seen that there are large numbers of both positive and negative concentration fluctuations. There appear to be two distinct flow situations here also, but the large-scale motion seems to influence all of the data. Given that $u'f' \simeq (\Delta u)(\Delta f)$, notice in the conditional sampling results that when the concentration fluctuation (Δf) is negative and the relative mean velocity (Δu) is positive, $u'f'<0$ and hence a negative mass transport coefficient. The same result is observed when the concentration fluctuation is positive. The data within the large-scale structure can be separated by observing the large jump in relative mean velocity and transport coefficient. One again, a small number of data samples appears to be responsible for the jomority of the axial mass transport. If the data with $f' <-0.2$ or $f'>.1$ is considered not part of the large scale, a weighted average of the large-scale data gives 36% of the samples accounting for 77% of the axial mass transport. The weighted average is calculated as the mean mass transport ratio for the large-scale data multiplied by the percent of the total number of samples that are included in the large-scale data.

Finally, Figure 11 is an example of data containing no large-scale structure. There are no large concentration fluctuations and the relative mean velocitites are very small. This location is inside the recirculation zone in the outer region of the flow.

Precisely which concentration fluctuation ranges are included in the large-scale motion is an admittedly somewhat subjective decision. The conditional sampling program was run on axial and radial velocity concentration data at axial locations of 13, 51, 102, 152, 203, 254, and 305mm for the non-swirling case. It was run at 13, 25, 51, 102, and 152mm for the swirling flow case since Roback & Johnson (12) found that complete mixing occurred much more rapidly in this flow. In all cases, the data within the large-scale structure were separated out based on concentration fluctuation, as well as the clear jumps in relative mean velocity and mass transport coefficient. This technique, when applied to the Johnson & Bennett data set, resulted in a basically consistent set of results; it is thought that the scatter found in some of the results is due to the limited large-scale data available for the present investigation. Despite this, the hypothesis that large positive or negative concentration fluctuations can be used to identify large-scale motion appears to be valid. As stated earlier, the true test of a detector is the completeness of the pattern it yields. Once the concentration-velocity data for the large-scale structures were extracted, much information about the influence of these structures was available. The results, to be discussed, support this choice of detector and the resulting pattern is in fact well defined.

RESULTS

As mentioned previously, the data sets used for the present investigation were acquired by Johnson & Bennett (11) for non-swirling flow and Roback & Johnson (12) for swirling flow. The results reported here are those associated with the large-scale structures. As discussed in the Analysis section, these results were obtained using conditional sampling techniques; the large-scale samples were detected using the concentration fluctuations as the criterion.

Several parameters were examined using the output of the conditional sampling program. The complete set of results for the non-swirling flow at the axial station at 152mm is contained in Appendix B and consists of numerous sets of results for various r/R_O: axial velocity or radial velocity, each taken simultaneously with concentration.

Using the procedures already described, several flow parameters were investigated as functions of r/R_O for each axial location. The first parameter studied was the large-scale fraction defined as the ratio of samples with large concentration excursions compared to the total sample size. For the non-swirling flow, plots are included for the axial velocity (Figs. 12-19) and radial velocity (Figs. 20-25) data. In each case, the percentage appears to be maximized in the shear layer where the large scales are known to exist from flow visualization done previously (11). As already stated, the data acquisition rate was oriented toward repeatable overall statistics. Therefore the distribution between large-scale and non-large-scale data is believed to be representative of the actual flow.

It is seen that, with increasing downstream distance, the percentage of data in the large scale becomes a weaker function of radius, with the peak in the shear layer becoming less pronounced in the axial data. At 102mm (Fig. 14) there is a large peak in the shear layer at $r/R_0 \simeq .2$ where over 40% of the data is in the large scale. This drops off rapidly and by $r/R_0 \simeq .4$ is close to zero. At 152mm (Fig. 15) the curve is not as steep. From $r/R_0 =$ 0 to $r/R_0 \simeq .25$, 30-40% of the data is in the large scale. The percentage approached 0 at $r/R_0 \simeq .5$; but overall, more of the data is in the large-scale structure at this axial location. By 203mm (Fig. 16) the curve is still flatter. From $r/R_0 = 0$ to $r/R_0 \simeq .2$, 50-60% of the data is in the large scale, not approaching zero until $r/R_0 \simeq .6$. Overall, a still larger percentage of the flow is part of the large-scale structure than in previous cases. Combining the axial velocity plots, a contour plot of percentage of data that is part of the large-scale structure was done (Fig. 19). It is seen that the largest percentage is located within the shear layer and spreads radially, moving shownsteam as the shear layer spreads also.

The radial velocity plots exhibit similar characteristics to the axial plots, with the peak spreading as the axial location increases. Figures 22 and 24 have curves that aren't quite so smooth as the others but the overall trend is similar. The percentage of data in the large scale must be the same for radial data as for axial; this is the case here for the most part. Any discrepancies can be attributed to the limited amount of large-scale data available.

Next, a calculation was made of the percentage of mass transport attributable to the large-scale portion of the flow. This was done for each radial location at a given axial station. This data, plotted as a function of r/R_0 for each axial station, is shown in Figures 26 through 38 for the non-swirling flow. The axial mass transport percentage plots (Figs. 26-32) are typified by Figure 27, at z = 51mm, which shows that the percentage attributable to the large scale is a maximum within the shear layer between the jets. It is well in excess of 50% throughout the shear layer.

Looking at the radial mass transport percentage plots at 13mm and 51mm (Figs. 33 and 34), they are similar to their axial counterparts (Figs. 26 and 27) although the percentage is higher for the radial data. Further downstream, these plots (Figs. 35-38) were considerably more involved, again with higher peak percentages than for the corresponding axial ones (Figs. 28-31).

Combining all of these results, it is possible to plot contours of percentage contribution to the mass transport due to the large-scale data. The axial mass transport plot (Fig. 39) shows that throughout the shear layer, 50-90% of the transport can be attributed to the large-scale motion. The increased complexity for radial mass transport became very evident when attempting to plot a similar contour plot for it. The limited locations with available data make it impossible to complete this figure. The existing data showed promise of a plot with similar features to the axial one, with somewhat higher percentages, but more data is needed to accurately complete this plot.

Looking at Figures 19 and 39, it is seen that there is qualitative agreement between the percentage of data that is part of the large-scale motion and the percentage contribution of the large scales to the mass transport. In the region where at least 50% of the mass transport is attributed to the large-scale motion, at least 10% of the data is part of these large scales. In the peak region of 80-90% contribution, at least 20% of the data is part of the large-scale motion. These plots certainly substantiate the importance of large-scale motion in the mass transport of the flow.

Figure 40 is a summary of the transport zones for axial mass transport. It is adapted from Figure 2 and includes the boundary of the region which Johnson & Bennett (10) found did not follow the traditional gradient transport model, as well as the boundary of the region for which the large-scale structure exerts a strong influence on the axial mass transport. The boundary of the large-scale region is based on a 50% contribution to the mass transport, although other values may be used by overlaying Figure 2 with Figure 40. The boundaries of these two regions are observed to follow each other very closely. This leads to the conclusion that consideration of the large-scale structures is essential in accounting for the axial mass transport in this region where the gradient transport model is inadequate. Of course, the presence of the large-scale structures means the flow includes multiple scales; gradient transport should not be expected to apply in such regions.

For the swirling flow, plots of large-scale fraction (Figs. 41-43) and mass transport percentage (Figs. 44-46) are included for axial velocity at axial stations of 13, 25, and 51mm. As Roback & Johnson (12) found, mixing for the swirling flow case occurs in approximately one third the downstream distance that it takes for the non-swirling flow. For this reason, large-scale structures were found to be influential in a much smaller region than for the non-swirling flow.

At 13mm (Fig. 41) the large-scale fraction peaks at approximately 30% of the data samples while at 25mm (Fig. 42) the peak is closer to 40%. In both cases the maximum occurs within the shear layer between the inner and annular jets as expected. By 51mm (Fig 43) the large-scale fraction is peaking at over 60% but the peak has shifted to the centerline. This is apparently due to the unsteadiness associated with the leading edge of the recirculation zone which occurs for the swirling flow and is consistent with the findings of Roback & Johnson (12). As expected, these percentages are somewhat higher at the same axial locations for the swirling flow than for the non-swirling flow.

The largest difference between swirling and non-swirling flow occurs at the 51mm location. The high values there are almost certainly associated with the unsteady motion of the recirculation zone noted earlier. Flow visualization (12) at this point clearly shows the very large structures present near the centerline. Also, as seen in the non-swirling flow, the overall percentage of data within the large-scale motion increases with downstream distance.

Swirling flow data were analyzed for large-scale structures at the 102 and 152mm locations. Though some indication of large structures was found, it represented, at most, 3% of the total samples at any one location. These results are not included as the statistics contain significant uncertainty due to the small sample size. We would agree with Roback & Johnson that large-scale structures exist at 102mm at least; but if the sample set is representative of the large-scale fraction, the large-scale structures are of no significance at this point.

The swirling flow mass transport percentage plots (Figs. 44-46) also exhibit some similarities to the non-swirling case. In each case the percentage is a maximum in the shear layer between the jets and the region of large-scale influence spreads radially with downstream distance. As already stated, the swirling flow mixes very rapidly and these plots reflect this. The percentages are high, like the non-swirl flow, but spread into the centerline much sooner axially than for the non-swirl flow.

A result of the rapid mixing for the swirling flow is that changes from station to station are much larger than for the non-swirl case. This makes it difficult to draw contours. As with the non-swirling flow, the influence of the large-scale motion is large and also consistent throughout the flow field.

An effort was undertaken to utilize the two-component velocity data to look at the large-scale contribution to the momentum transport. It was necessary to select a new detector to separate the large-scale data since there is no concentration data available in this case. A modified conditional sampling program was written to try to find such a trigger. A flow chart is included in Figure 47 and a program listing is in Appendix A. This program was used on the concentration-velocity data previously sampled for the non-swirling flow using concentration fluctuation as a trigger. Calculations were made of a conditional mean velocity and rms velocity fluctuation based on the same concentration range already selected. These were then compared to the overall mean and rms for the data. A typical output from this program is shown (Fig. 48) together with a plot of the data (Fig. 49). This figure shows the velocity distribution, in this case, a radial velocity data set. The overall data exhibits the nearly normal distribution. The large-scale data is more skewed, with a significantly different mean velocity and somewhat different rms fluctuation velocity than the overall. It had been hoped that radial velocity or velocity fluctuation might be used as a detector for the large-scale structure in the two-component velocity data. However, based on the results typified by this figure, there is no way to use either to separate the large-scale data. Use of axial velocity as a trigger was ruled out also when plots of this type showed similar results.

Plots of mean velocity and rms velocity fluctuation as functions of r/R_0 were done for simultaneous non-swirling concentration-velocity (axial and radial) data at various axial stations. The overall and large-scale values were plotted together for comparison purposes. Figure 50 is a typical plot for axial velocity. The mean velocity for the overall data and that for the large-scale data have very small differences, indicating that the coherent structures are moving at approximately the same axial velocity as the rest of the flow. This result for free shear layers is consistent with the results of Kovasznay et al (27) and several others (reviewed by Cantwell 18) who found large structure convection velocities in wall-bounded flows between 80 and 90 percent of the free stream mean velocity. Roshko (17) noted that for plane-mixing layers the large-scale vortices convect at approximately the average velocity of the two streams, with the velocity and density ratios having some influence.

Plots of mean radial velocity vs. r/R_0 are included for axial stations of 51, 102, 152, and 203mm. Figure 51 shows a negligible difference between the large-scale and overall data at 51mm. At 102mm, the differences are very significant (Fig. 52). For $0\leq r/R_0<.2$, the large-scale structures have a larger negative radial velocity than the mean flow. From $.2\leq r/R_0\leq.4$, the large-scale structures have a larger positive radial velocity than the mean flow, with the difference increasing with r/R_0. In this region, the shear layer is spreading radially, assuming that the large-scale structures identify the shear region.

Further downstream, at 152mm (Fig. 53), there is a negligible difference between large-scale motion and overall data for $r/R_0<.2$. This difference is significant, however, for $.275\leq r/R_0\leq.475$ and is approximately constant in this range. Again the coherent structures have a significantly larger radial velocity than indicated by the mean velocity of all the data.

At 203mm (Fig. 54), there are very small differences for $0 \leq r/R_0 \leq .3$. Large differences are found between the large-scale flow and overall for $.3 < r/R_0 \leq .6$. The radial mean velocity appears to be a linearly increasing function of r/R_0 for the large-scale and overall data, although the large-scale increase at a faster rate.

If the extent of the shear layer is assumed to correspond to the region where large-scale structures are found, the spreading rate of the shear layer for the non-swirling flow can be examined using Figures 12 through 17. Table 1 shows the radial extent of the large-scale structures for each axial station taken directly from the figures. Data were not taken at the same radial locations for all axial locations; therefore, comparisons of the exact same radial locations are not always possible. The data base is complete enough to observe that the spreading rate of the shear layer, or region where large-scale structures exist, increases approximately linearly with increasing axial location. This is consistent with other work on free shear layers (29) and consistent with the positive radial velocity found by Johnson & Bennett (11). These results emphasize the need for multiple scale modeling (15) since the large scales and overall flow have different radial convection velocities.

Figures 55, 56, and 57 are plots of the large-scale relative mean velocity as a function of concentration fluctuation, at axial locations of 51, 102, and 152mm respectively, for the non-swirling flow. The large-scale relative mean velocity is defined, at each axial and radial location, as the mean velocity for a given concentration fluctuation range minus the mean velocity for all of the large-scale data at the location. These plots provide additional support for the selection of the large-scale structures in that the large-scale relative mean velocity is approximately zero, in each figure, for concentration fluctuation of zero.

At any location there is some fluctuation in the overall curve, attributed to eddy variations. Each curve has limited scatter though and the vortex like structures are quite well defined in that a given relative mean velocity suggests a preferred concentration fluctuation value. Since the structures are well defined, the lack of correlation reported by Johnson & Bennett (11) must be due to the random arrival times of the structures. This is also suggested by the 3-D calculations of Riley & Metcalfe (30) and leads to the conclusion that the present form of the structures is "3-D like" for the large-scales.

CONCLUSION

The initial or upstream development of shear flows is crucial to the performance of many aerodynamic components (i.e., combustors). Comparisons of experimental results with computer predictions show that present models are not sufficient for such flows. Historically, flow visualization has shown that large-scale structures are present within this upstream, non-equilibrium region. It has been generally hypothesized that any lack of agreement between prediction and experiment can be attributed to these structures. In general, no adequate model (including them) has been included in the numerical computer codes, primarily since little was known about them.

The present investigation set out to analyze the physical characteristics of large-scale structures in free shear layers and to evaluate their importance to turbulent transport (including the first ever results for mass transport). Utilizing previously acquired data, the conclusions are limited in that the data set was not optimized for this use. Regardless, several significant conclusions are possible; they include:

(1) The large concentration fluctuations are indicative of the large structures. First, the sign of the transport is predictable with a model consistent with these structures. Secondly, the region with significant large concentration fluctuations is consistent with the large-scale region noted from flow visualization.

(2) The large structures, where present, account for most of the mass transport; the obvious implication of multiple scales is consistent with the lack of agreement with a gradient transport model.

(3) The large structures are found to be convected axially with the overall mean velocity but radially at a faster speed; this further strengthens the need for a multiple scale model.

(4) Any investigation of the influence of large-scale structures on momentum transport in three-dimensional free shear layers will most probably require concentration detection.

(5) The effects of large-scale motion for the swirling flow case or limited, at least for the data available, to the region just upstream of the recirculation zone and to the shear region between the jets.

The present investigation therefore has documented the importance of the large-scale structures and the need for them to be modelled if computer predictions are to be accurate. It is strongly suggested that the development of such a model is of the highest priority. Experimentally, this suggests several projects for further investigation. They include:

(1) A detailed analysis of the flow development with the large structures. What is the structure in physical space? Whay type of mixing occurs within them (is it a two-step process as suggested for two-dimensional shear layers)?

(2) A detailed analysis of momentum transport associated with the large structures. Does if significantly affect the results as would be predicted from the present mass transport results and from the results for other shear flows?

(3) An investigation of the influence of initial conditions on large-scale development. Certainly, such initial conditions are required for any computer simulation. What effects do changes in initial conditions have and what are the implications for accurate models?

(4) An investigation of two-dimensional vs. Three-dimensional shear layers. Both the published experimental results and the recent computer simulations strongly suggest that such a delineation between two-dimensional and three-dimensional flows is not straightforward. What are the implications of such assumptions on the development of an accurate model?

TABLE 1 : SPREADING RATE OF SHEAR LAYER

STREAMWISE LOCATION z (mm)	EXTENT OF SHEAR LAYER , r/Ro
13	.250
51	.300
102	.400
152	.475
203	.600
254	.724

Fig. 1

SHEAR REGIONS OF COAXIAL JETS

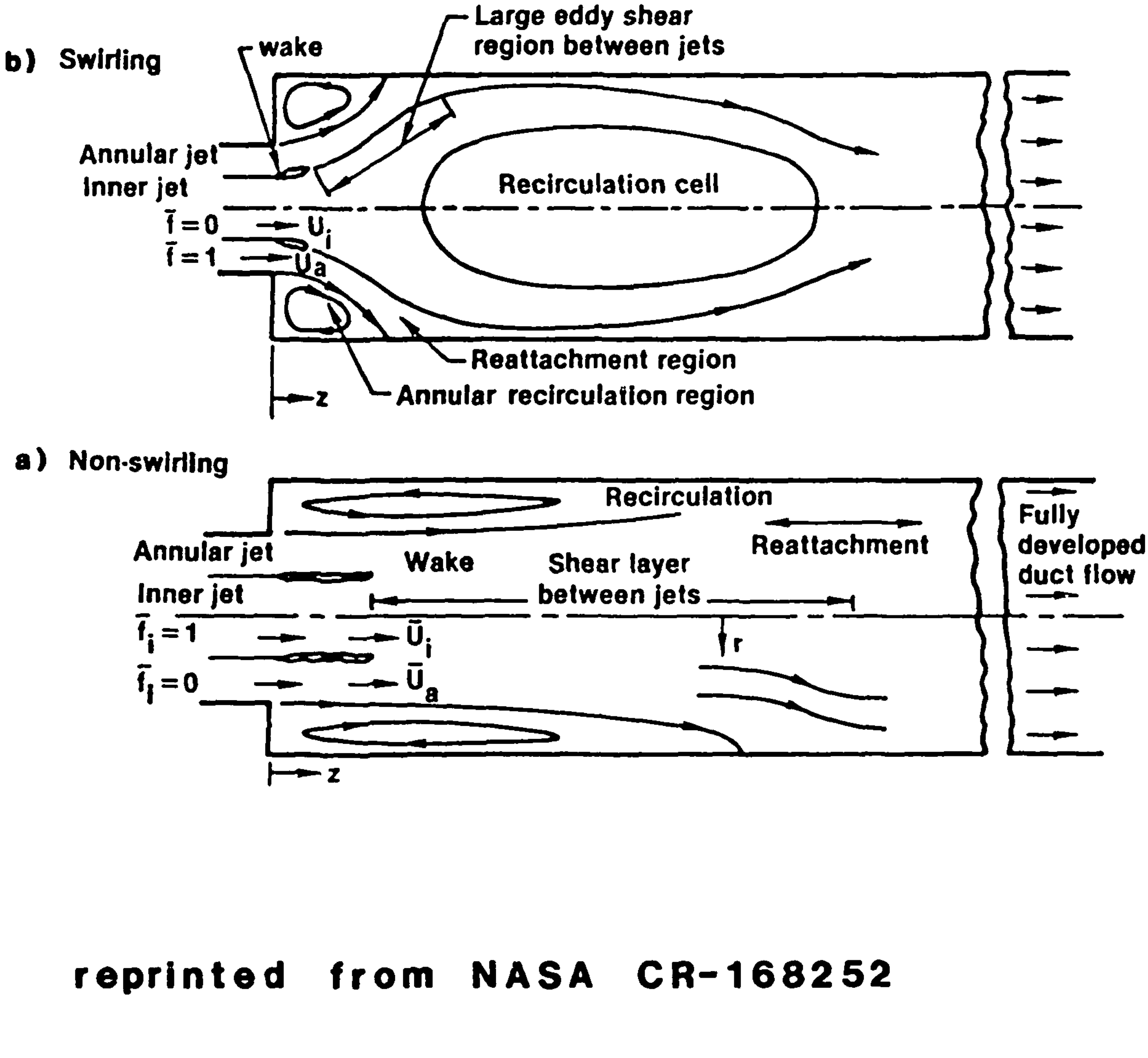

reprinted from NASA CR-168252

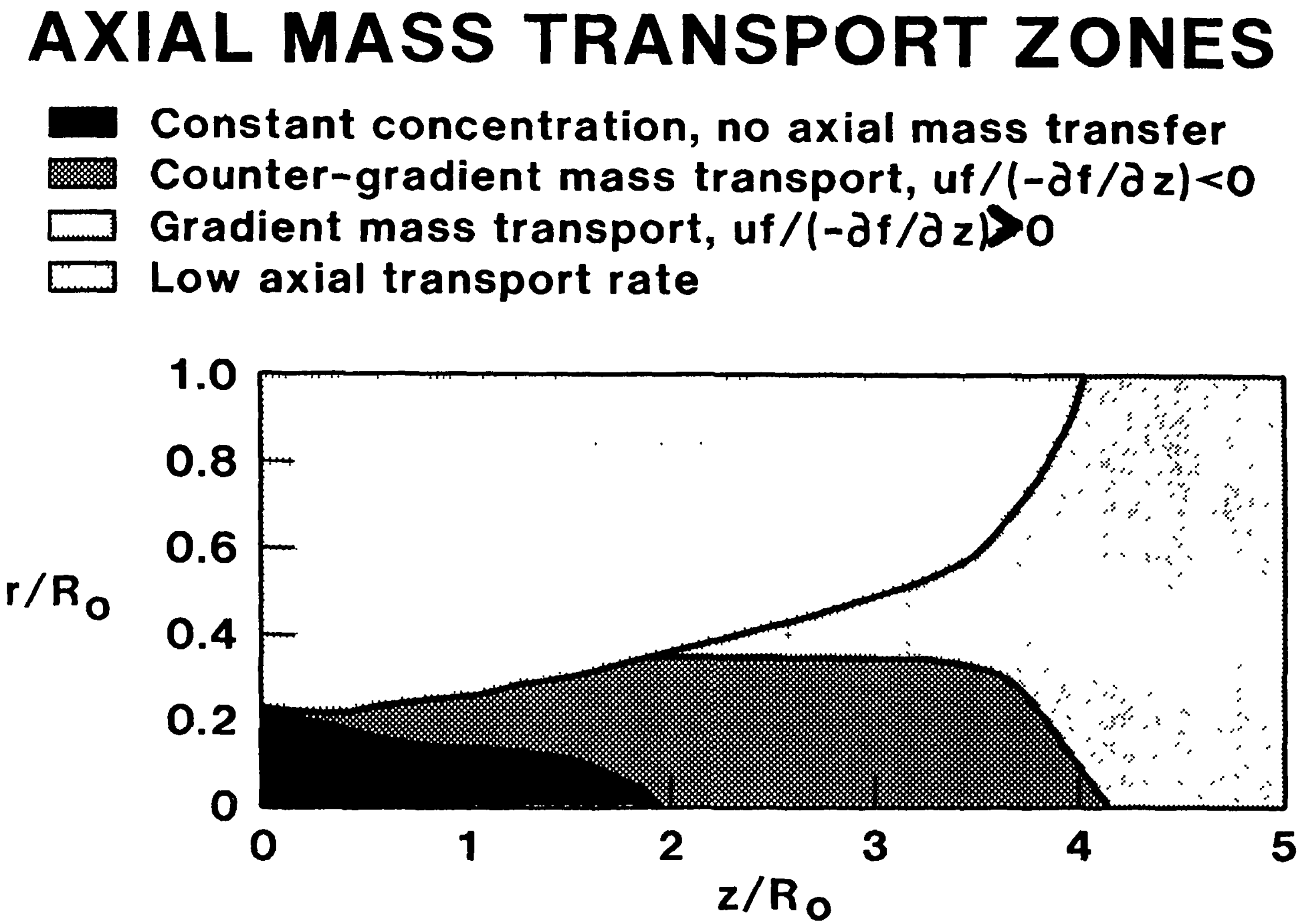
AXIAL MASS TRANSPORT ZONES
Constant concentration, no axial mass transfer
Counter-gradient mass transport, uf/(-∂f/∂z)<0
Gradient mass transport, uf/(-∂f/∂z)>0
Low axial transport rate
r/R_o
1.0
0.8
0.6
0.4
0.2
0
0
1
2
3
4
5
z/R_o

Fig. 2

ORIGINAL PAGE IS
OF POOR QUALITY

Fig. 3

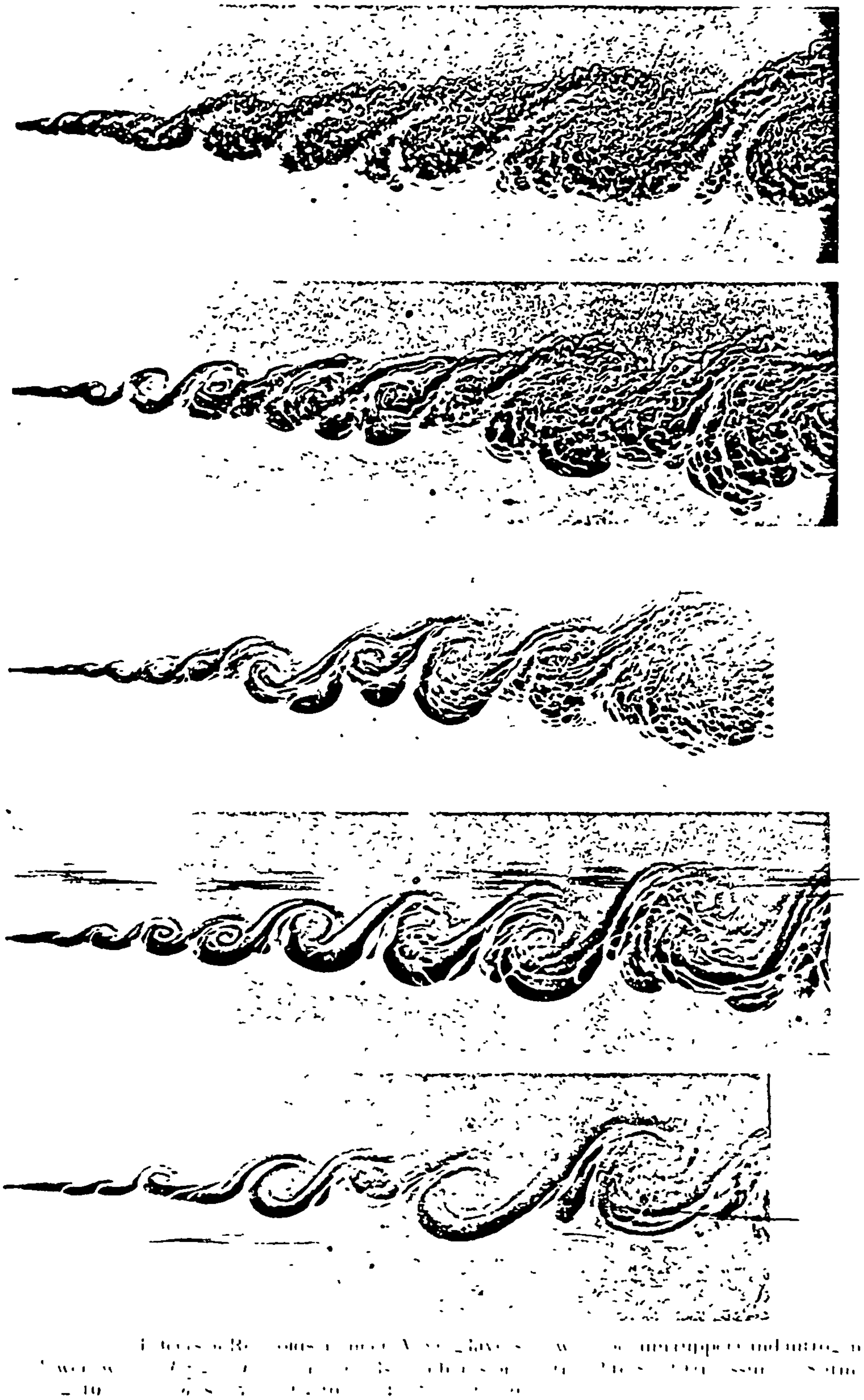

Fig. 4

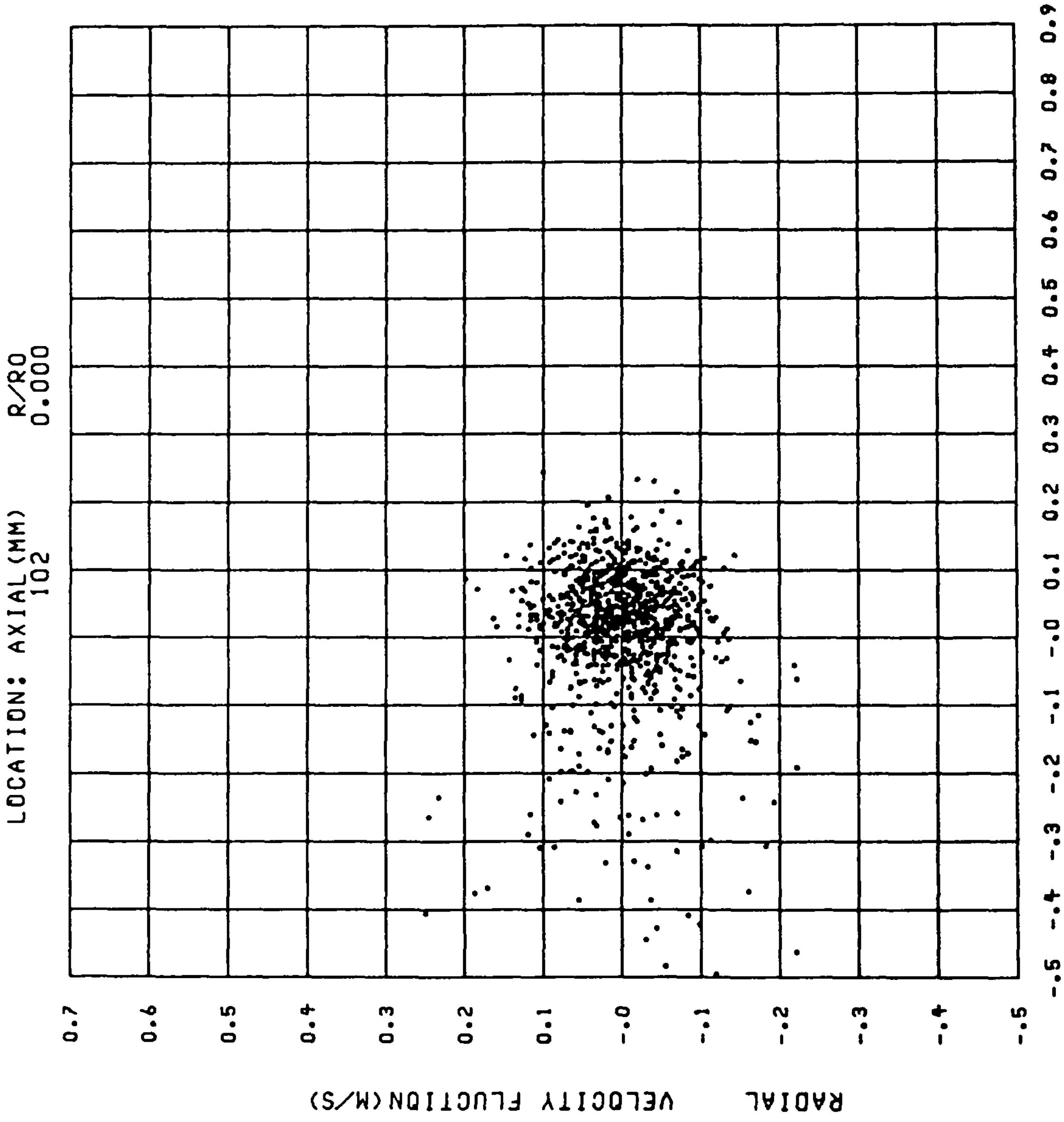
LOCATION: AXIAL(MM) 102
R/RO 0.000
CONCENTRATION FLUCTUATION
-.5 -.4 -.3 -.2 -.1 -.0 0.1 0.2 0.3 0.4 0.5 0.6 0.7 0.8 0.9
RADIAL VELOCITY FLUCTUATION(M/S)
0.7 0.6 0.5 0.4 0.3 0.2 0.1 -.0 -.1 -.2 -.3 -.4 -.5

Fig. 5

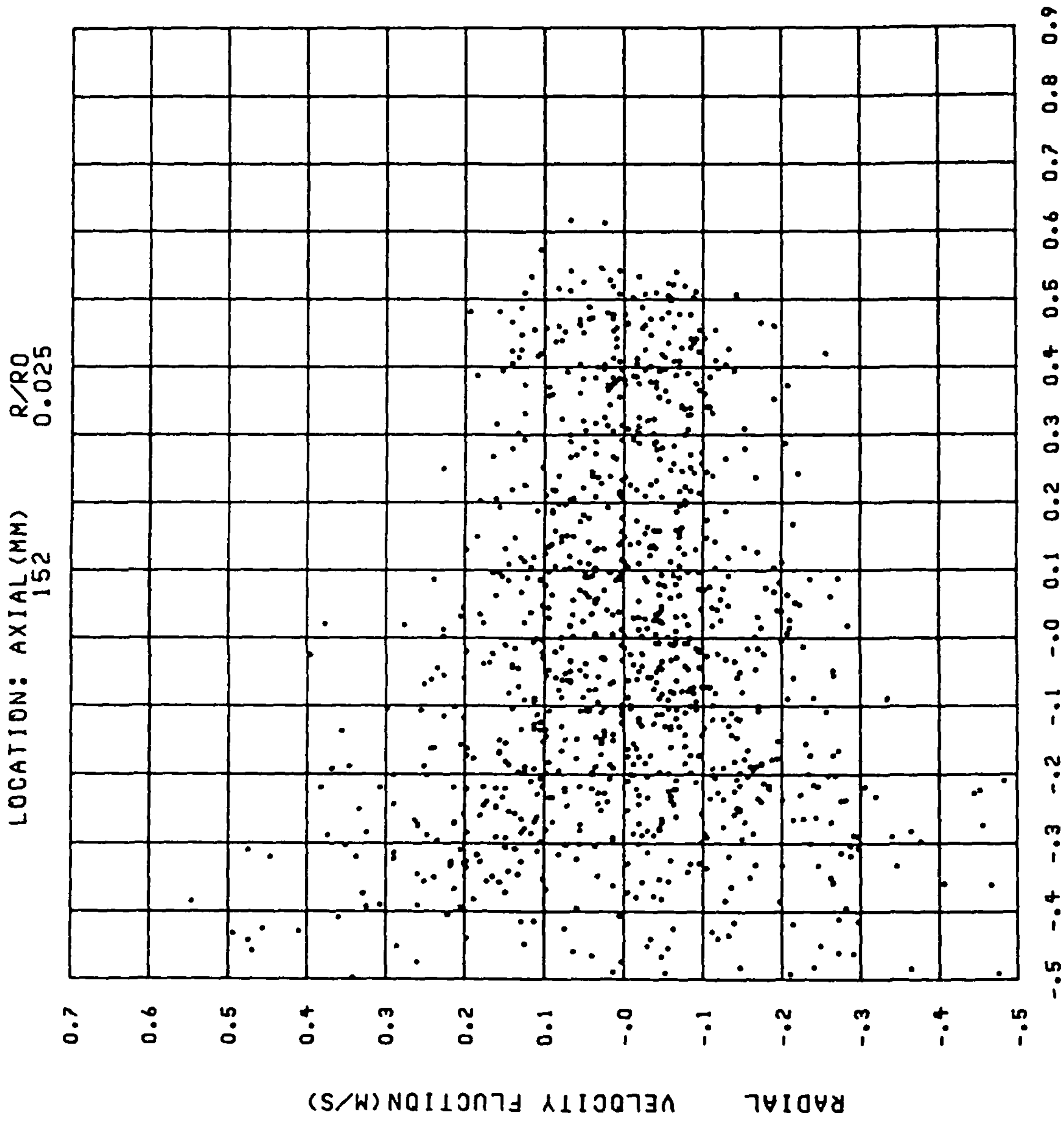
LOCATION: AXIAL(MM) 152
R/RO 0.025
-.5 -.4 -.3 -.2 -.1 -.0 0.1 0.2 0.3 0.4 0.5 0.6 0.7 0.8 0.9
CONCENTRATION FLUCTUATION
0.7 0.6 0.5 0.4 0.3 0.2 0.1 -.0 -.1 -.2 -.3 -.4 -.5
RADIAL VELOCITY FLUCTUATION(M/S)

Fig. 6

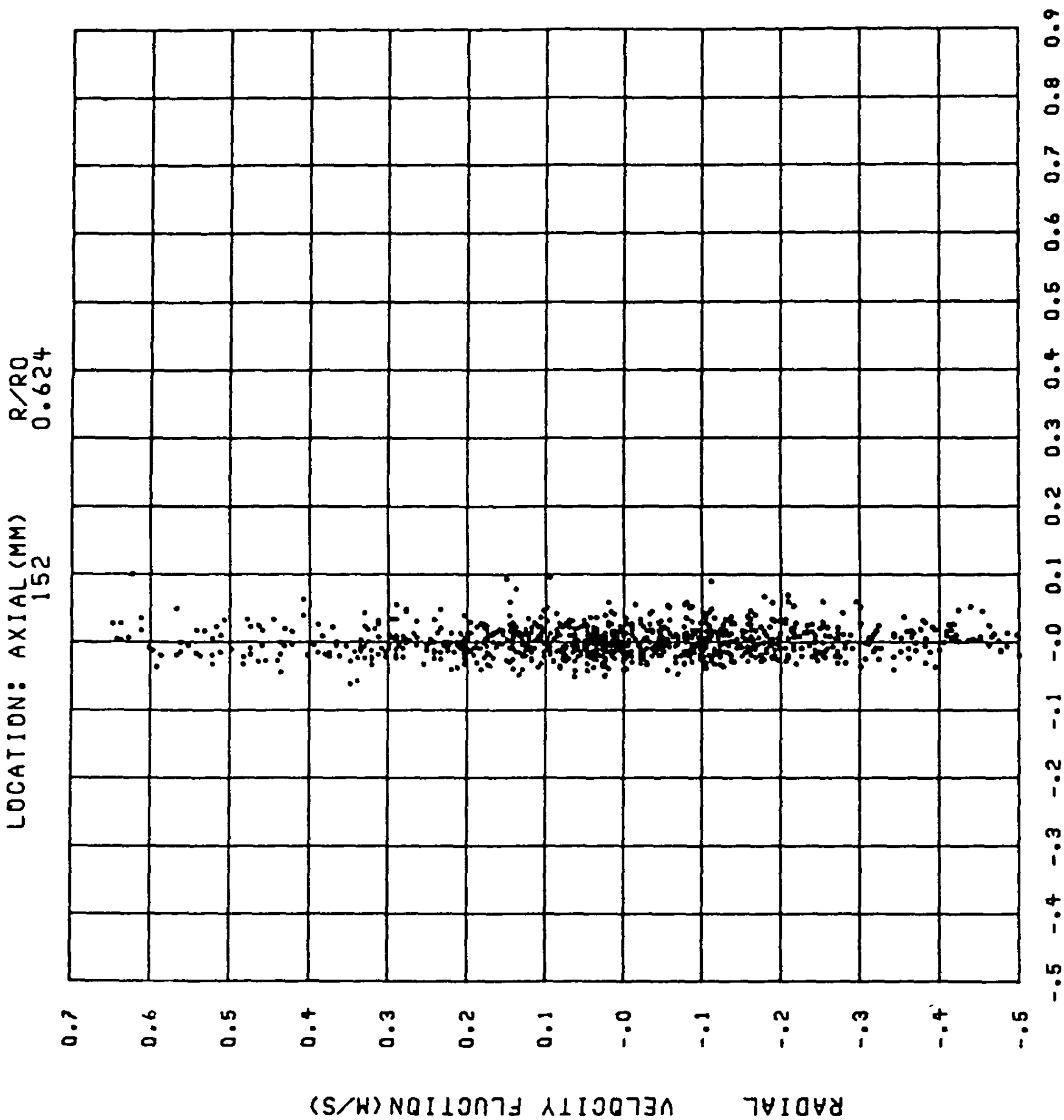
LOCATION: AXIAL (MM)
152
R/RO
0.624
CONCENTRATION FLUCTUATION
RADIAL VELOCITY FLUCTUATION (M/S)

Fig. 7

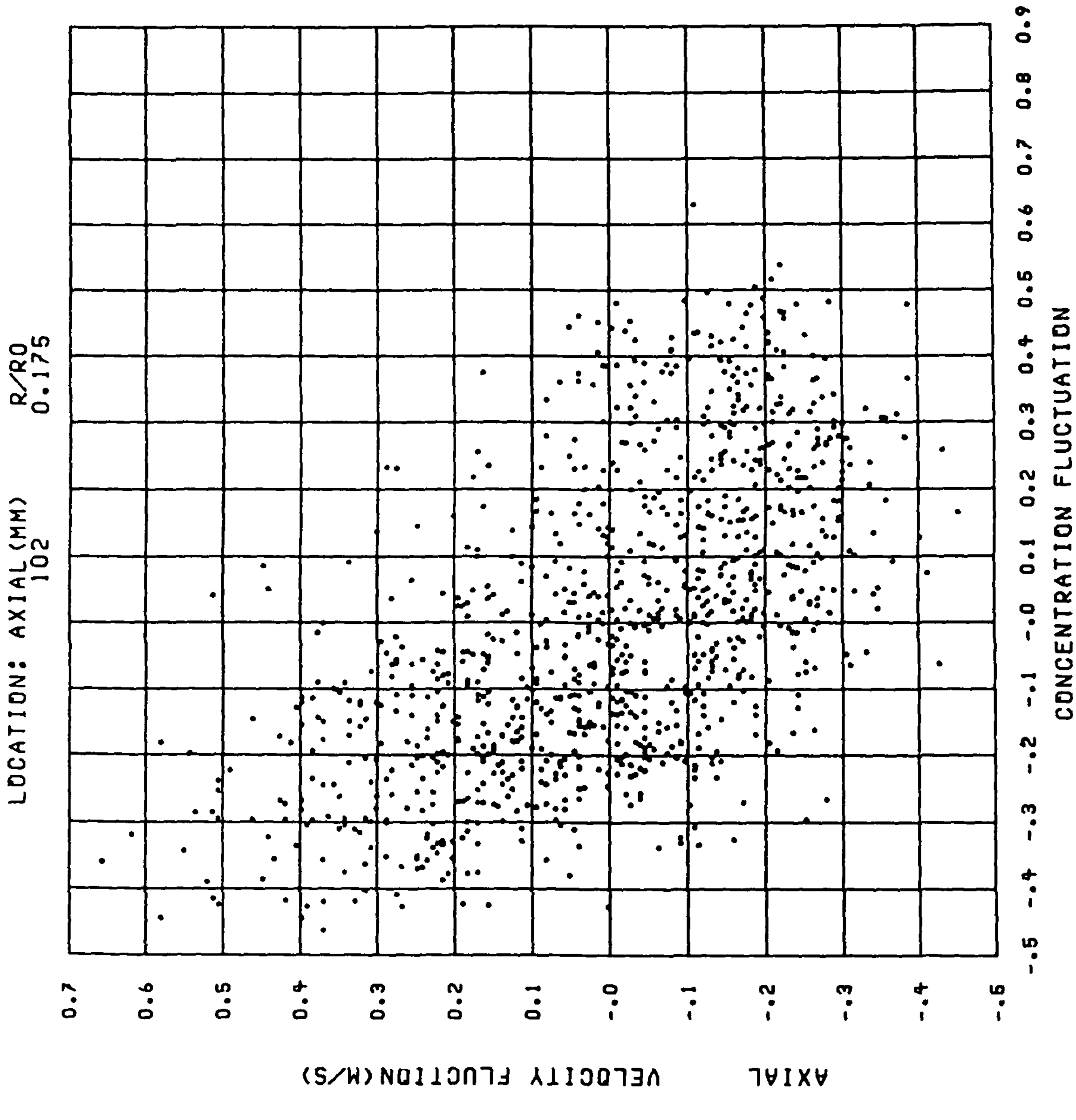
LOCATION: AXIAL(MM) 102
R/RO 0.175
CONCENTRATION FLUCTUATION
-.5 -.4 -.3 -.2 -.1 -.0 0.1 0.2 0.3 0.4 0.5 0.6 0.7 0.8 0.9
AXIAL VELOCITY FLUCTION(M/S)
0.7 0.6 0.5 0.4 0.3 0.2 0.1 -.0 -.1 -.2 -.3 -.4 -.5

Fig. 8

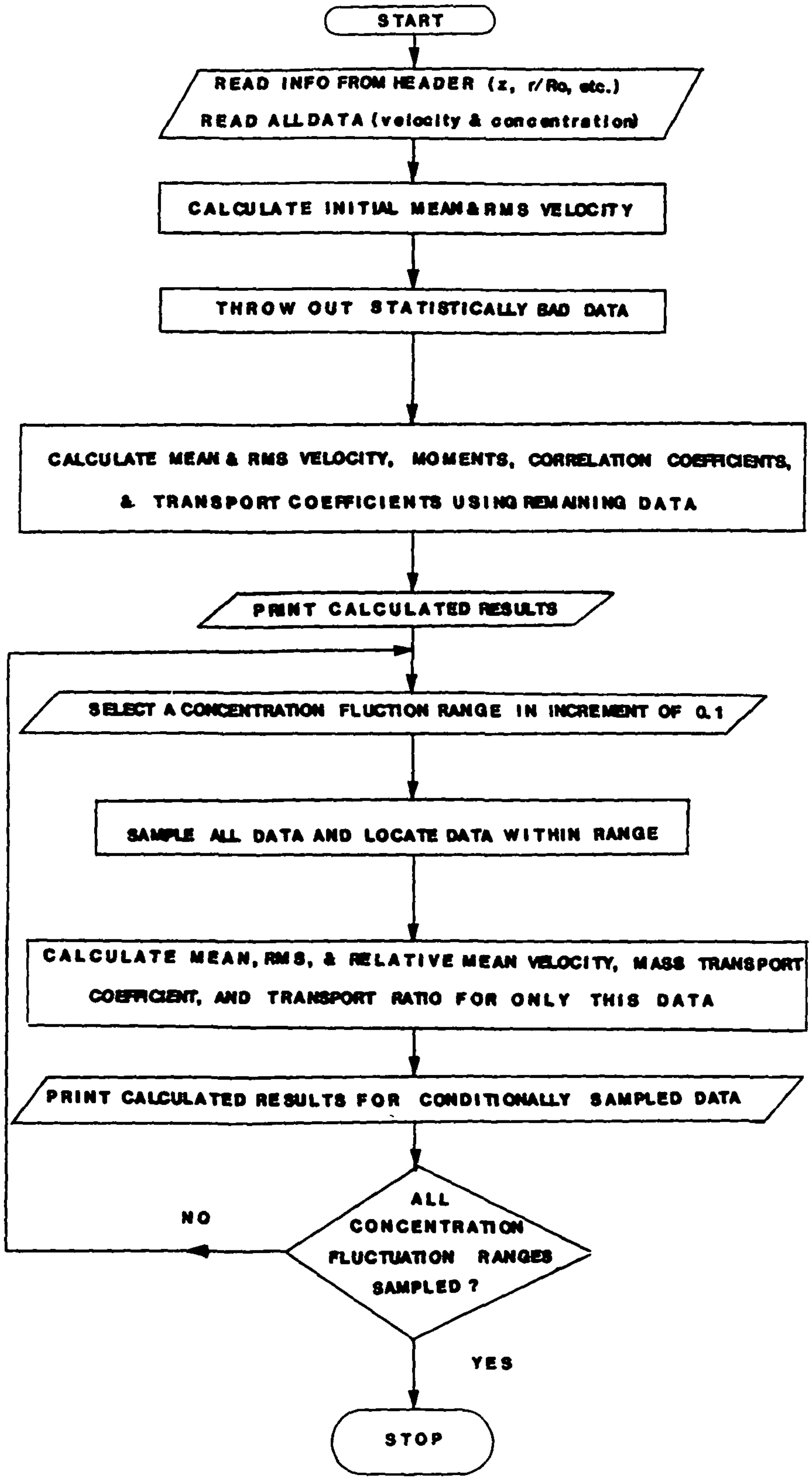
START
READ INFO FROM HEADER (z, r/Ro, etc.)
READ ALL DATA (velocity & concentration)
CALCULATE INITIAL MEAN & RMS VELOCITY
THROW OUT STATISTICALLY BAD DATA
CALCULATE MEAN & RMS VELOCITY, MOMENTS, CORRELATION COEFFICIENTS, & TRANSPORT COEFFICIENTS USING REMAINING DATA
PRINT CALCULATED RESULTS
SELECT A CONCENTRATION FLUCTION RANGE IN INCREMENT OF 0.1
SAMPLE ALL DATA AND LOCATE DATA WITHIN RANGE
CALCULATE MEAN, RMS, & RELATIVE MEAN VELOCITY, MASS TRANSPORT COEFFICIENT, AND TRANSPORT RATIO FOR ONLY THIS DATA
PRINT CALCULATED RESULTS FOR CONDITIONALLY SAMPLED DATA
ALL CONCENTRATION FLUCTUATION RANGES SAMPLED ?
NO
YES
STOP

```
SAMPLE 61.5
 SUCCESSFUL (TEMP) RESTORE RUN61F5 AS (TF5)
 CANCELLED: DDNAME RMDS     UNKNOWN

    DATA OUTPUT FOR RUN 61 POINT  5

AXIAL   VELOCITY VS CONCENTRATION
Z= 51 MM AND R/RO= 0.158
NO= 999 AND N4=985
VBAR=   0.7083 MPS
VRMS=   0.0894 MPS
THIRD MOMENT OF TURBULENCE= 0.15068E-03 MPS**3
THIRD CORRELATION COEFFICIENT=   0.2112
FOURTH MOMENT OF TURBULENCE= 0.20856E-03 MPS**4
FOURTH CORRELATION COEFFICIENT=   3.2709
CBAR=   0.775%
CRMS=   0.154%
CPVPBAR= -0.000522
OVERALL TRANSPORT COEFFICIENT= -0.038032
```

CONDITIONAL SAMPLING RESULTS

CONCENTRATION FLUCTUATION	NUMBER OF OCCURANCES	MEAN	RELATIVE MEAN	RMS	TRANSPORT COEFFICIENT	TRANSPORT RATIO
-1.0 - -0.9001	0					
-0.9 - -0.8001	0					
-0.8 - -0.7001	0					
-0.7 - -0.6001	1	0.8780	0.16968	0.00000	-7.72770	203.187
-0.6 - -0.5001	2	0.8580	0.14968	0.10100	-5.52904	145.377
-0.5 - -0.4001	17	0.7931	0.08480	0.10857	-2.70198	71.044
-0.4 - -0.3001	31	0.7270	0.01868	0.10087	-0.50036	13.156
-0.3 - -0.2001	76	0.7163	0.00798	0.10603	-0.18062	4.749
-0.2 - -0.1001	101	0.7006	-0.00775	0.10964	0.06358	-1.672
-0.1 - -0.0001	160	0.6896	-0.01873	0.08799	0.05972	-1.570
-0.0 - 0.0999	304	0.7002	-0.00813	0.07993	-0.00778	0.204
0.1 - 0.1999	262	0.7167	0.00834	0.07600	0.08703	-2.288
0.2 - 0.2999	31	0.7417	0.03338	0.07767	0.53998	-14.198
0.3 - 0.3999	0					
0.4 - 0.4999	0					
0.5 - 0.5999	0					
0.6 - 0.6999	0					
0.7 - 0.7999	0					
0.8 - 0.8999	0					
0.9 - 0.9999	0					

```
END OF RUN 61 -POINT  5
 TERMINATED: STOP
```

Fig. 9

```
SAMPLE 61.6
 SUCCESSFUL (TEMP) RESTORE RUN61F6 AS (TF6)
 CANCELLED: DDNAME RMDS      UNKNOWN

    DATA OUTPUT FOR RUN 61 POINT  6

AXIAL   VELOCITY VS CONCENTRATION
Z= 51 MM AND R/RO= 0.208
NO= 999 AND N4=999
VBAR=   1.0037 MPS
VRMS=   0.2193 MPS
THIRD MOMENT OF TURBULENCE= 0.32597E-02 MPS**3
THIRD CORRELATION COEFFICIENT=   0.3090
FOURTH MOMENT OF TURBULENCE= 0.58079E-02 MPS**4
FOURTH CORRELATION COEFFICIENT=   2.5103
CBAR=   0.367%
CRMS=   0.171%
CPVPBAR= -0.018305
OVERALL TRANSPORT COEFFICIENT= -0.488753
```

CONDITIONAL SAMPLING RESULTS

CONCENTRATION FLUCTUATION	NUMBER OF OCCURANCES	MEAN	RELATIVE MEAN	RMS	TRANSPORT COEFFICIENT	TRANSPORT RATIO
-1.0 - -0.9001	0					
-0.9 - -0.8001	0					
-0.8 - -0.7001	0					
-0.7 - -0.6001	0					
-0.6 - -0.5001	0					
-0.5 - -0.4001	0					
-0.4 - -0.3001	11	1.2878	0.28411	0.12489	-2.43854	4.989
-0.3 - -0.2001	92	1.1762	0.17253	0.18350	-1.09923	2.249
-0.2 - -0.1001	217	1.0975	0.09381	0.20346	-0.39192	0.802
-0.1 - -0.0001	226	1.0394	0.03572	0.20658	-0.06921	0.142
-0.0 - 0.0999	199	0.9664	-0.03726	0.20343	-0.05765	0.118
0.1 - 0.1999	117	0.8656	-0.13807	0.17301	-0.52990	1.084
0.2 - 0.2999	73	0.8365	-0.16718	0.14165	-1.07212	2.194
0.3 - 0.3999	46	0.8497	-0.15402	0.12301	-1.38951	2.843
0.4 - 0.4999	19	0.8247	-0.17897	0.08073	-2.11066	4.318
0.5 - 0.5999	2	0.7225	-0.28121	0.03950	-4.07154	8.330
0.6 - 0.6999	0					
0.7 - 0.7999	0					
0.8 - 0.8999	0					
0.9 - 0.9999	0					

```
END OF RUN 61 -POINT  6
 TERMINATED: STOP
```

Fig. 10

```
SAMPLE 52,14
 SUCCESSFUL (TEMP) RESTORE RUN52F14 AS (TF11)
 CANCELLED: DDNAME RMDS     UNKNOWN

    DATA OUTPUT FOR RUN 52 POINT 14

RADIAL  VELOCITY VS CONCENTRATION
Z=102 MM AND R/RO= 0.550
NO= 999 AND N4=992
VBAR=   0.0422 MPS
VRMS=   0.2275 MPS
THIRD MOMENT OF TURBULENCE= 0.13084E-02 MPS**3
THIRD CORRELATION COEFFICIENT=   0.1111
FOURTH MOMENT OF TURBULENCE= 0.89393E-02 MPS**4
FOURTH CORRELATION COEFFICIENT=   3.3354
CBAR=   0.008%
CRMS=   0.016%
CPVPBAR= -0.000505
OVERALL TRANSPORT COEFFICIENT= -0.139573
```

CONDITIONAL SAMPLING RESULTS

CONCENTRATION FLUCTUATION	NUMBER OF OCCURANCES	MEAN	RELATIVE MEAN	RMS	TRANSPORT COEFFICIENT	TRANSPORT RATIO
-1.0 - -0.9001	0					
-0.9 - -0.8001	0					
-0.8 - -0.7001	0					
-0.7 - -0.6001	0					
-0.6 - -0.5001	0					
-0.5 - -0.4001	0					
-0.4 - -0.3001	0					
-0.3 - -0.2001	0					
-0.2 - -0.1001	0					
-0.1 - -0.0001	521	0.0665	0.02432	0.22888	-0.13017	0.933
-0.0 - 0.0999	471	0.0153	-0.02690	0.22297	-0.15001	1.075
0.1 - 0.1999	0					
0.2 - 0.2999	0					
0.3 - 0.3999	0					
0.4 - 0.4999	0					
0.5 - 0.5999	0					
0.6 - 0.6999	0					
0.7 - 0.7999	0					
0.8 - 0.8999	0					
0.9 - 0.9999	0					

```
END OF RUN 52 -POINT 14
 TERMINATED: STOP
```

Fig. 11

ORIGINAL PAGE IS
OF POOR QUALITY

Fig. 12

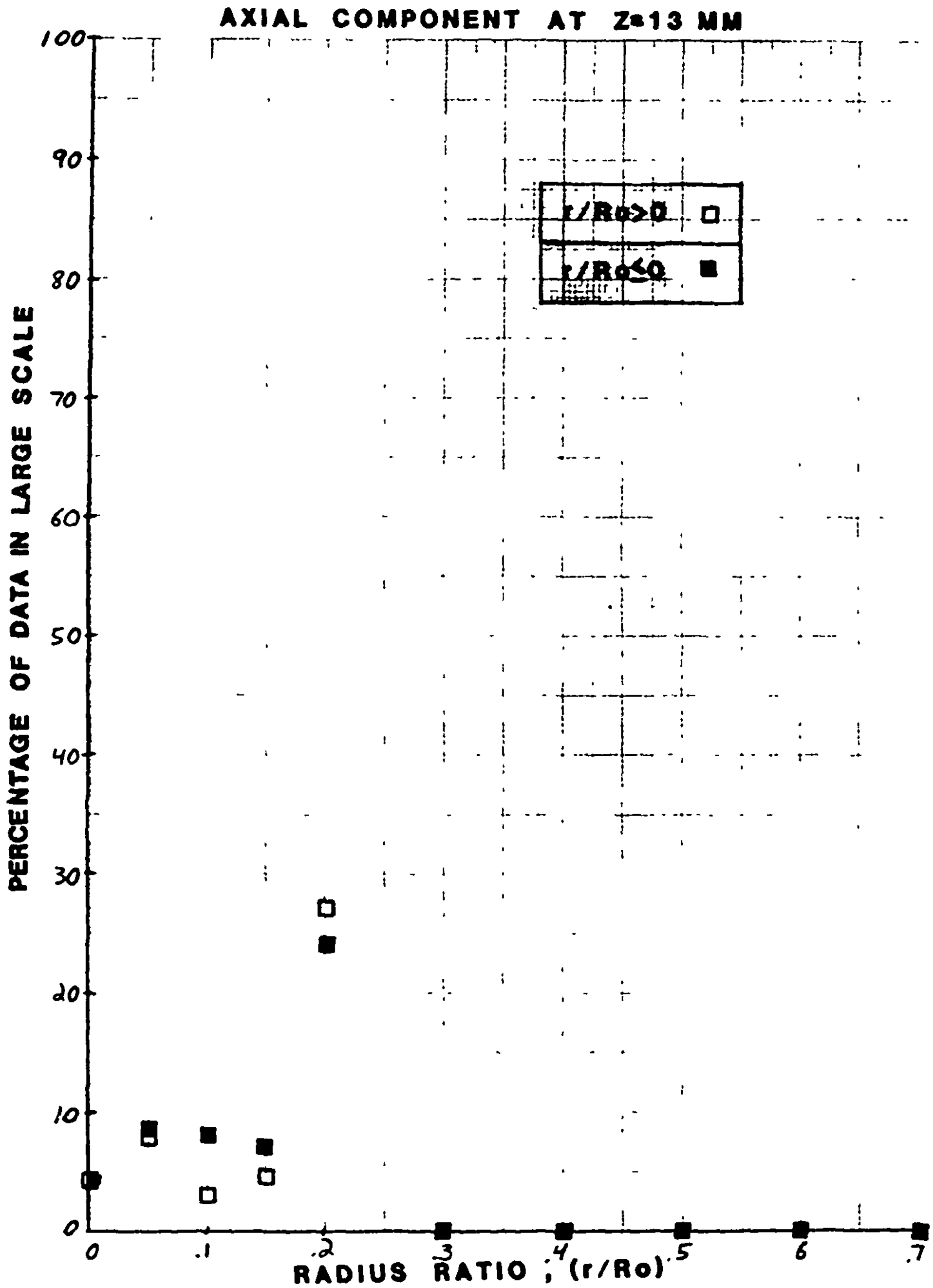

Fig. 13

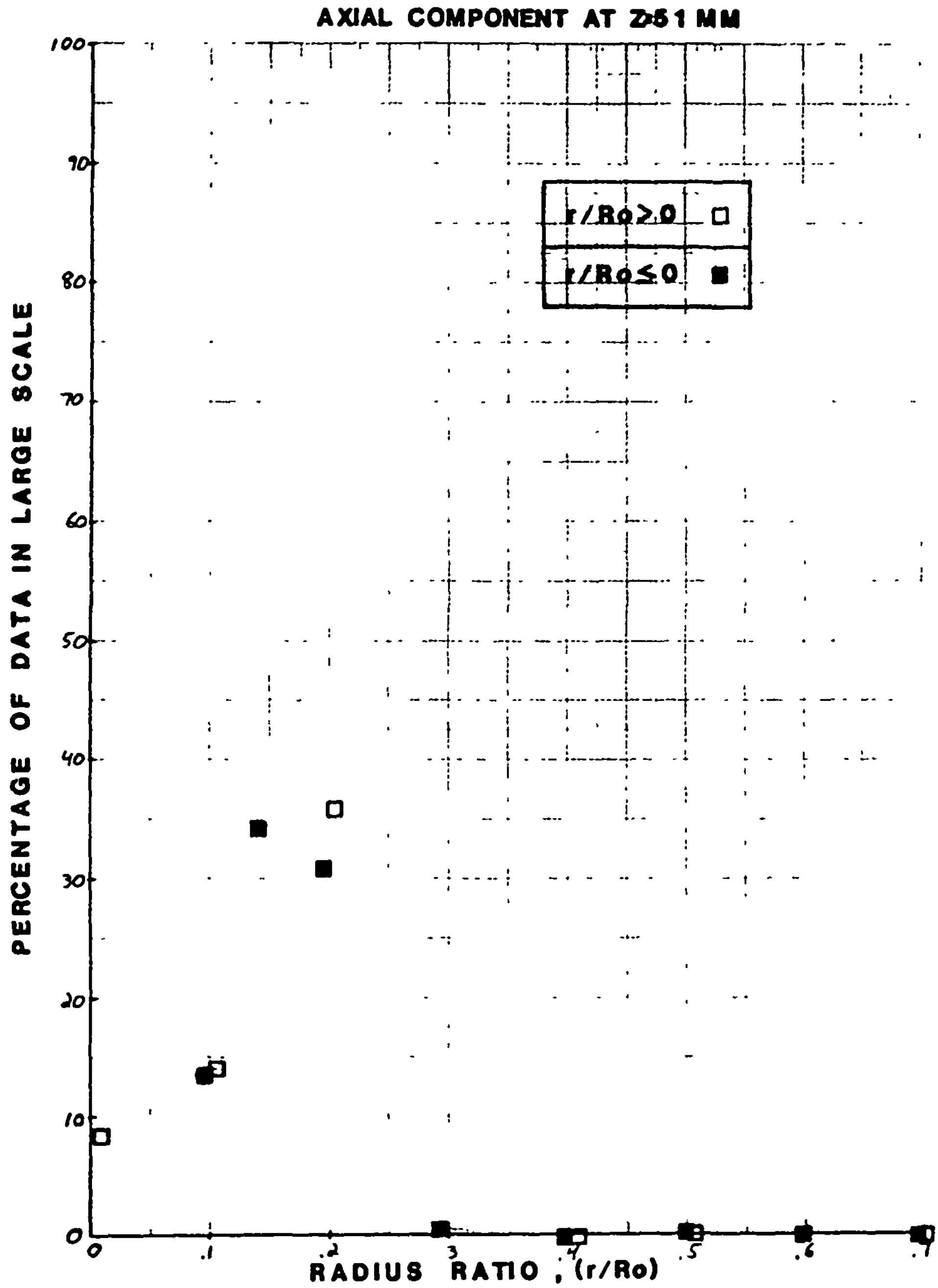
AXIAL COMPONENT AT Z>51 MM
100
90
80
70
60
50
40
30
20
10
0
PERCENTAGE OF DATA IN LARGE SCALE
r/Ro≥0
r/Ro≤0
0
.1
.2
.3
.4
.5
.6
.7
RADIUS RATIO , (r/Ro)

Fig. 14

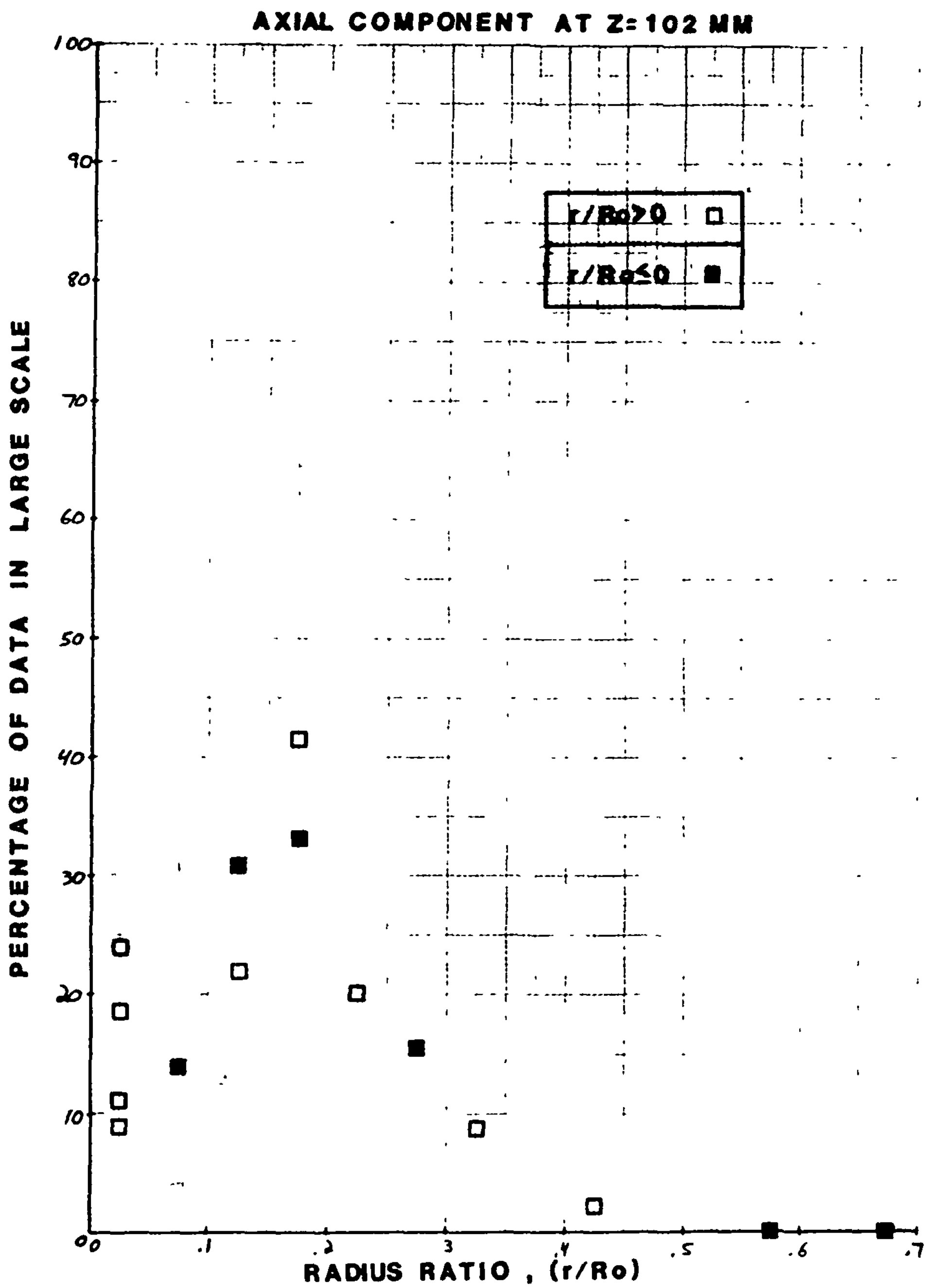

AXIAL COMPONENT AT Z=102 MM
PERCENTAGE OF DATA IN LARGE SCALE
RADIUS RATIO , (r/Ro)
r/Ro>0
r/Ro≤0
100
90
80
70
60
50
40
30
20
10
0
0
.1
.2
.3
.4
.5
.6
.7

ORIGINAL PAGE IS
OF POOR QUALITY

Fig. 15

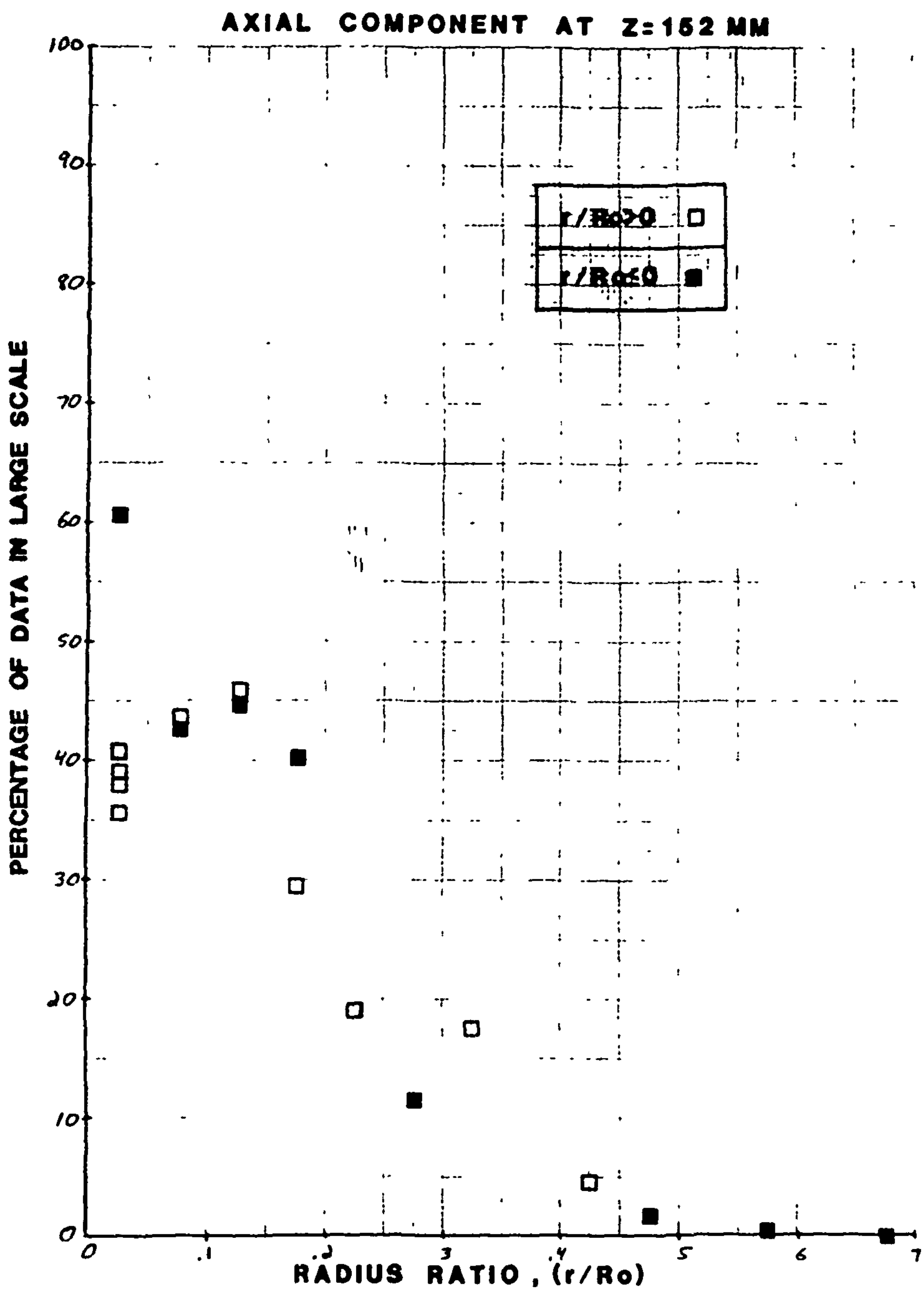

Fig. 16

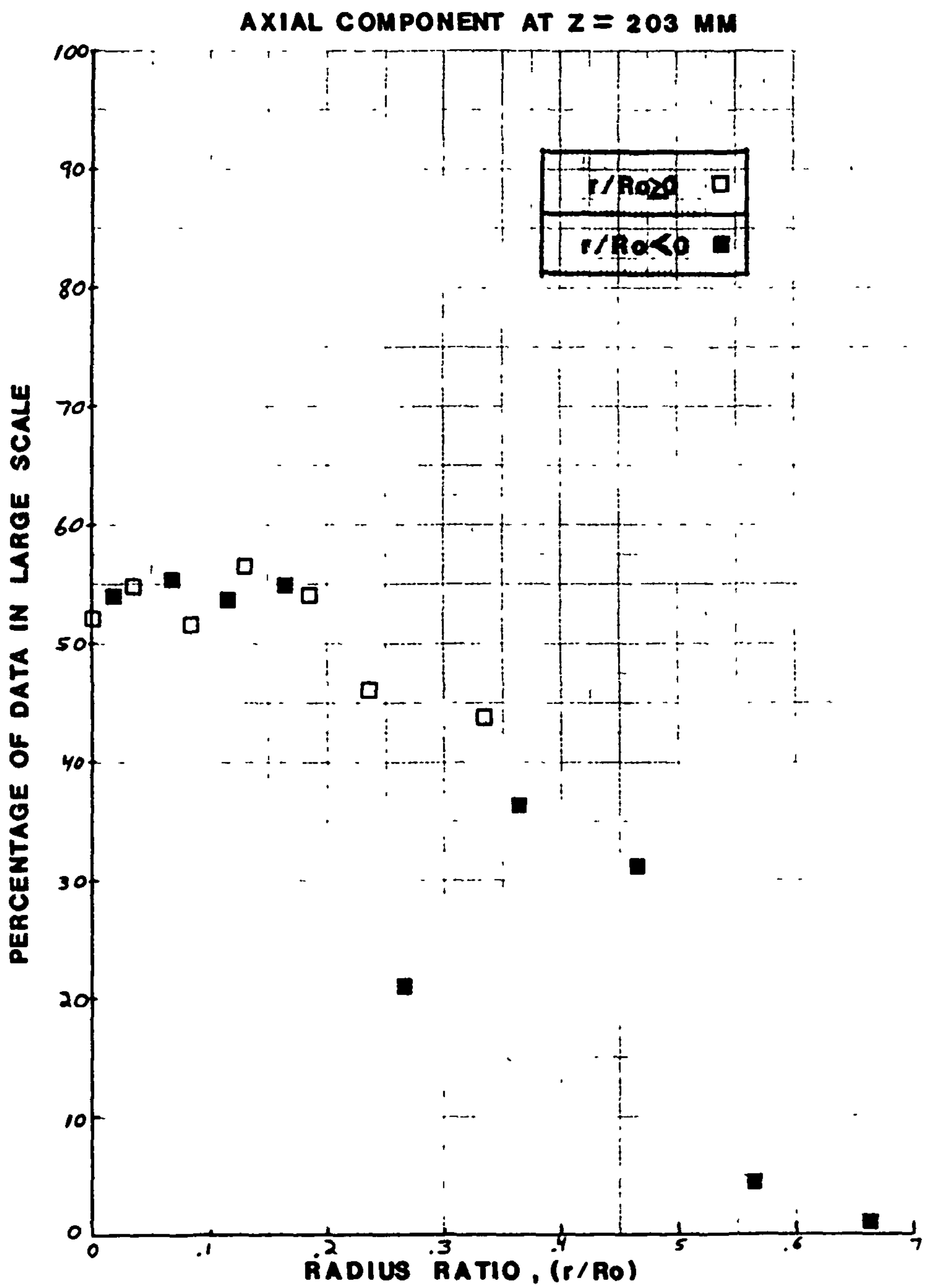
AXIAL COMPONENT AT Z = 203 MM
PERCENTAGE OF DATA IN LARGE SCALE
RADIUS RATIO, (r/Ro)
r/Ro≥0
r/Ro<0
100
90
80
70
60
50
40
30
20
10
0
0
.1
.2
.3
.4
.5
.6
.7

ORIGINAL PAGE IS
OF POOR QUALITY

Fig. 17

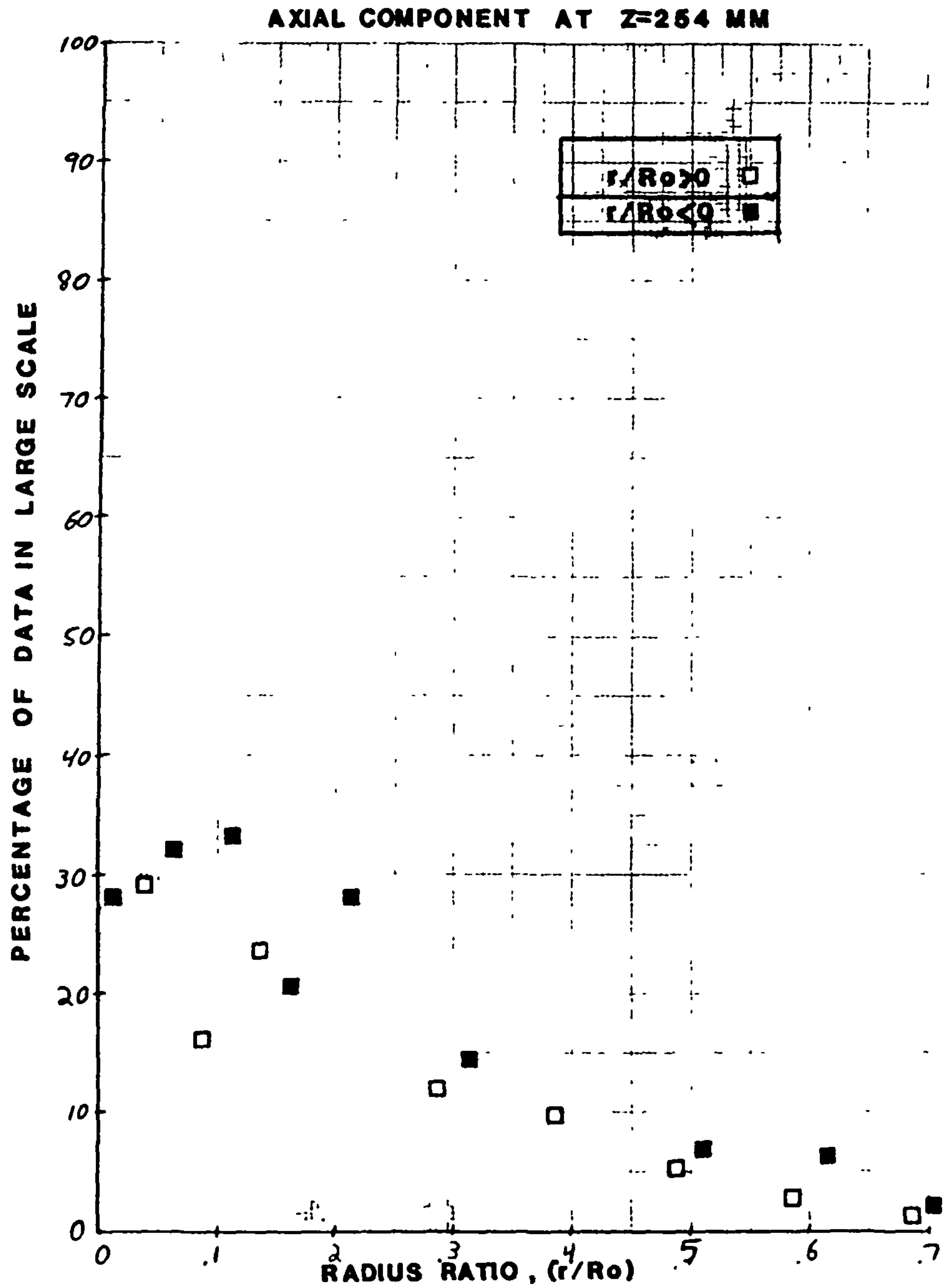

Fig. 18

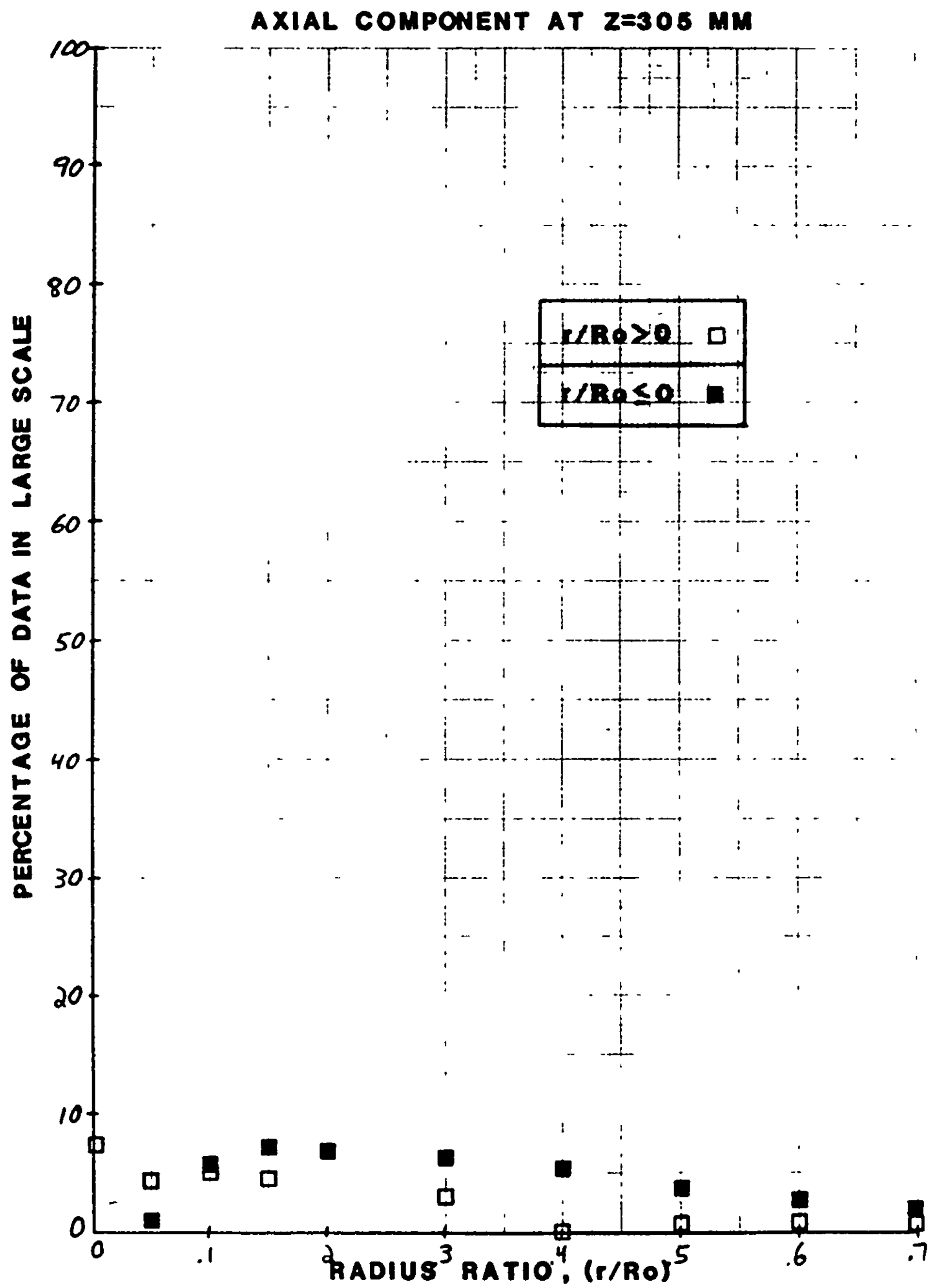
AXIAL COMPONENT AT Z=305 MM
PERCENTAGE OF DATA IN LARGE SCALE
RADIUS RATIO, (r/Ro)
r/Ro≥0
r/Ro≤0
0
10
20
30
40
50
60
70
80
90
100
.1
.2
.3
.4
.5
.6
.7

Fig. 19

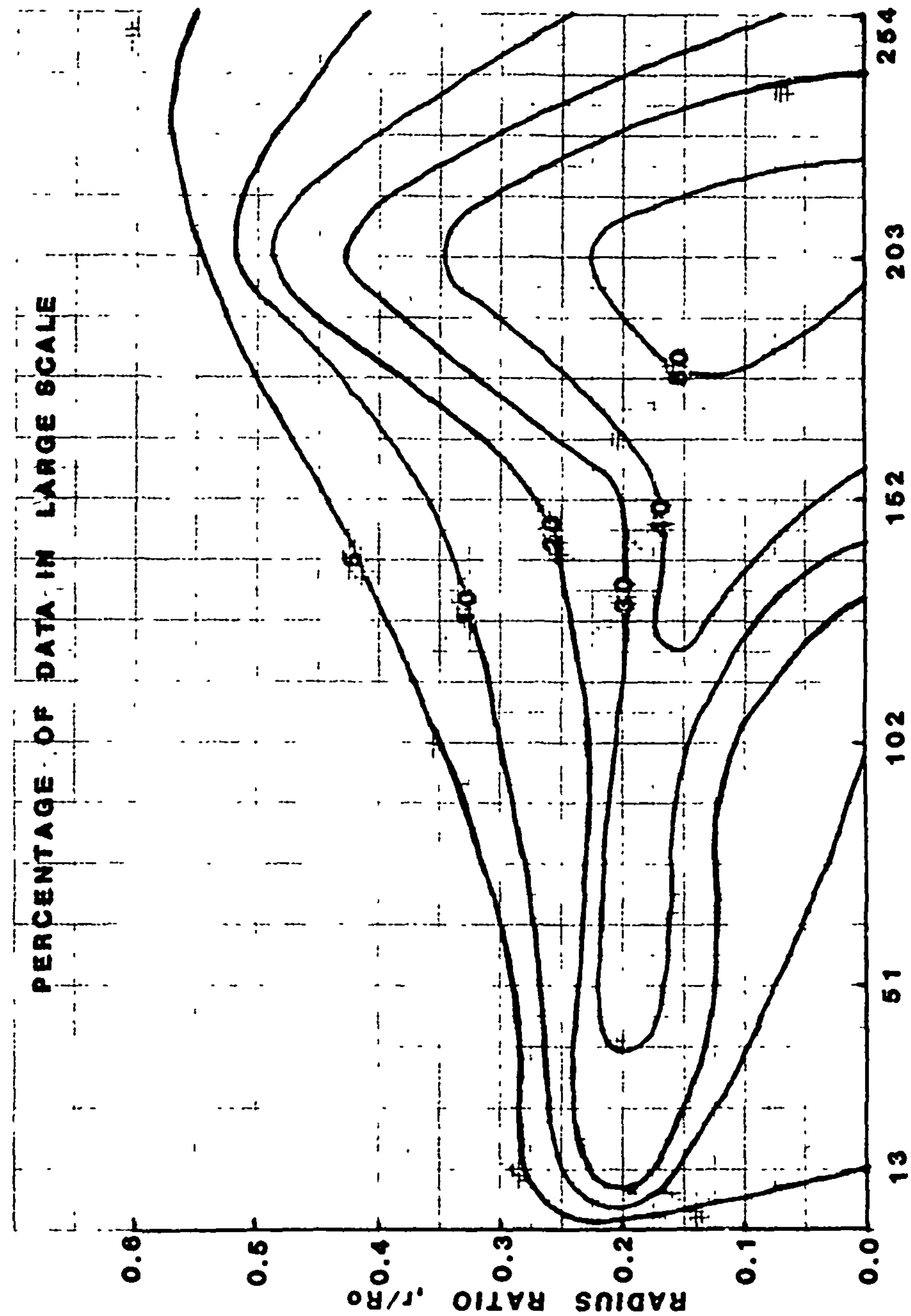
PERCENTAGE OF DATA IN LARGE SCALE
5
10
20
30
40
50
0.6
0.5
0.4
0.3
0.2
0.1
0.0
RADIUS RATIO ,r/Ro
13
51
102
152
203
254
AXIAL POSITION , Z (mm)

Fig. 20

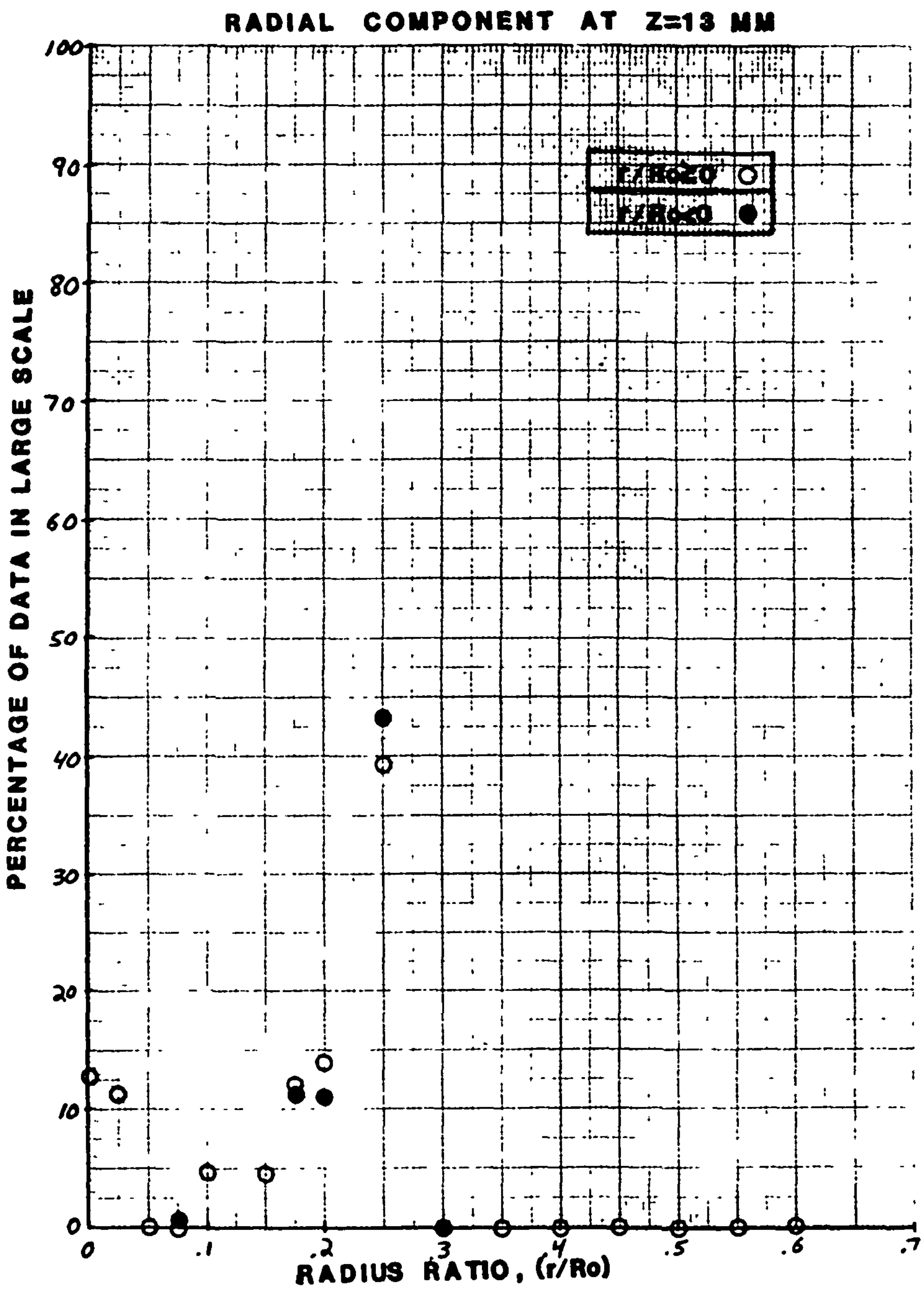

RADIAL COMPONENT AT Z=13 MM
r/Ro≥0
r/Ro<0
PERCENTAGE OF DATA IN LARGE SCALE
100
90
80
70
60
50
40
30
20
10
0
0
.1
.2
.3
.4
.5
.6
.7
RADIUS RATIO, (r/Ro)

ORIGINAL PAGE IS
OF POOR QUALITY

Fig. 21

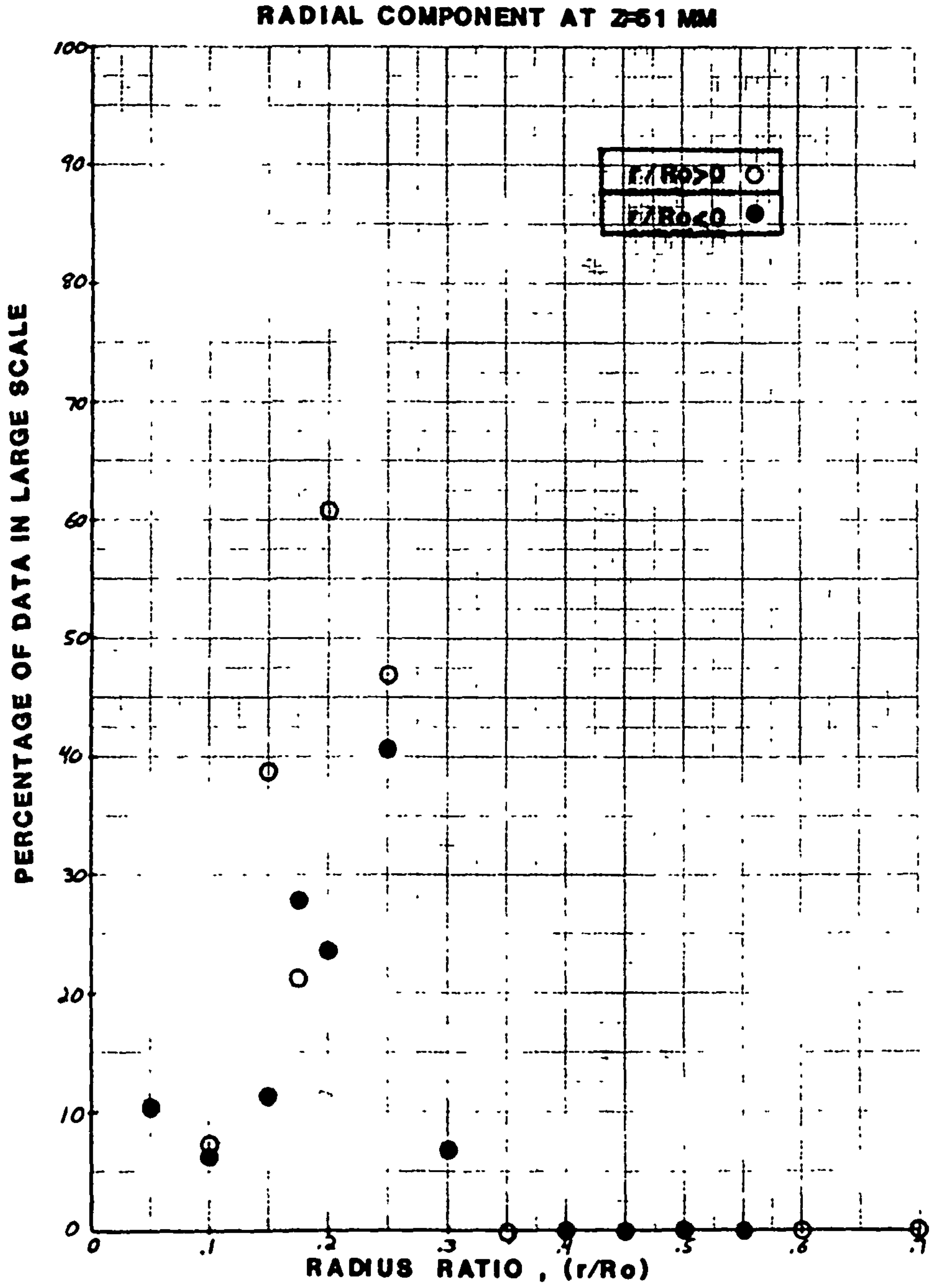

Fig. 22

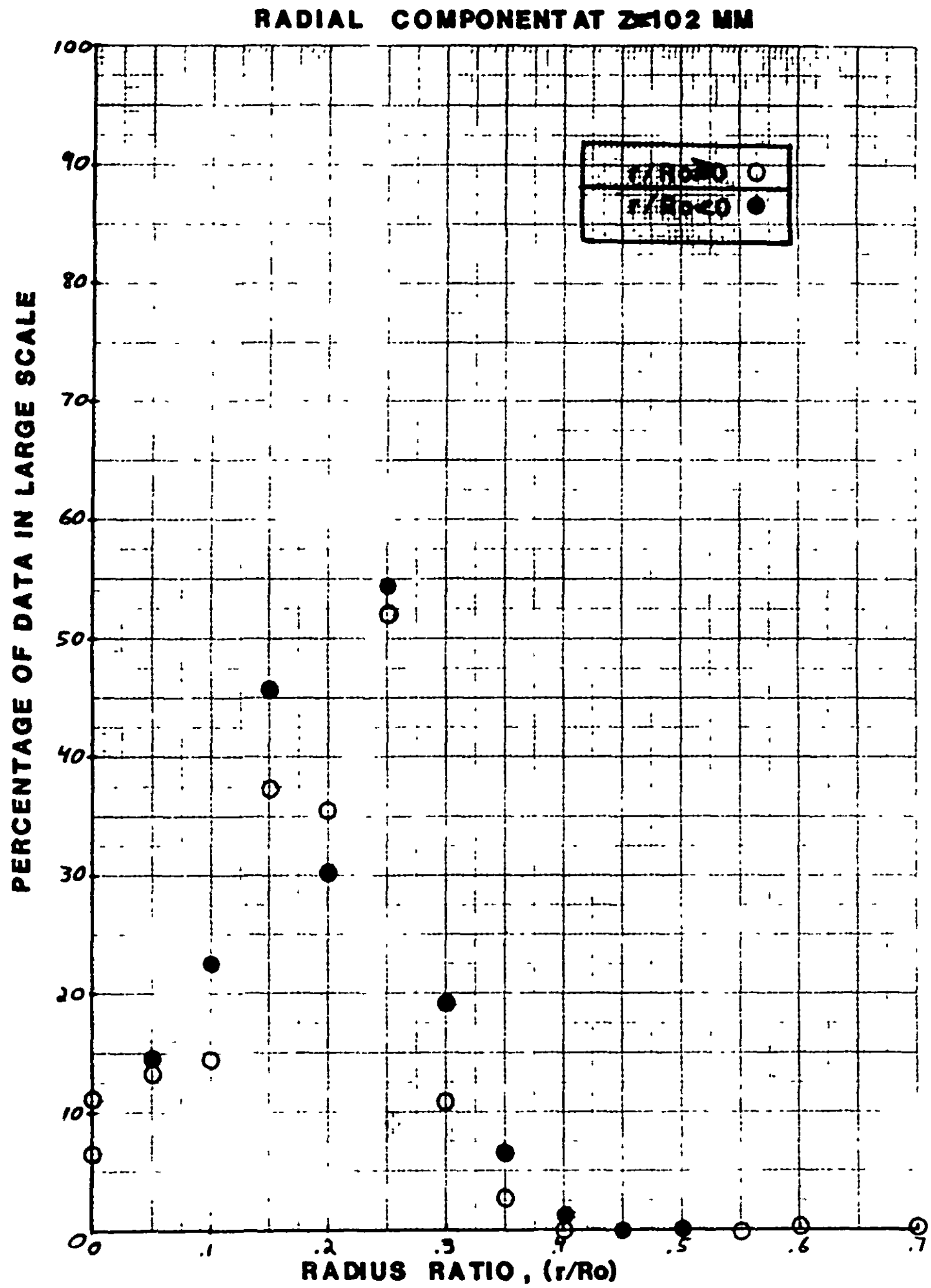
RADIAL COMPONENT AT Z=102 MM
PERCENTAGE OF DATA IN LARGE SCALE
RADIUS RATIO, (r/Ro)
100
90
80
70
60
50
40
30
20
10
0
0
.1
.2
.3
.4
.5
.6
.7
r/Ro>0
r/Ro<0

ORIGINAL PAGE IS
OF POOR QUALITY

Fig. 23

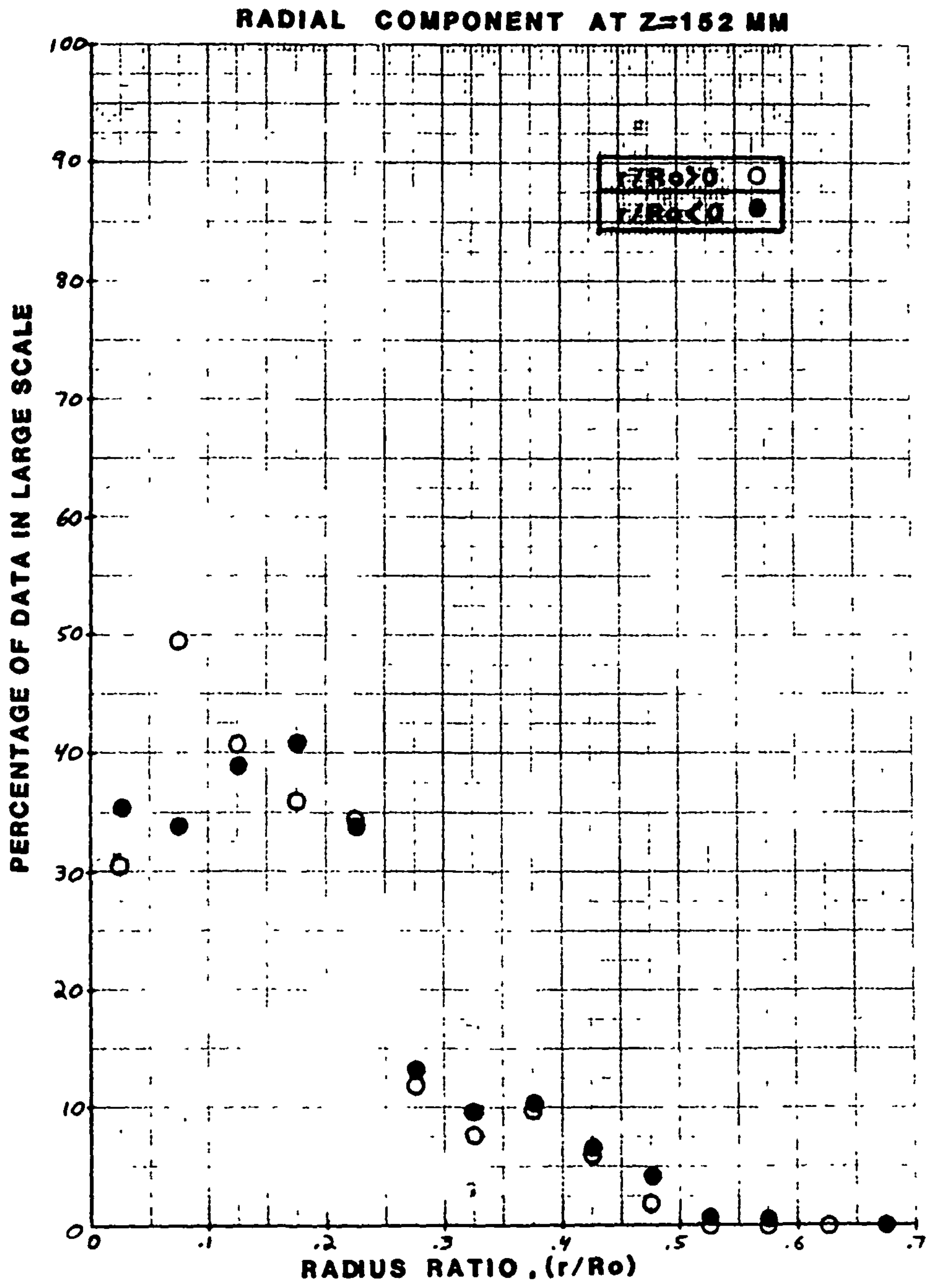

Fig. 24

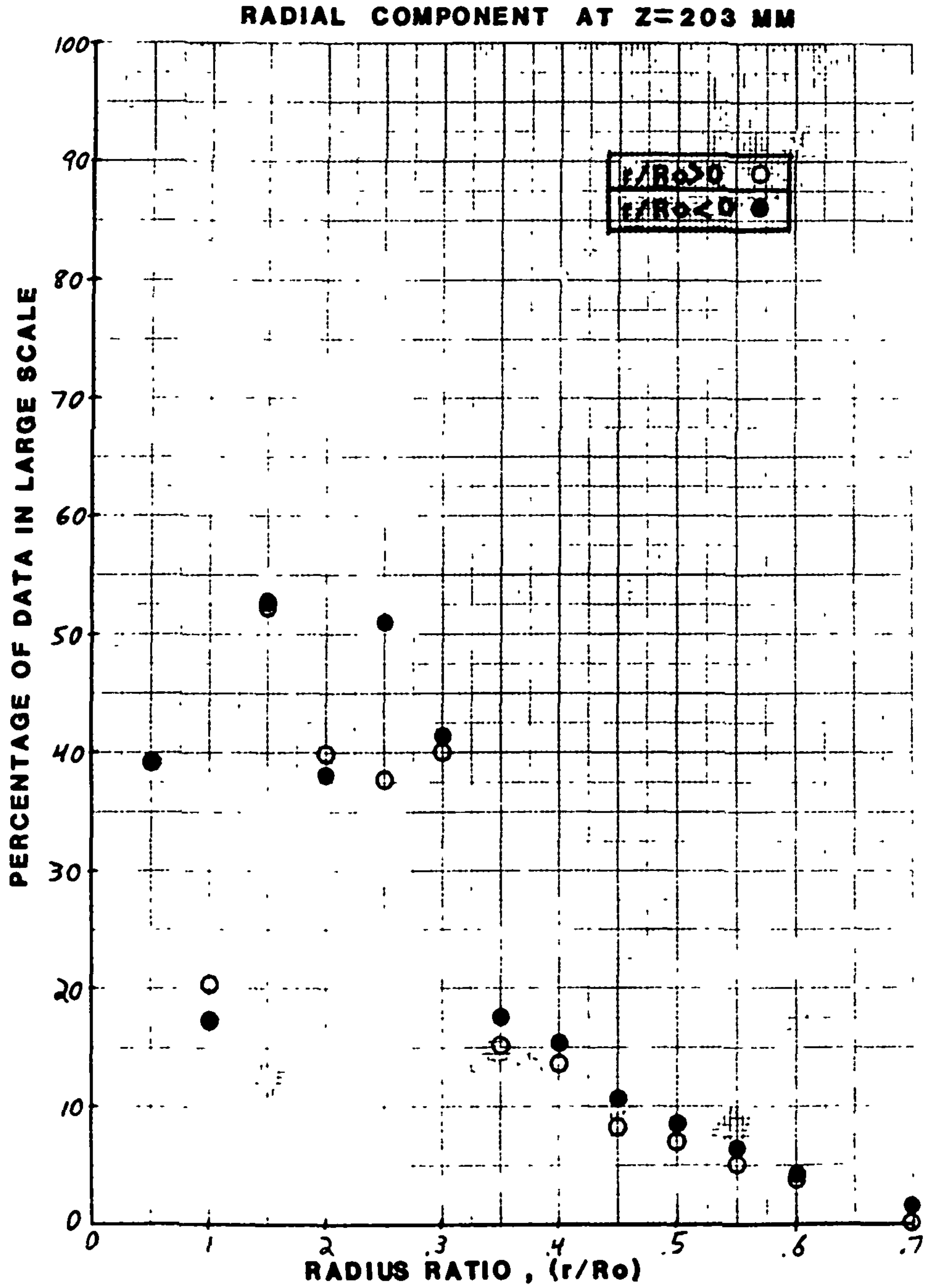

RADIAL COMPONENT AT Z=203 MM
PERCENTAGE OF DATA IN LARGE SCALE
RADIUS RATIO , (r/Ro)
r/Ro>0
r/Ro<0
100
90
80
70
60
50
40
30
20
10
0
0
.1
.2
.3
.4
.5
.6
.7

Fig. 25

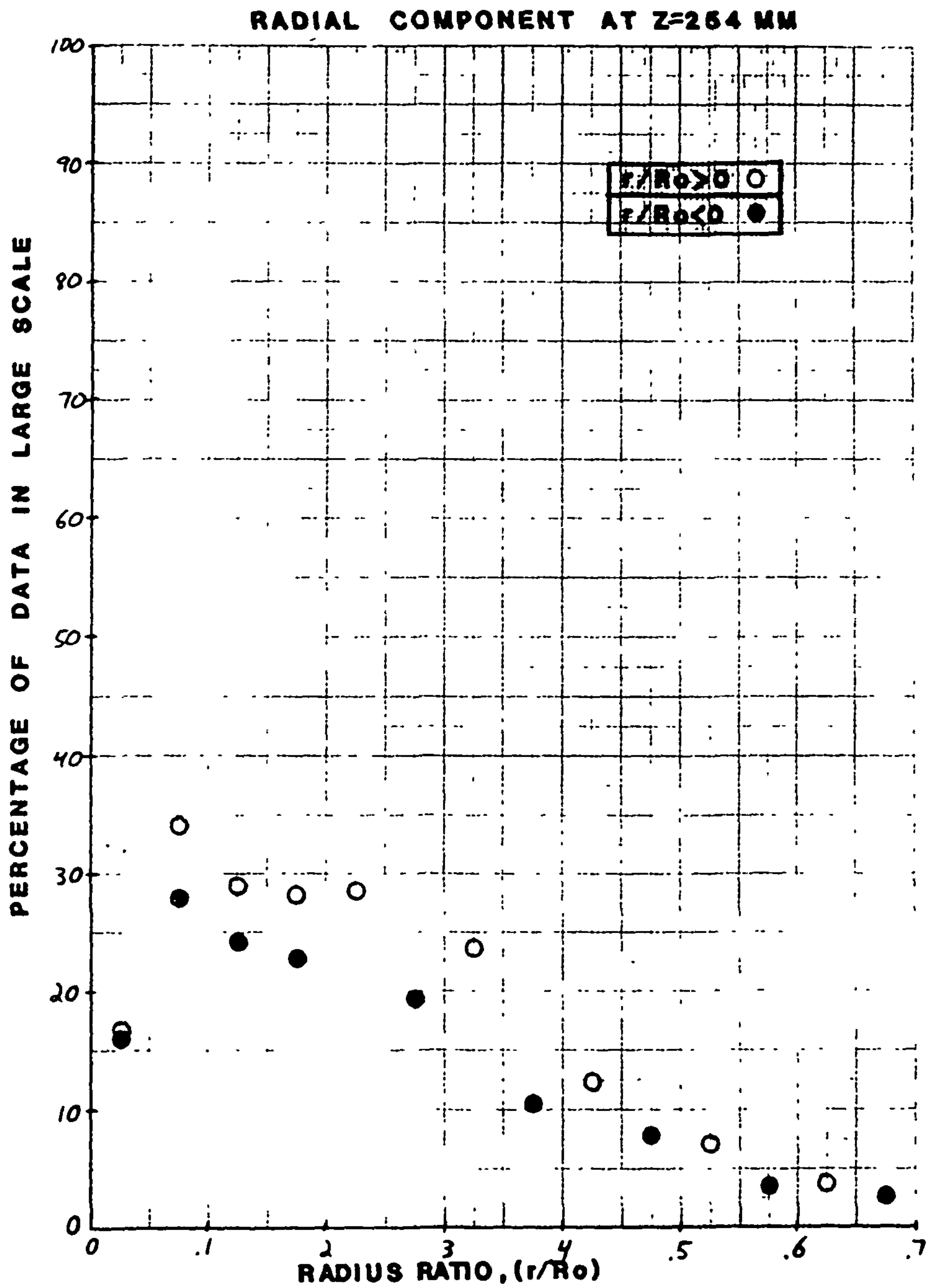

RADIAL COMPONENT AT Z=254 MM
PERCENTAGE OF DATA IN LARGE SCALE
r/Ro>0
r/Ro<0
100
90
80
70
60
50
40
30
20
10
0
0
.1
.2
.3
.4
.5
.6
.7
RADIUS RATIO, (r/Ro)

Fig. 26

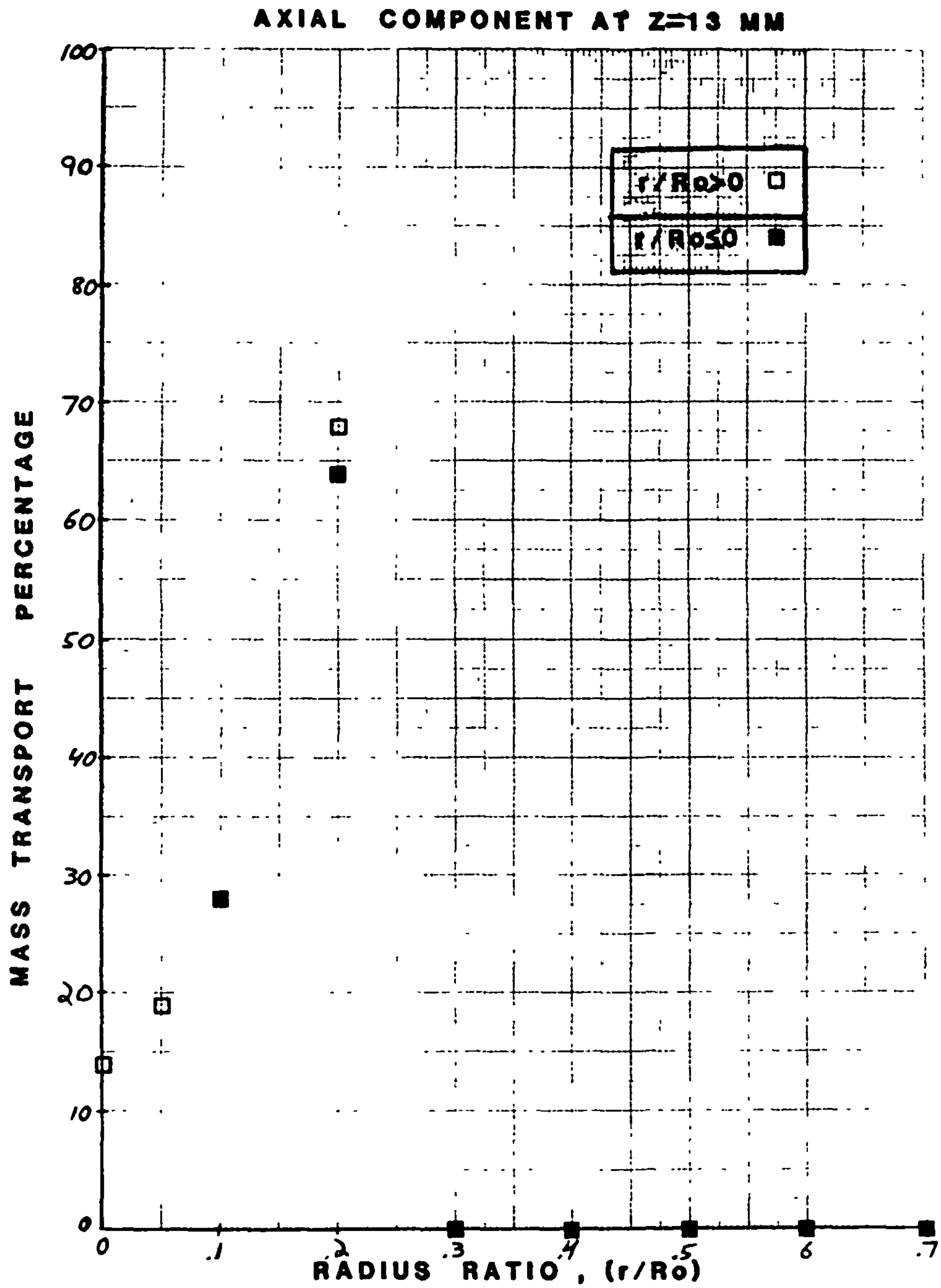
AXIAL COMPONENT AT Z=13 MM
MASS TRANSPORT PERCENTAGE
RADIUS RATIO, (r/Ro)
r/Ro>0
r/Ro≤0
100
90
80
70
60
50
40
30
20
10
0
0
.1
.2
.3
.4
.5
6
.7

Fig. 27

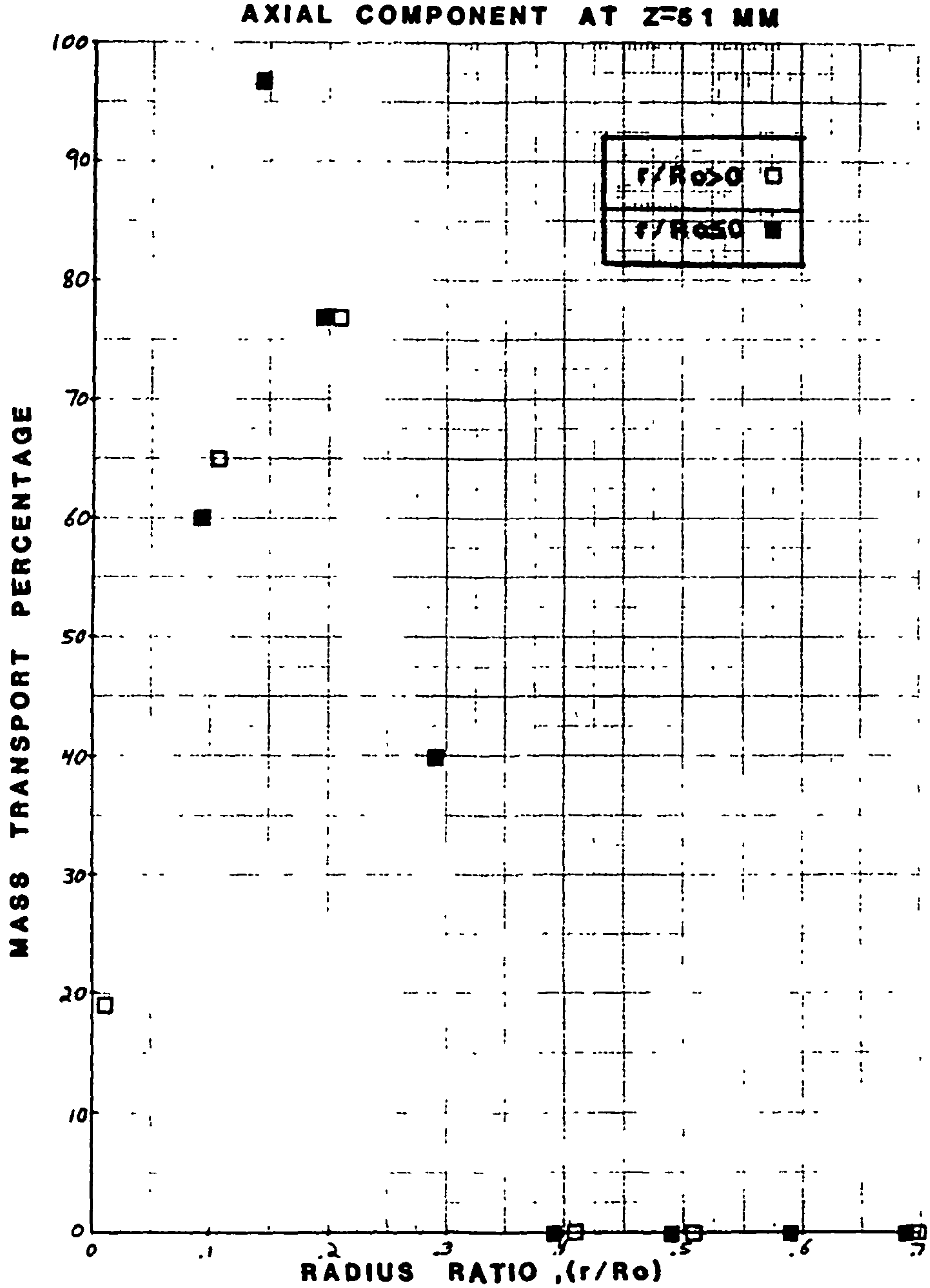

AXIAL COMPONENT AT Z=51 MM
100
90
80
70
60
50
40
30
20
10
0
MASS TRANSPORT PERCENTAGE
0
.1
.2
.3
.4
.5
.6
.7
RADIUS RATIO ,(r/Ro)
r/Ro>0
r/Ro≤0

Fig. 28

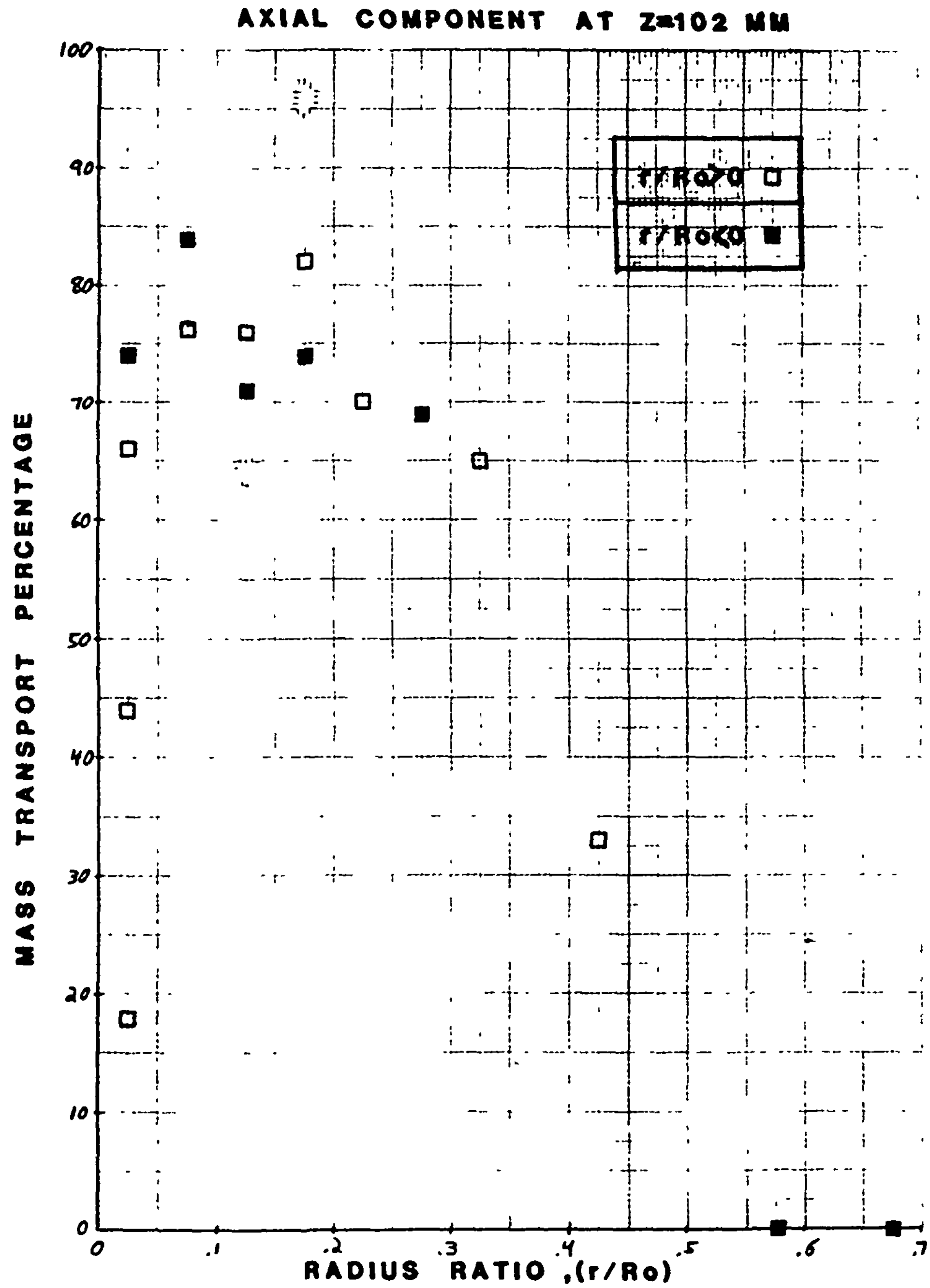

AXIAL COMPONENT AT Z=102 MM
MASS TRANSPORT PERCENTAGE
100
90
80
70
60
50
40
30
20
10
0
r/Ro>0
r/Ro<0
0
.1
.2
.3
.4
.5
.6
.7
RADIUS RATIO ,(r/Ro)

ORIGINAL PAGE IS
OF POOR QUALITY

Fig. 29

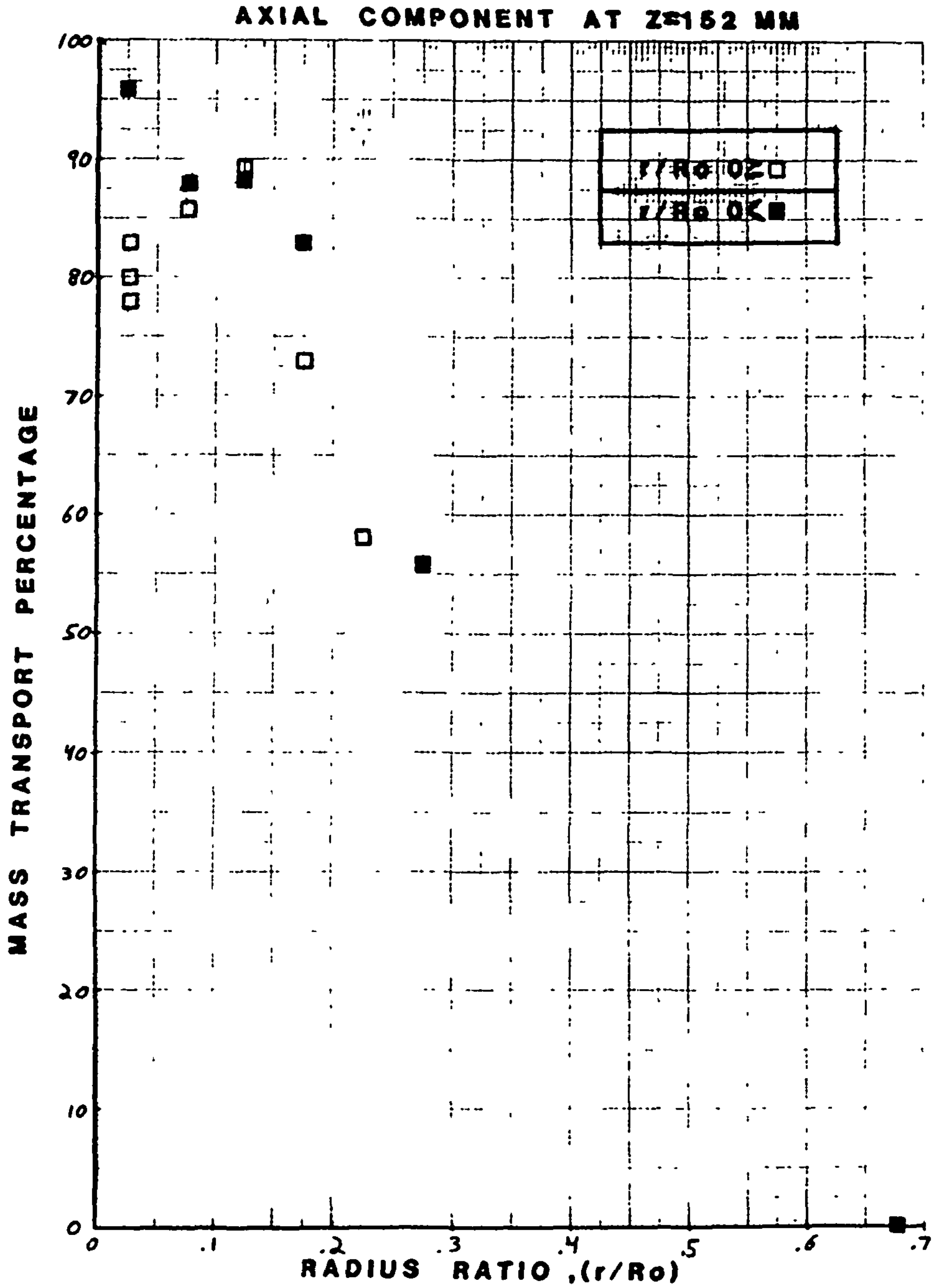

Fig. 30

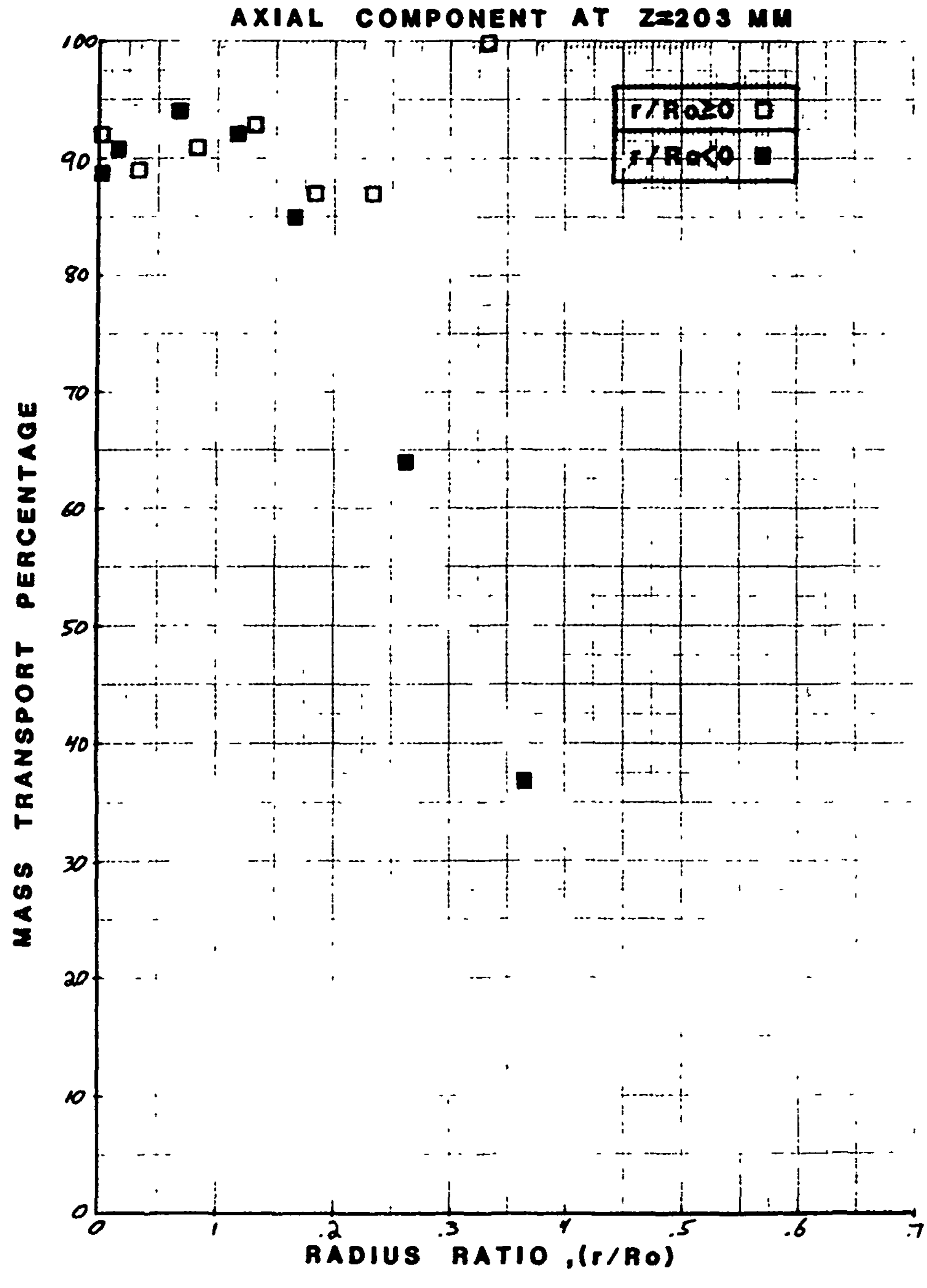
AXIAL COMPONENT AT Z=203 MM
r/Ro≥0
r/Ro<0
MASS TRANSPORT PERCENTAGE
RADIUS RATIO ,(r/Ro)
100
90
80
70
60
50
40
30
20
10
0
0
.1
.2
.3
.4
.5
.6
.7

ORIGINAL PAGE IS
OF POOR QUALITY

Fig. 31

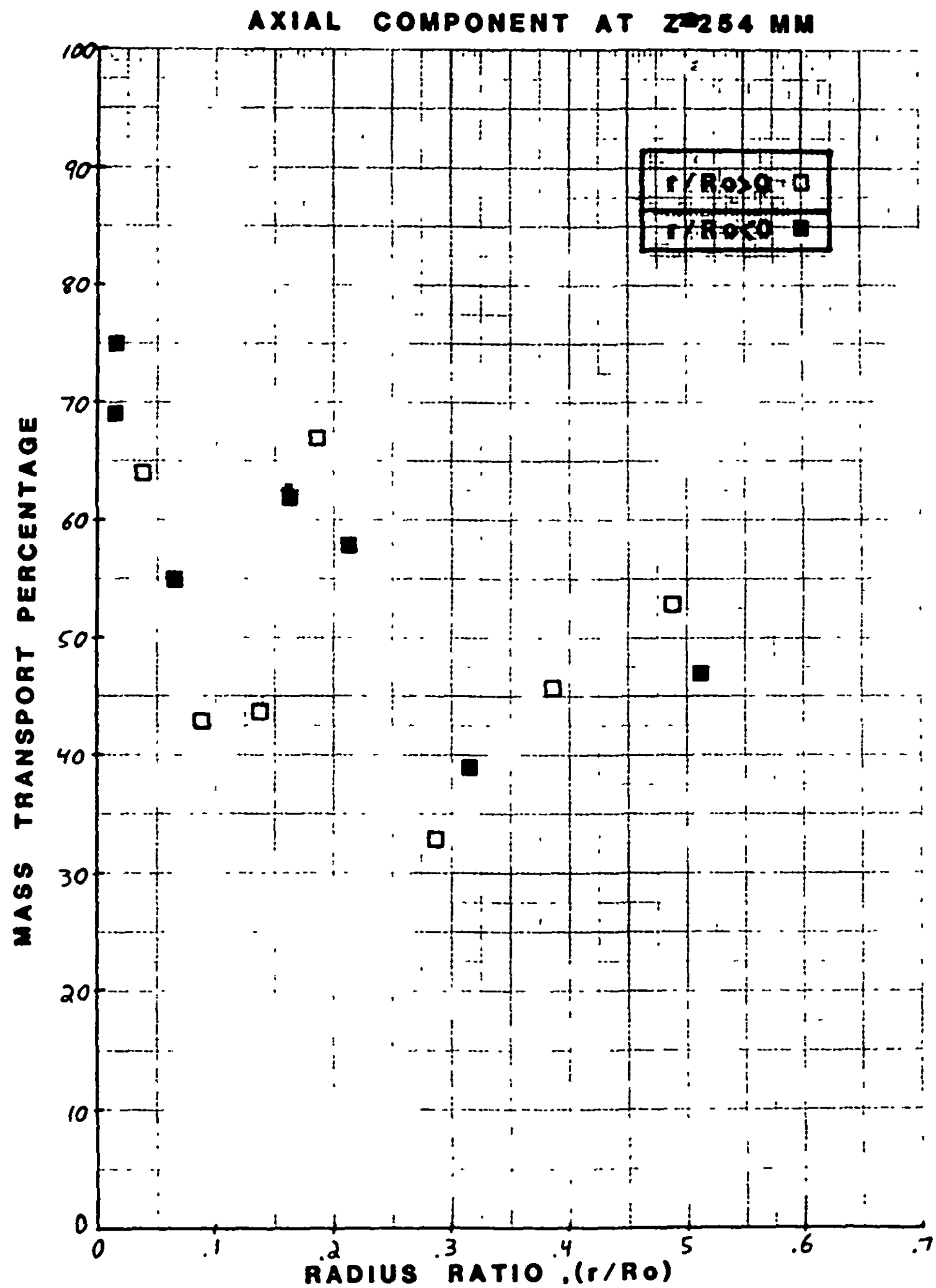

Fig. 32

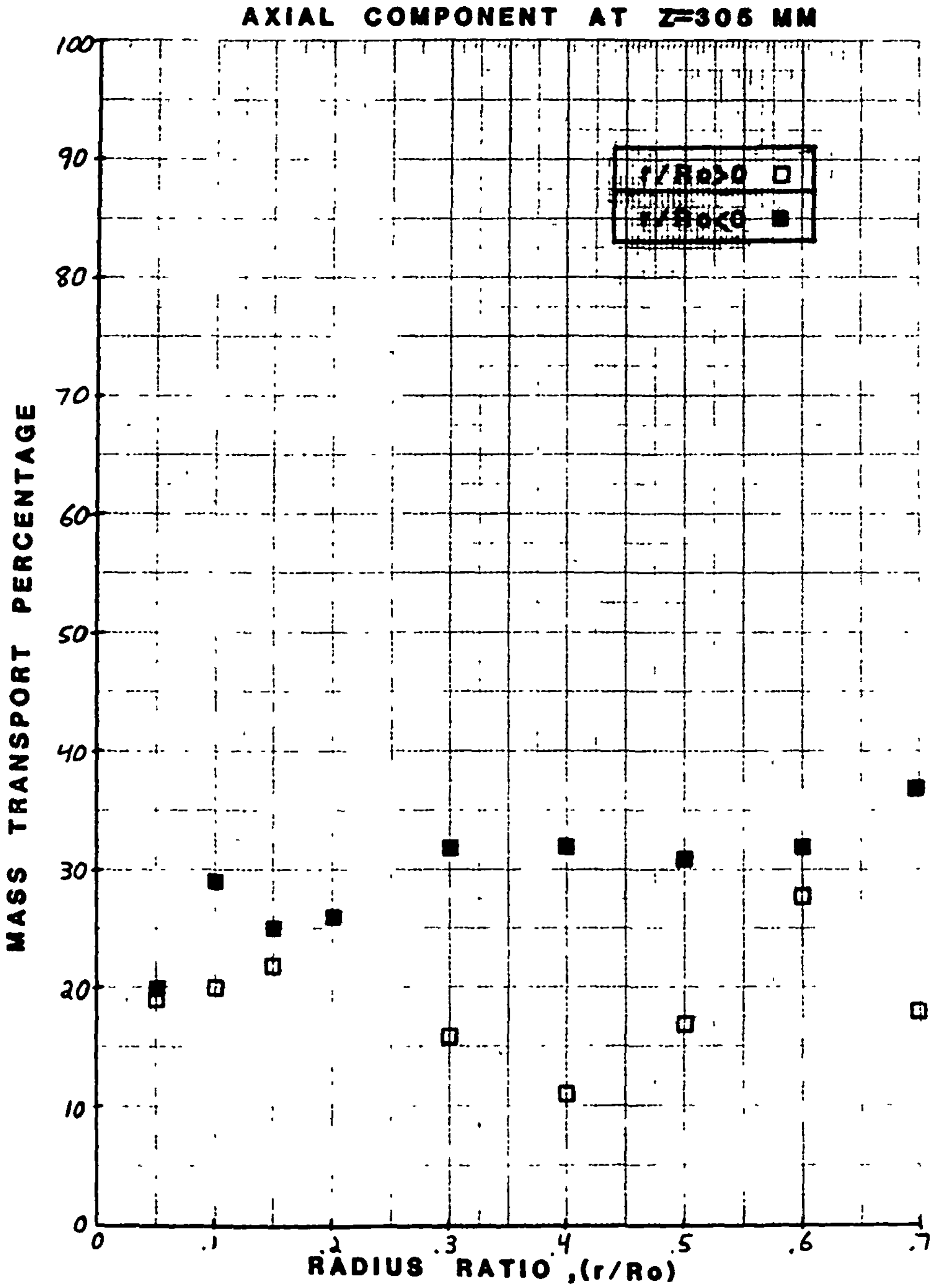
AXIAL COMPONENT AT Z=305 MM
MASS TRANSPORT PERCENTAGE
RADIUS RATIO ,(r/Ro)
r/Ro>0
r/Ro<0
100
90
80
70
60
50
40
30
20
10
0
0
.1
.2
.3
.4
.5
.6
.7

Fig. 33

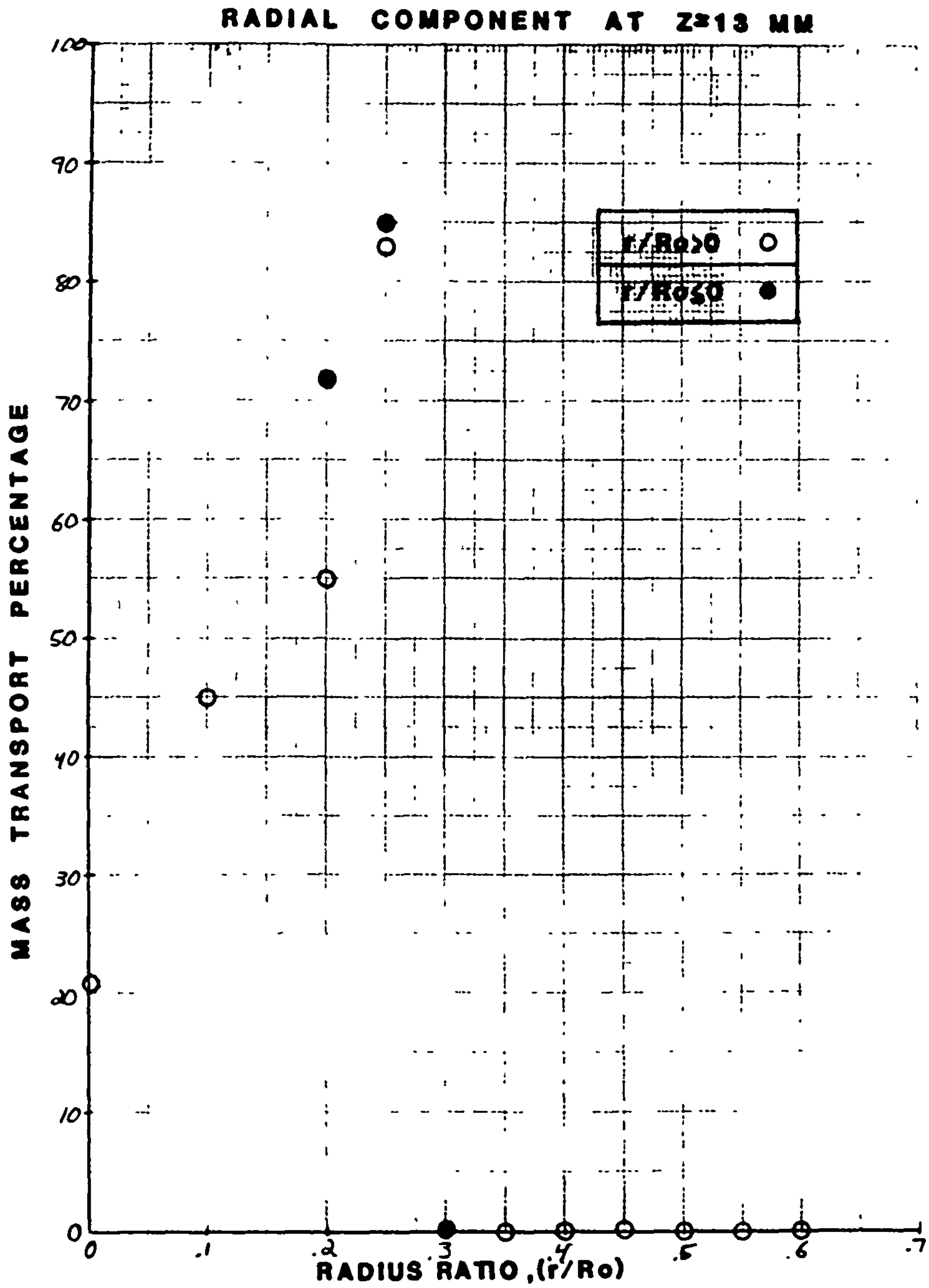
RADIAL COMPONENT AT Z=13 MM
MASS TRANSPORT PERCENTAGE
RADIUS RATIO ,(r/Ro)
r/Ro>0
r/Ro<0
0
10
20
30
40
50
60
70
80
90
100
0
.1
.2
.3
.4
.5
.6
.7

Fig. 34

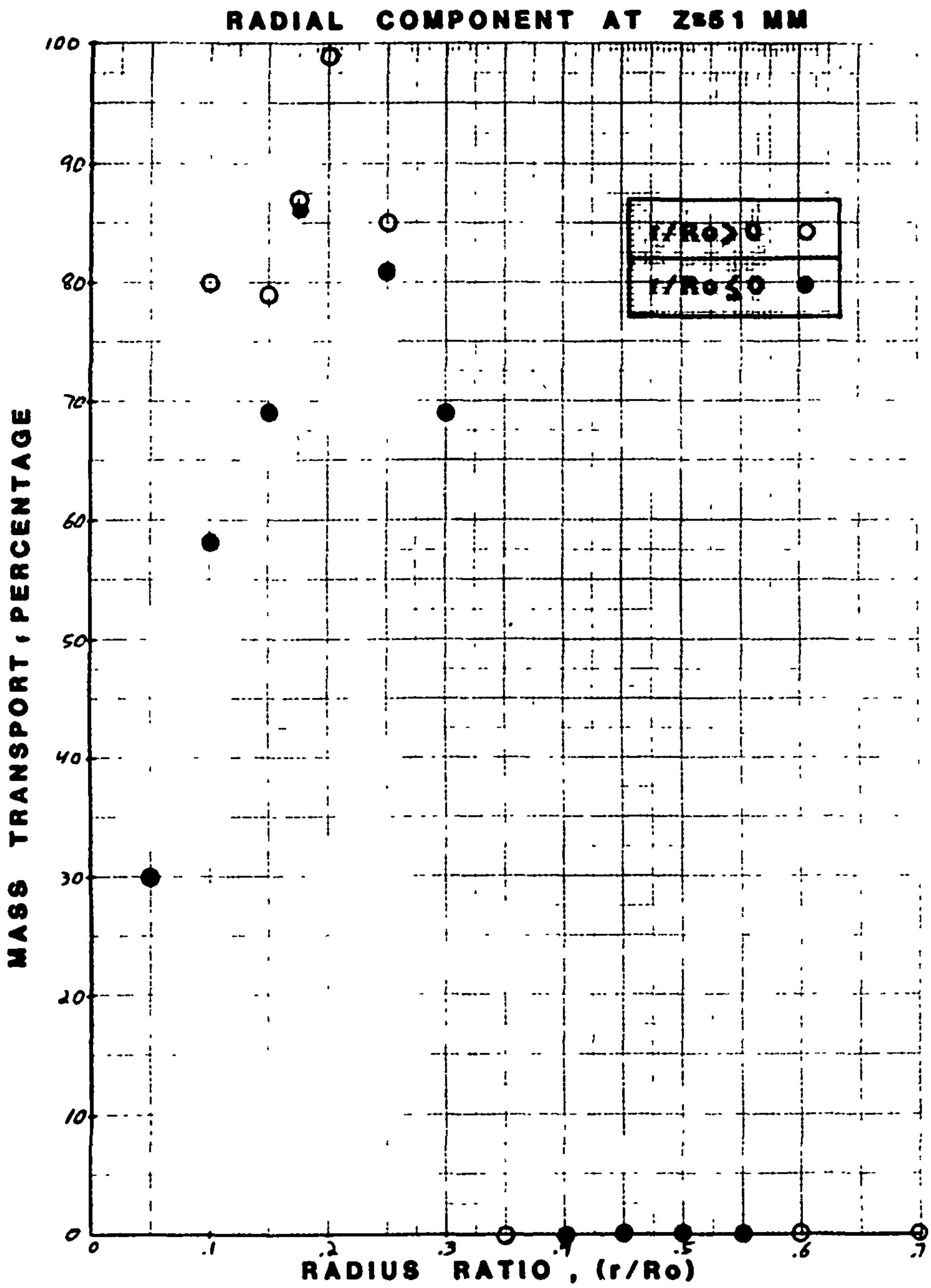

RADIAL COMPONENT AT Z=51 MM
100
90
80
70
60
50
40
30
20
10
0
MASS TRANSPORT , PERCENTAGE
r/Ro>0
r/Ro≤0
0
.1
.2
.3
.4
.5
.6
.7
RADIUS RATIO , (r/Ro)

ORIGINAL PAGE IS
OF POOR QUALITY

Fig. 35

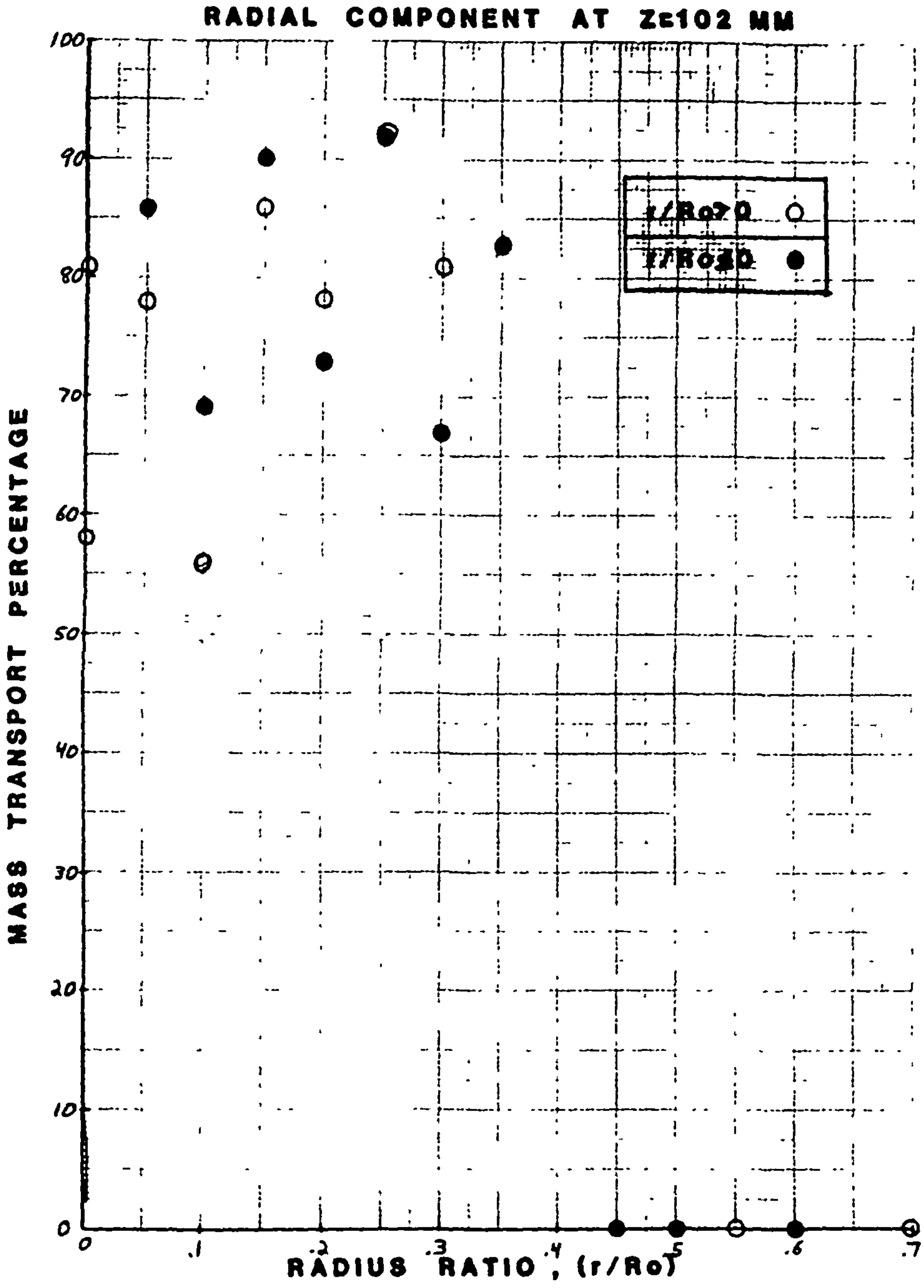

Fig. 36

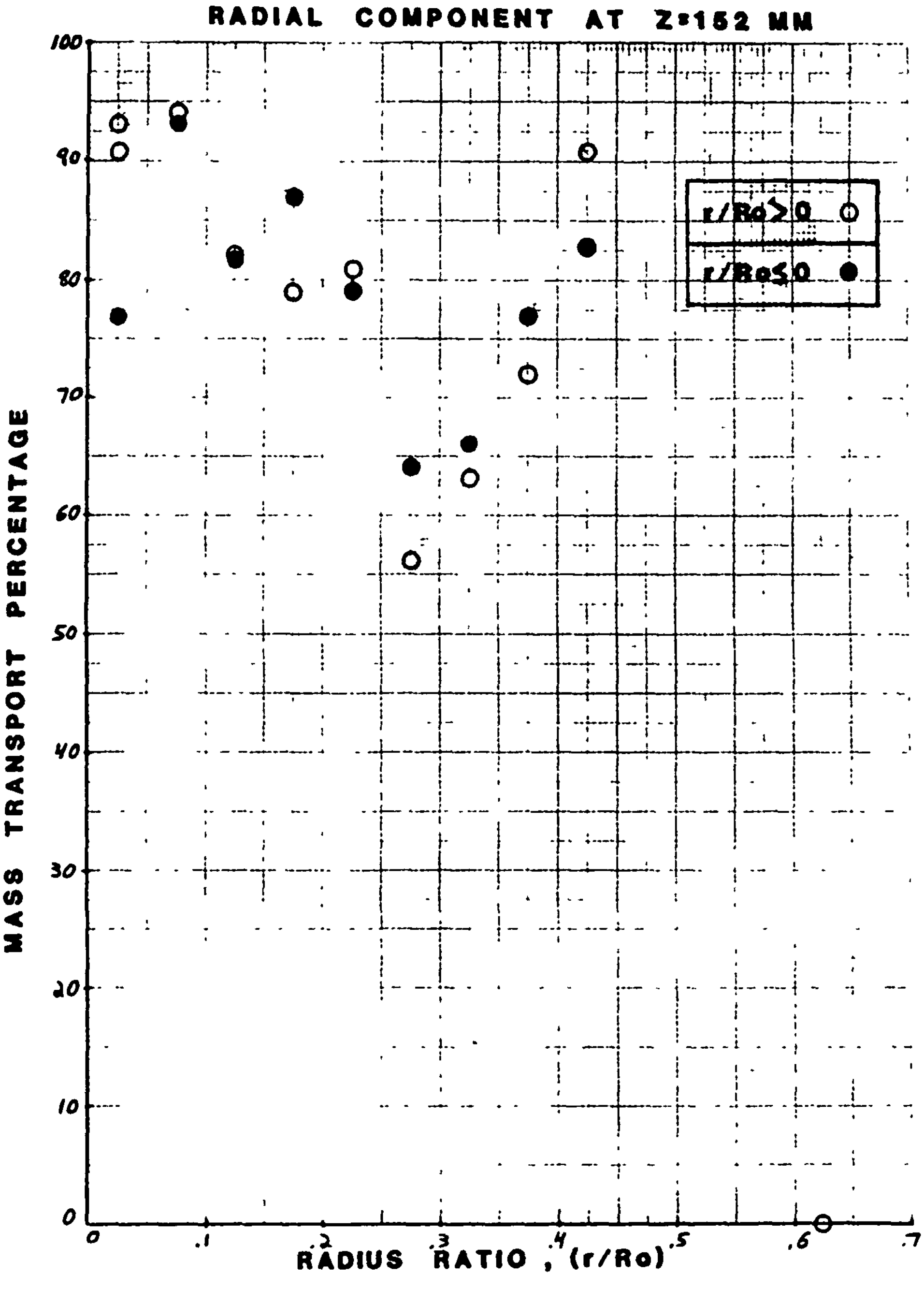
RADIAL COMPONENT AT Z=152 MM
MASS TRANSPORT PERCENTAGE
RADIUS RATIO, (r/Ro)
r/Ro>0
r/Ro≤0
100
90
80
70
60
50
40
30
20
10
0
.1
.2
.3
.4
.5
.6
.7

Fig. 37

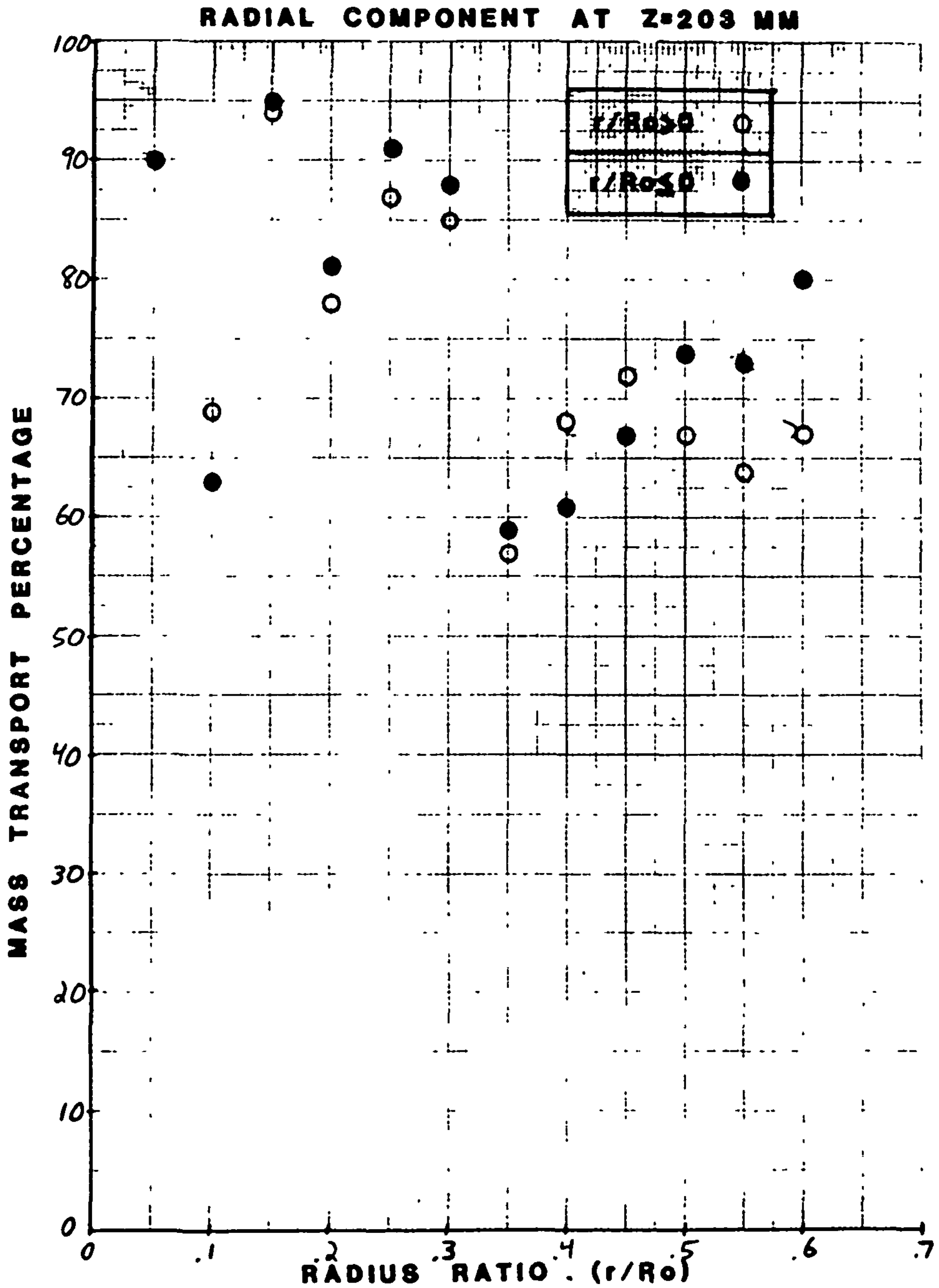

RADIAL COMPONENT AT Z=203 MM
r/Ro>0
r/Ro<0
MASS TRANSPORT PERCENTAGE
RADIUS RATIO . (r/Ro)
100
90
80
70
60
50
40
30
20
10
0
0
.1
.2
.3
.4
.5
.6
.7

Fig. 38

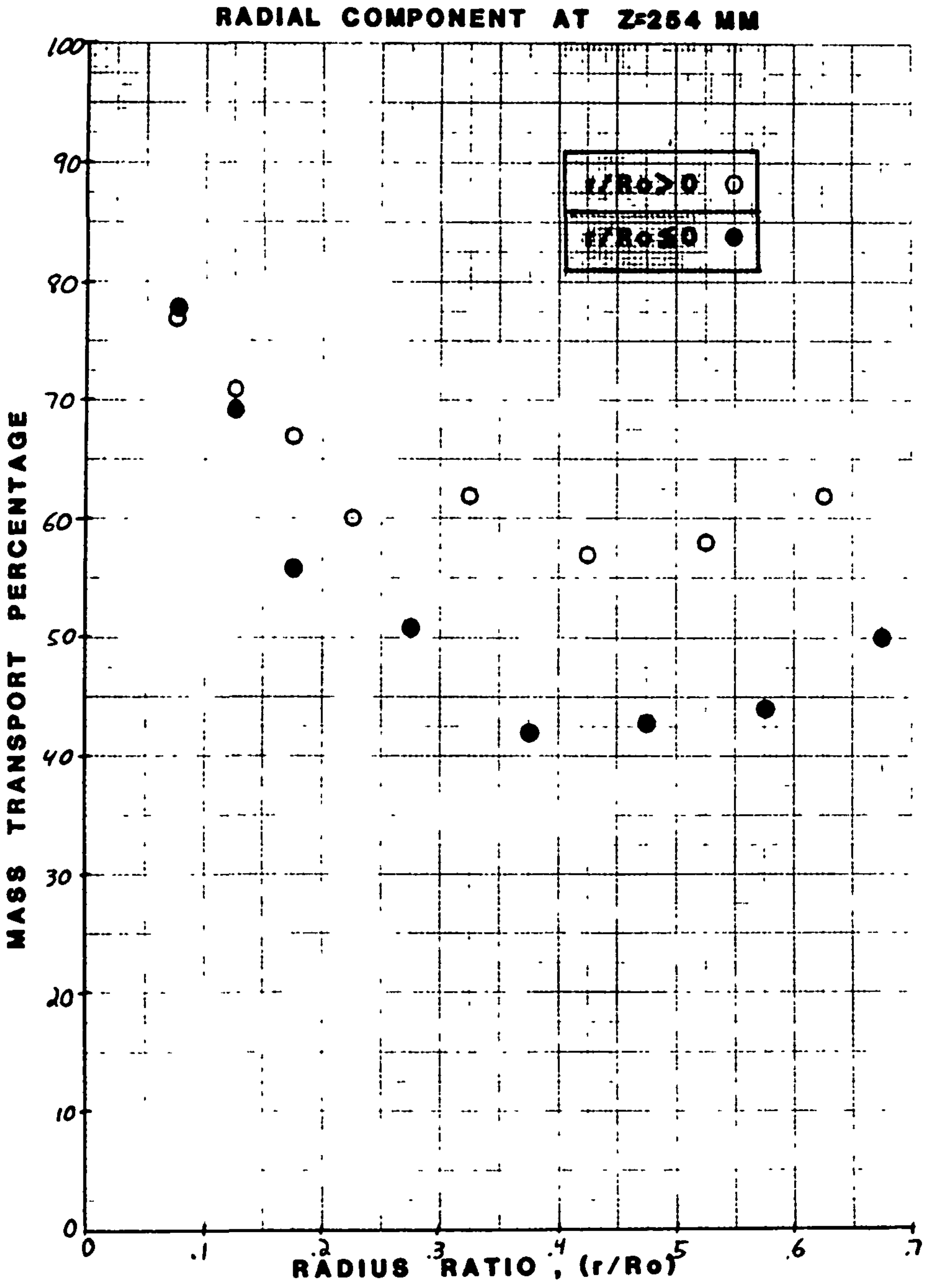
RADIAL COMPONENT AT Z=254 MM
MASS TRANSPORT PERCENTAGE
RADIUS RATIO , (r/Ro)
r/Ro>0
r/Ro≤0
0
10
20
30
40
50
60
70
80
90
100
0
.1
.2
.3
.4
.5
.6
.7

Fig. 39

AXIAL MASS TRANSPORT
LARGE SCALE CONTRIBUTION

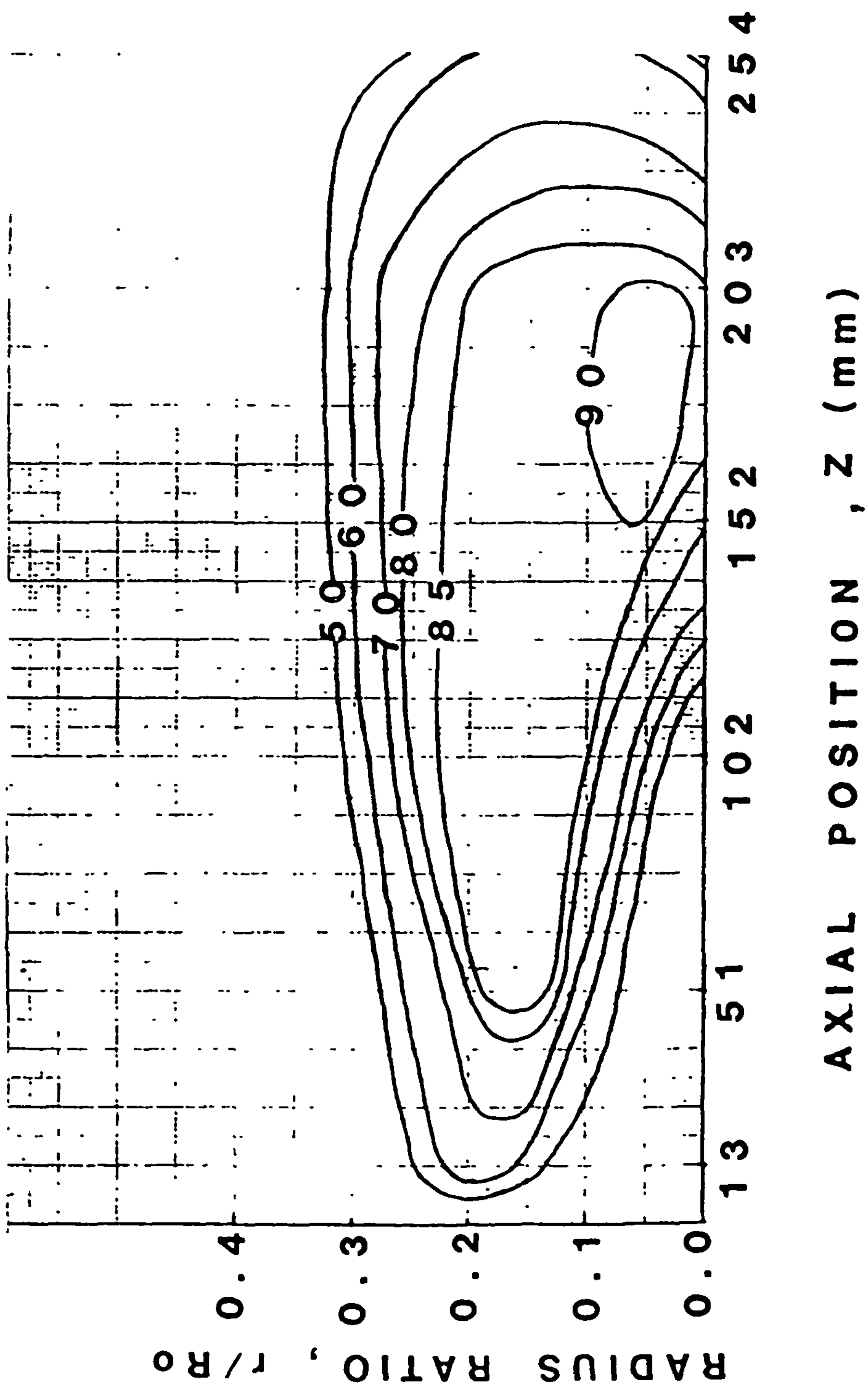

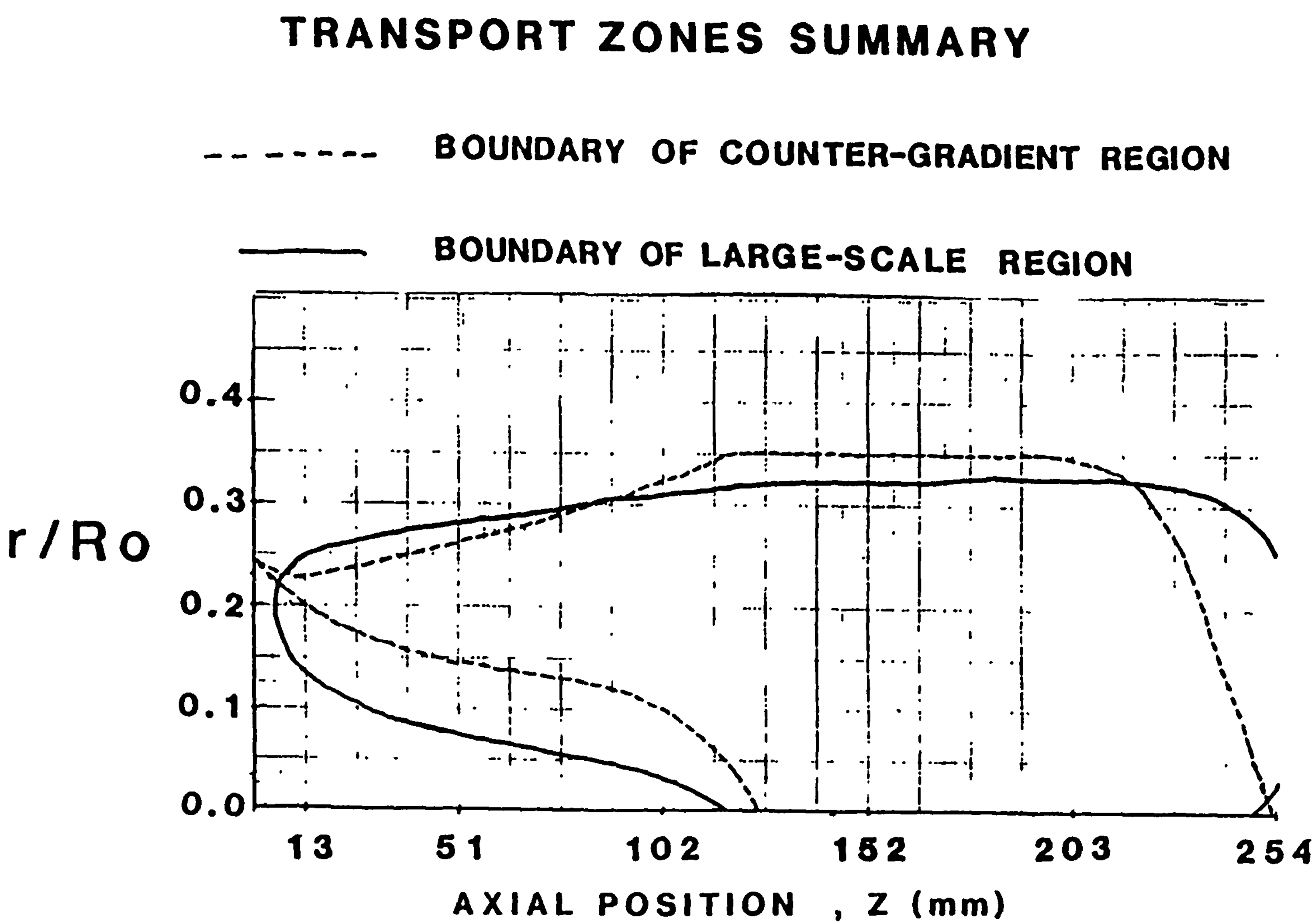
TRANSPORT ZONES SUMMARY
BOUNDARY OF COUNTER-GRADIENT REGION
BOUNDARY OF LARGE-SCALE REGION
r/Ro
0.4
0.3
0.2
0.1
0.0
13
51
102
152
203
254
AXIAL POSITION , Z (mm)

Fig. 40

Fig. 41

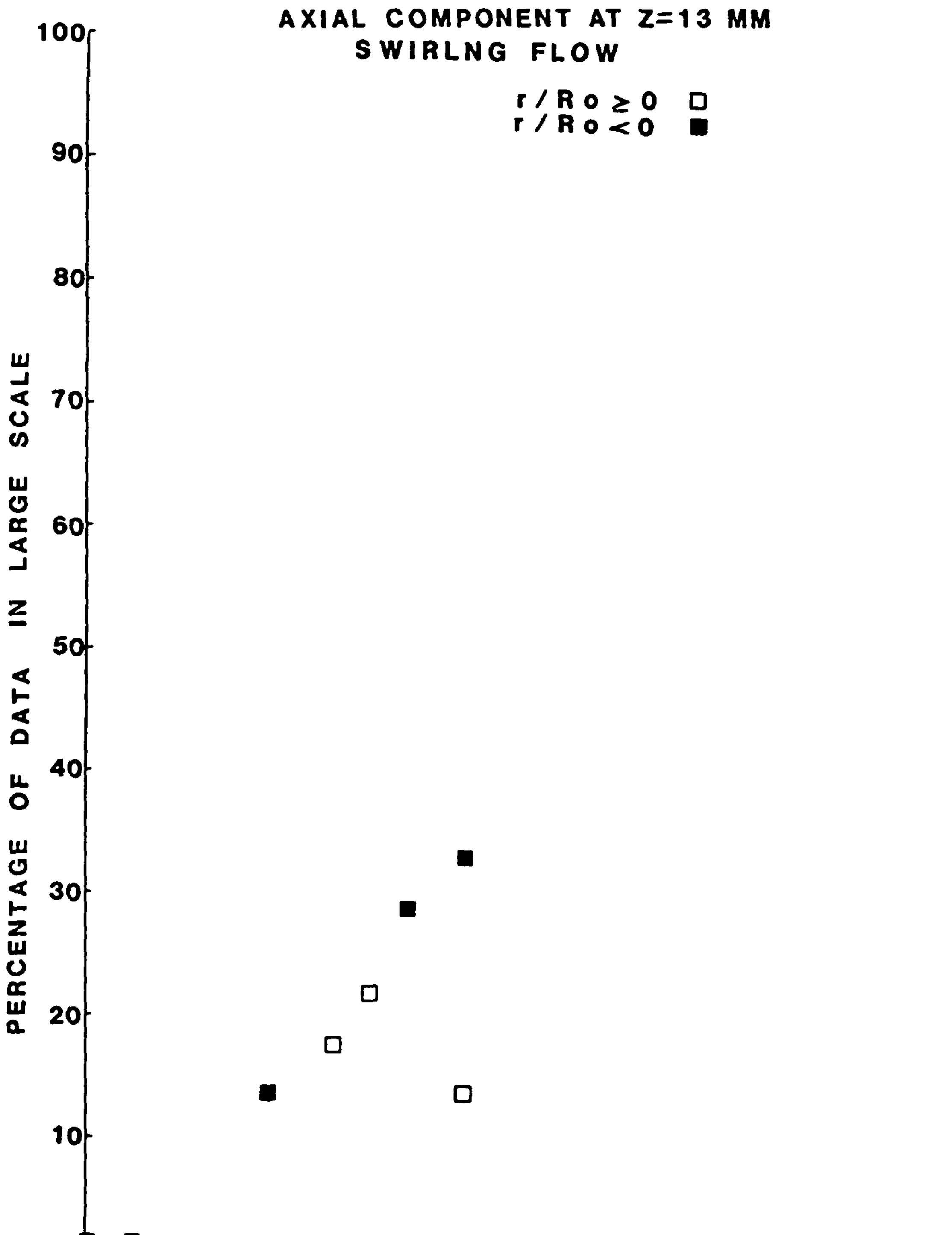

AXIAL COMPONENT AT Z=13 MM
SWIRLNG FLOW
r / R o ≥ 0
r / R o < 0
PERCENTAGE OF DATA IN LARGE SCALE
100
90
80
70
60
50
40
30
20
10
0
0
.1
.2
.3
.4
.5
.6
.7
RADIUS RATIO ,(r/Ro)

Fig. 42

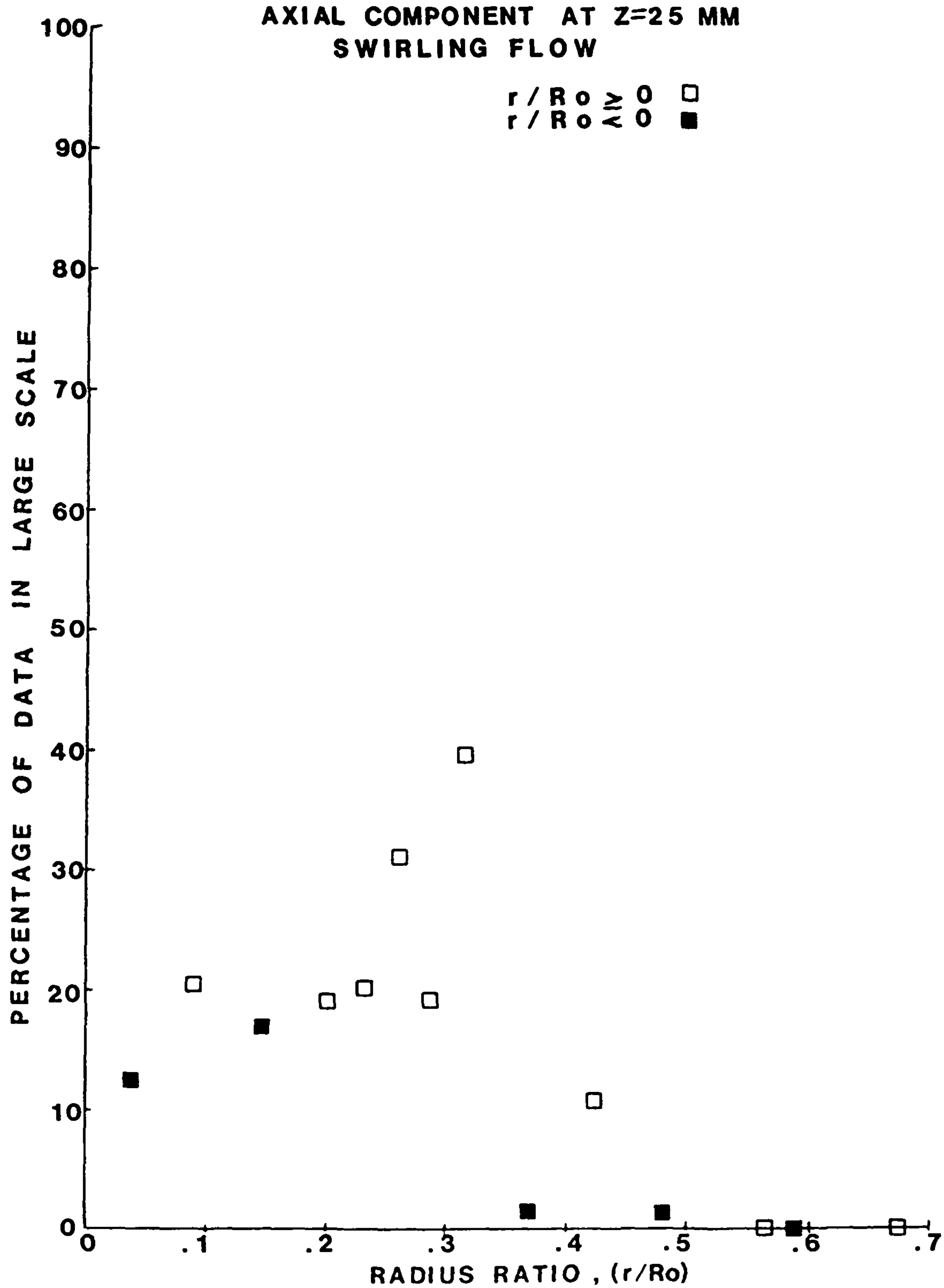
AXIAL COMPONENT AT Z=25 MM
SWIRLING FLOW
r / R o ≥ 0
r / R o < 0
PERCENTAGE OF DATA IN LARGE SCALE
100
90
80
70
60
50
40
30
20
10
0
0
.1
.2
.3
.4
.5
.6
.7
RADIUS RATIO , (r/Ro)

Fig. 43

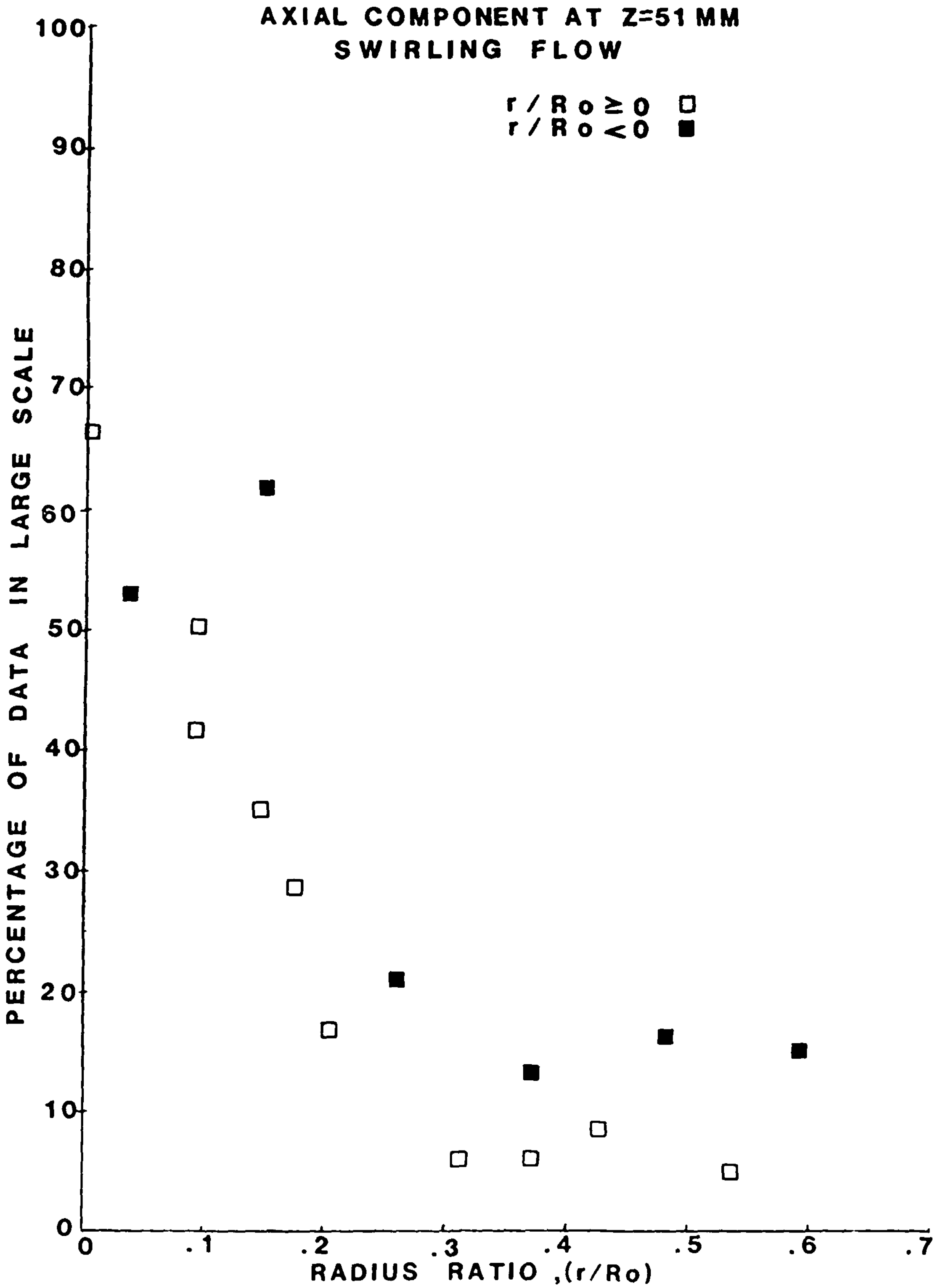
AXIAL COMPONENT AT Z=51 MM
SWIRLING FLOW
r / R o ≥ 0
r / R o < 0
PERCENTAGE OF DATA IN LARGE SCALE
100
90
80
70
60
50
40
30
20
10
0
0
.1
.2
.3
.4
.5
.6
.7
RADIUS RATIO ,(r/Ro)

Fig. 44

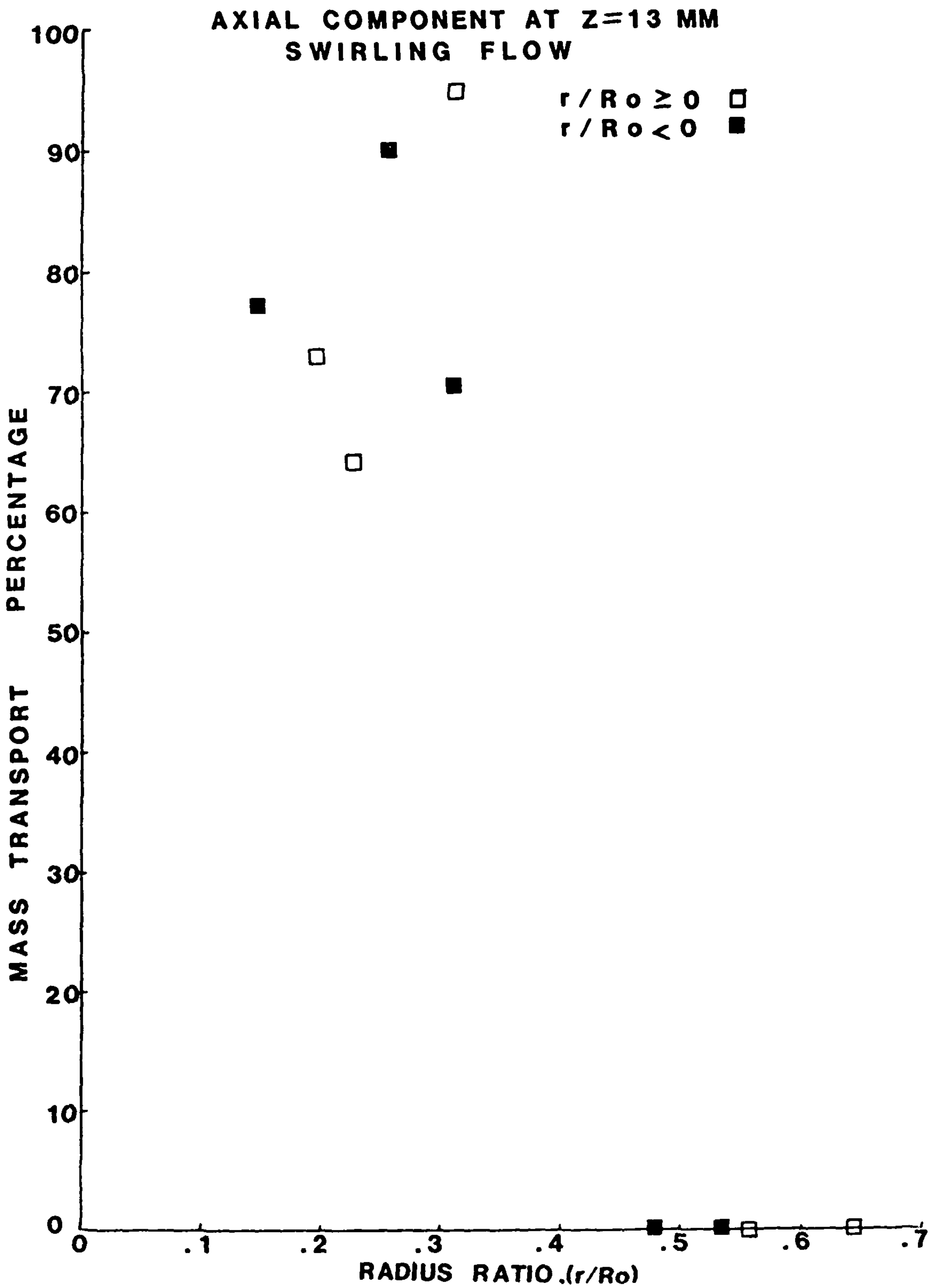
AXIAL COMPONENT AT Z=13 MM
SWIRLING FLOW
r/Ro ≥ 0
r/Ro < 0
MASS TRANSPORT PERCENTAGE
100
90
80
70
60
50
40
30
20
10
0
0
.1
.2
.3
.4
.5
.6
.7
RADIUS RATIO,(r/Ro)

Fig. 45

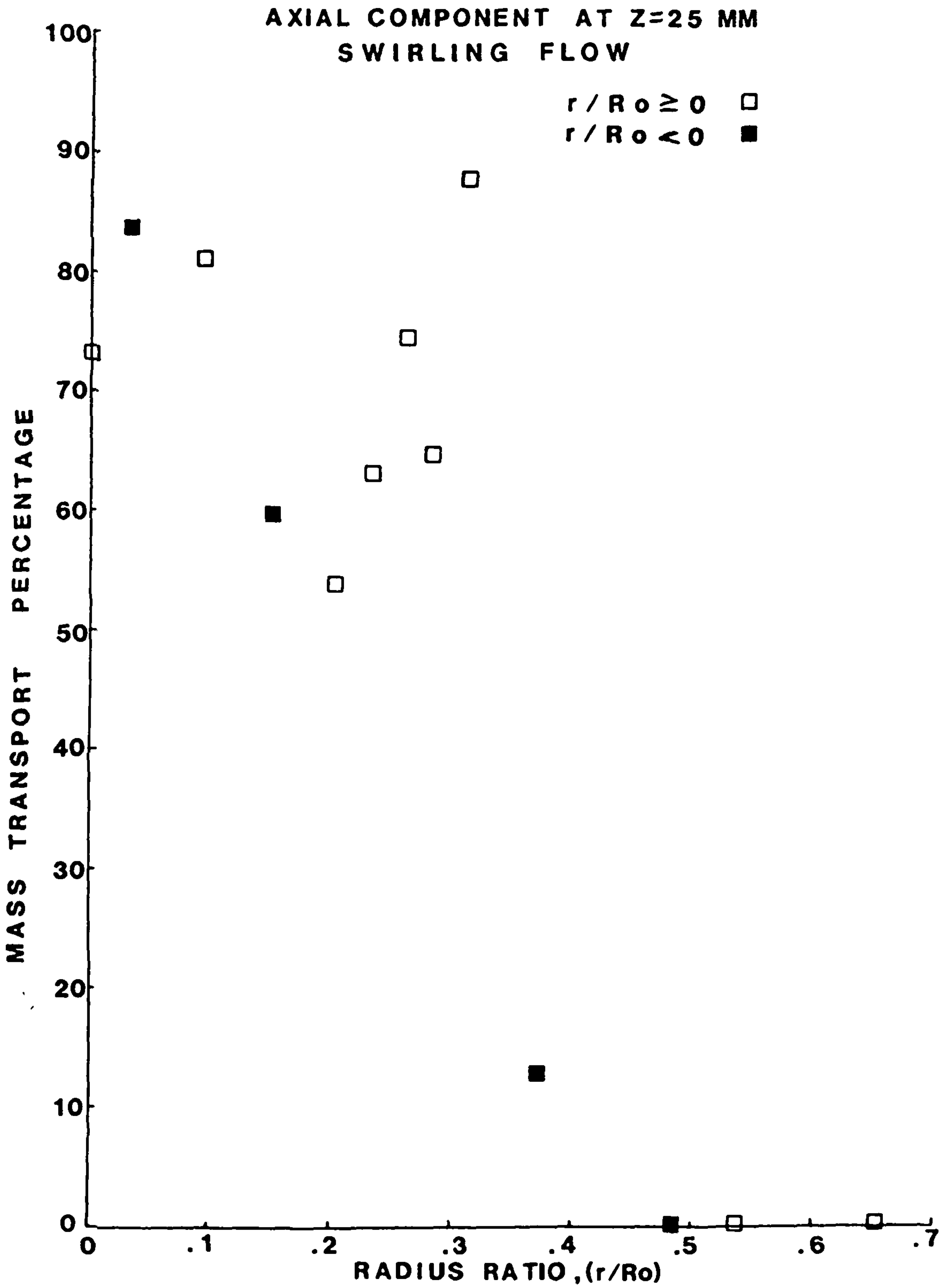

AXIAL COMPONENT AT Z=25 MM
SWIRLING FLOW
r/Ro ≥ 0
r/Ro < 0
MASS TRANSPORT PERCENTAGE
RADIUS RATIO, (r/Ro)
100
90
80
70
60
50
40
30
20
10
0
0
.1
.2
.3
.4
.5
.6
.7

Fig. 46

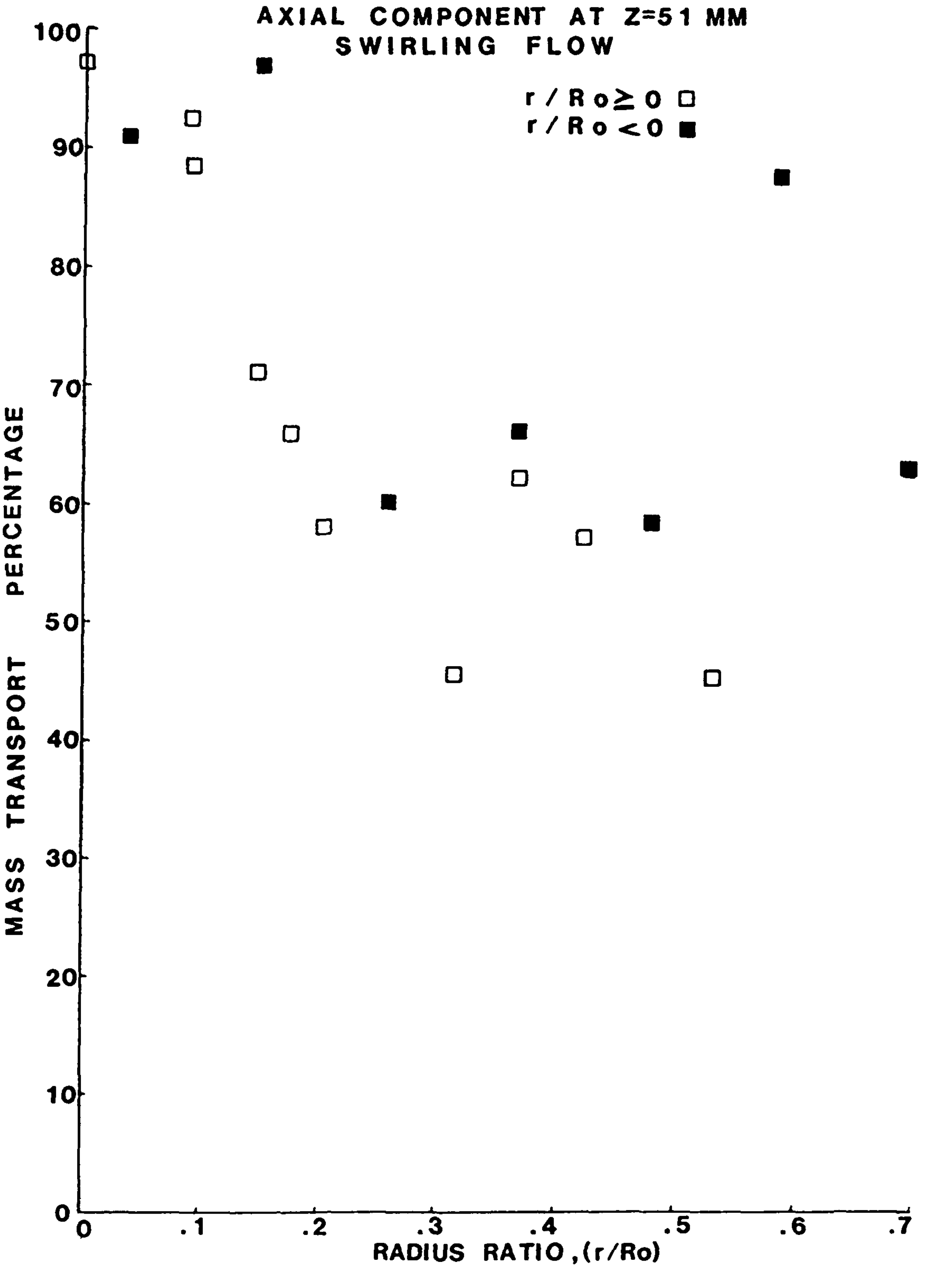
AXIAL COMPONENT AT Z=51 MM
SWIRLING FLOW
r/Ro≥0
r/Ro<0
MASS TRANSPORT PERCENTAGE
100
90
80
70
60
50
40
30
20
10
0
0
.1
.2
.3
.4
.5
.6
.7
RADIUS RATIO,(r/Ro)

Fig. 47

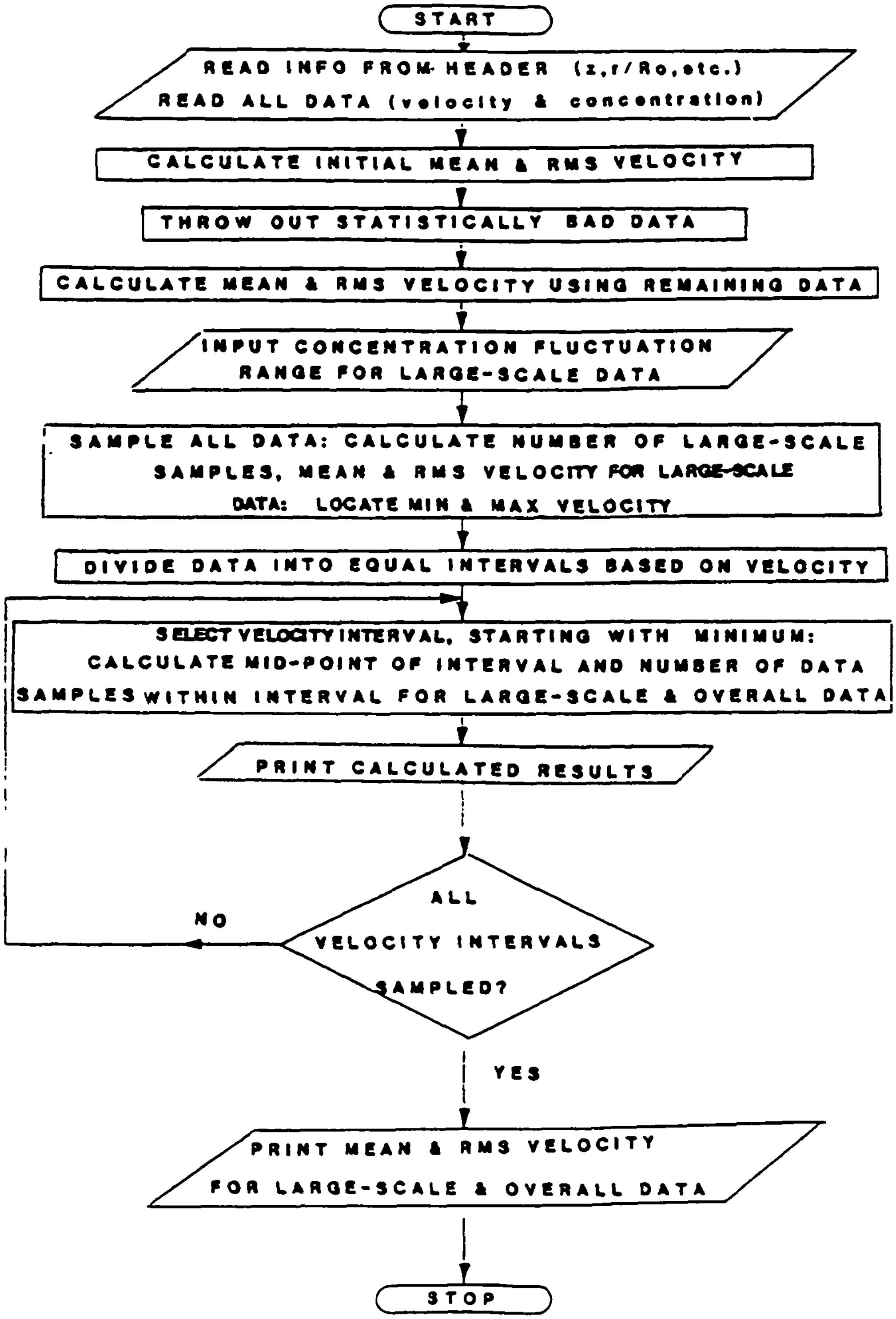
START
READ INFO FROM HEADER (z,r/Ro,etc.)
READ ALL DATA (velocity & concentration)
CALCULATE INITIAL MEAN & RMS VELOCITY
THROW OUT STATISTICALLY BAD DATA
CALCULATE MEAN & RMS VELOCITY USING REMAINING DATA
INPUT CONCENTRATION FLUCTUATION RANGE FOR LARGE-SCALE DATA
SAMPLE ALL DATA: CALCULATE NUMBER OF LARGE-SCALE SAMPLES, MEAN & RMS VELOCITY FOR LARGE-SCALE DATA: LOCATE MIN & MAX VELOCITY
DIVIDE DATA INTO EQUAL INTERVALS BASED ON VELOCITY
SELECT VELOCITY INTERVAL, STARTING WITH MINIMUM: CALCULATE MID-POINT OF INTERVAL AND NUMBER OF DATA SAMPLES WITHIN INTERVAL FOR LARGE-SCALE & OVERALL DATA
PRINT CALCULATED RESULTS
ALL VELOCITY INTERVALS SAMPLED?
NO
YES
PRINT MEAN & RMS VELOCITY FOR LARGE-SCALE & OVERALL DATA
STOP

Fig. 48

```
PROB 51,15
 SUCCESSFUL  TEMP) RESTORE RUN51P15 AS (TP15)
 CANCELLED: JDNAME RMOS      UNKNOWN


    DATA OUTPUT FOR RUN 51 POINT 15


RADIAL  VELOCITY VS CONCENTRATION
Z=152 MM AND R/RO= 0.324

  SELECT MINIMUM POSITIVE AND NEGATIVE CONCENTRATION FLUCTUATION
TO BE INCLUDED IN LARGE SCALE STRUCTURE USING F4.1 FORMAT:
 CPPOS=
0.2
 CPNEG=
-1.0

NUMBER OF SAMPLES: ORIGINAL=999 GOOD DATA=984  LARGE SCALE= 76
```

		NUMBER OF SAMPLES	
I	VMID(M/S)	L.S.	OVERALL
1	-0.522	0	2
2	-0.500	0	2
3	-0.478	0	2
4	-0.456	0	3
5	-0.434	0	2
6	-0.412	0	9
7	-0.390	0	1
8	-0.368	0	8
9	-0.346	0	9
10	-0.324	0	6
11	-0.302	0	8
12	-0.280	0	12
13	-0.258	0	15
14	-0.236	0	24
15	-0.214	0	17
16	-0.192	2	22
17	-0.170	0	31
18	-0.148	0	24
19	-0.126	2	36
20	-0.104	0	27
21	-0.082	0	35
22	-0.059	1	27
23	-0.037	2	47
24	-0.015	3	46
25	0.007	3	53
26	0.029	2	48
27	0.051	1	55
28	0.073	5	53
29	0.095	2	46
30	0.117	4	57
31	0.139	0	25
32	0.161	7	45
33	0.183	1	16
34	0.205	5	38
35	0.227	5	31
36	0.249	1	12
37	0.271	5	24
38	0.293	5	18
39	0.315	4	10
40	0.337	6	10
41	0.359	5	9
42	0.381	0	1
43	0.403	0	3
44	0.425	1	2
45	0.447	1	4
46	0.470	2	4
47	0.492	0	2
48	0.514	1	2
49	0.536	0	0
50	0.558	0	1

```
MEAN VELOCITY(M/S): OVERALL= 0.018 : LARGE SCALE= 0.188
RMS VELOCITY(M/S): OVERALL= 0.184 : LARGE SCALE= 0.155
CBAR= 0.087  CPPOS= 0.200   CPNEG=-1.000
 TERMINATED: STOP
```

Fig. 49

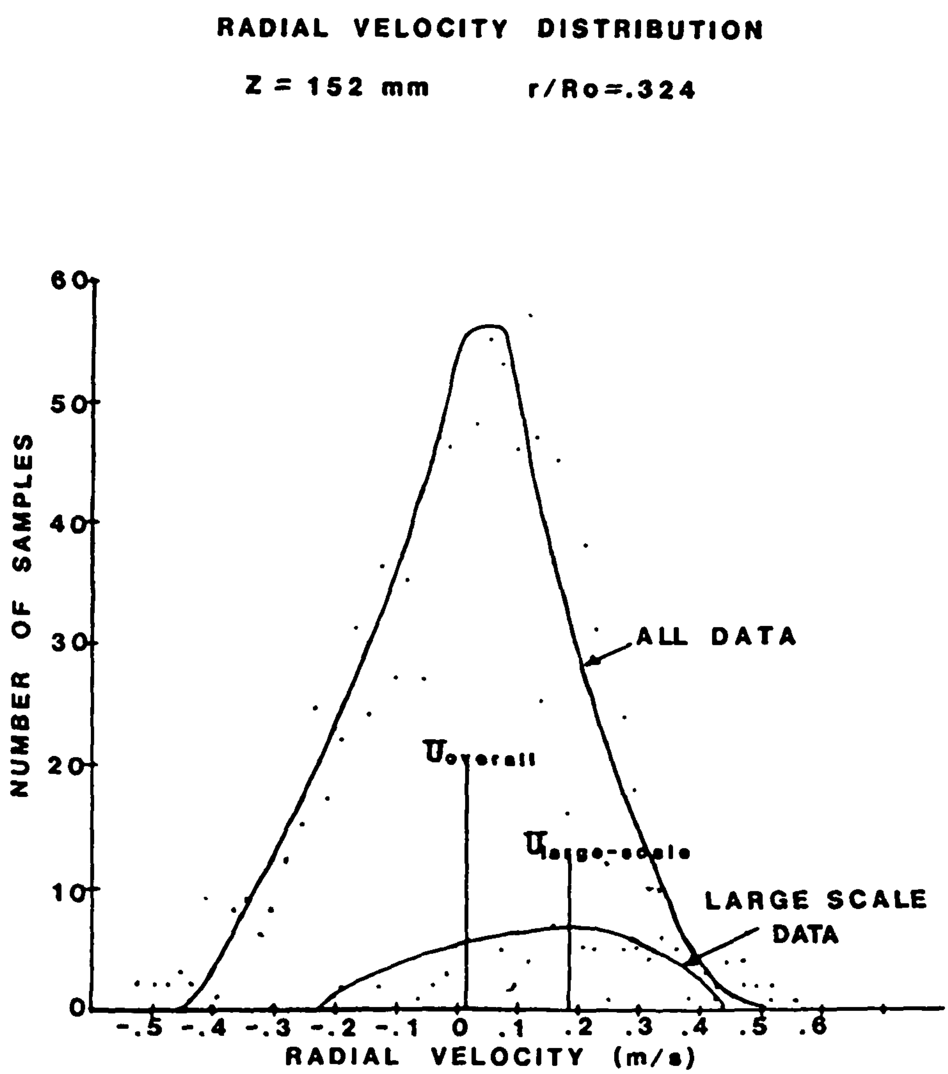
RADIAL VELOCITY DISTRIBUTION
Z = 152 mm
r/Ro=.324
60
50
40
30
20
10
0
NUMBER OF SAMPLES
ALL DATA
$\overline{U}_{overall}$
$\overline{U}_{large-scale}$
LARGE SCALE DATA
-.5 -.4 -.3 -.2 -.1 0 .1 .2 .3 .4 .5 .6
RADIAL VELOCITY (m/s)

Fig. 50

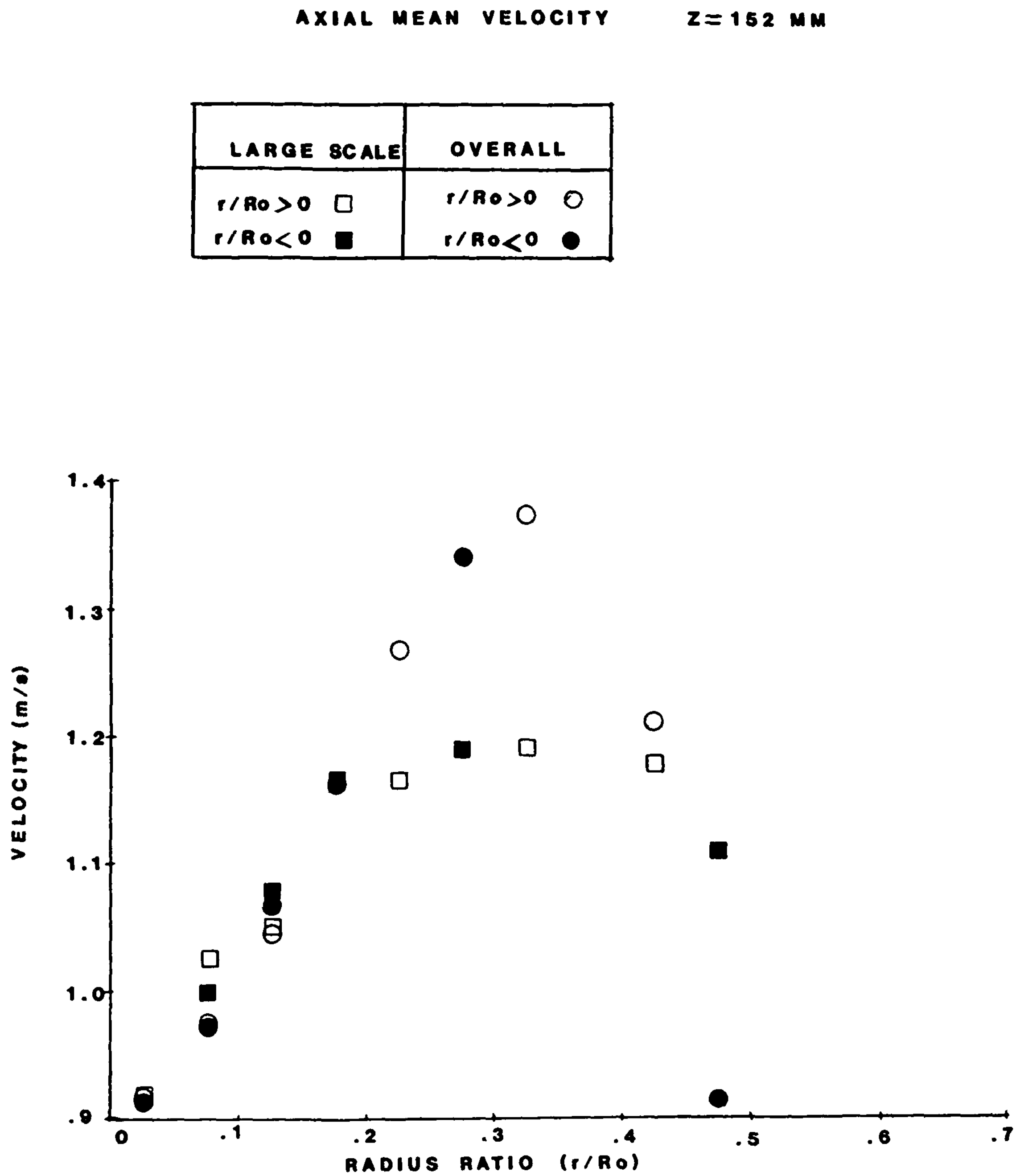
AXIAL MEAN VELOCITY Z=152 MM
LARGE SCALE
OVERALL
r/Ro>0
r/Ro<0
r/Ro>0
r/Ro<0
VELOCITY (m/s)
1.4
1.3
1.2
1.1
1.0
.9
0
.1
.2
.3
.4
.5
.6
.7
RADIUS RATIO (r/Ro)

Fig. 51

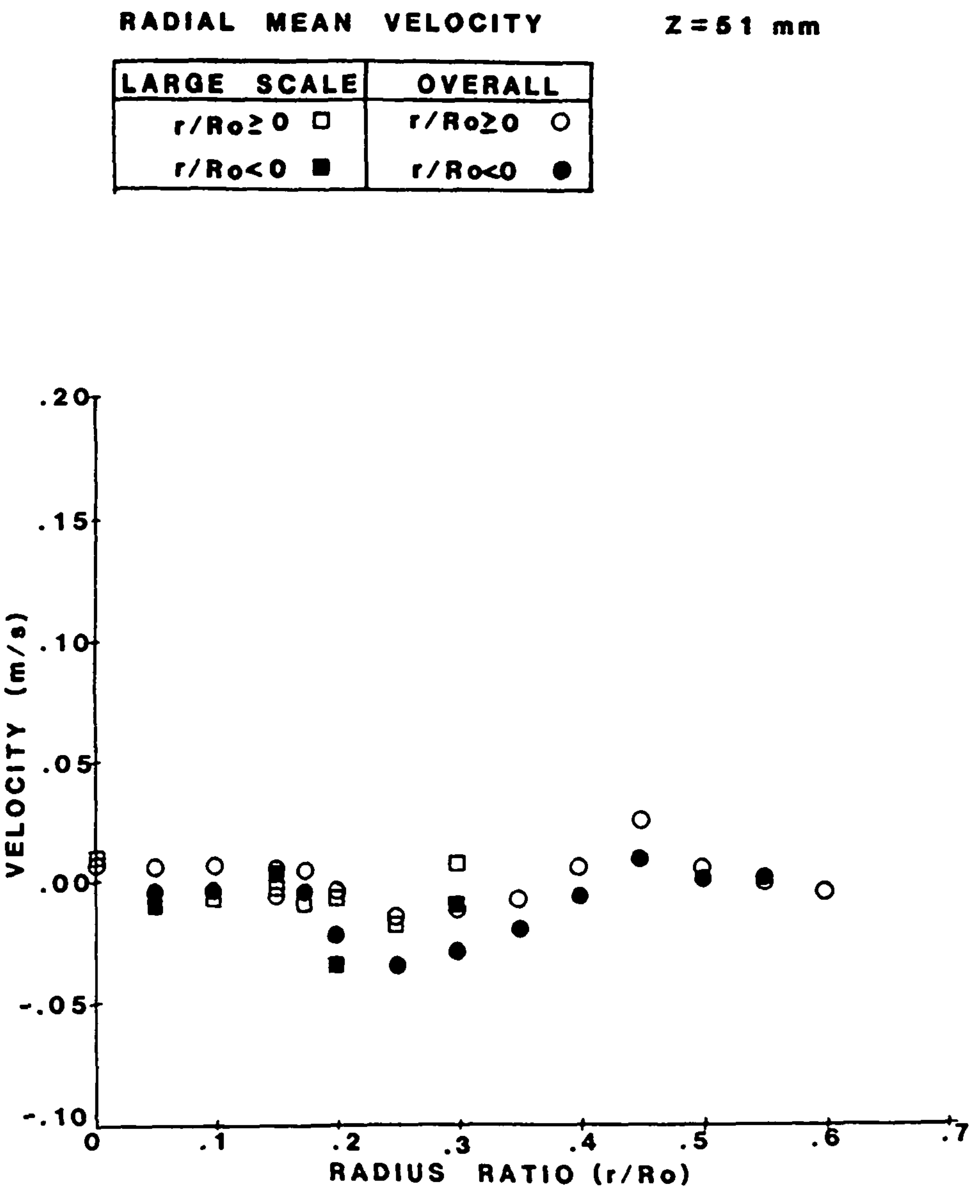
RADIAL MEAN VELOCITY
Z=51 mm
LARGE SCALE
OVERALL
r/Ro≥0
r/Ro<0
.20
.15
.10
.05
.00
-.05
-.10
VELOCITY (m/s)
0
.1
.2
.3
.4
.5
.6
.7
RADIUS RATIO (r/Ro)

Fig. 52

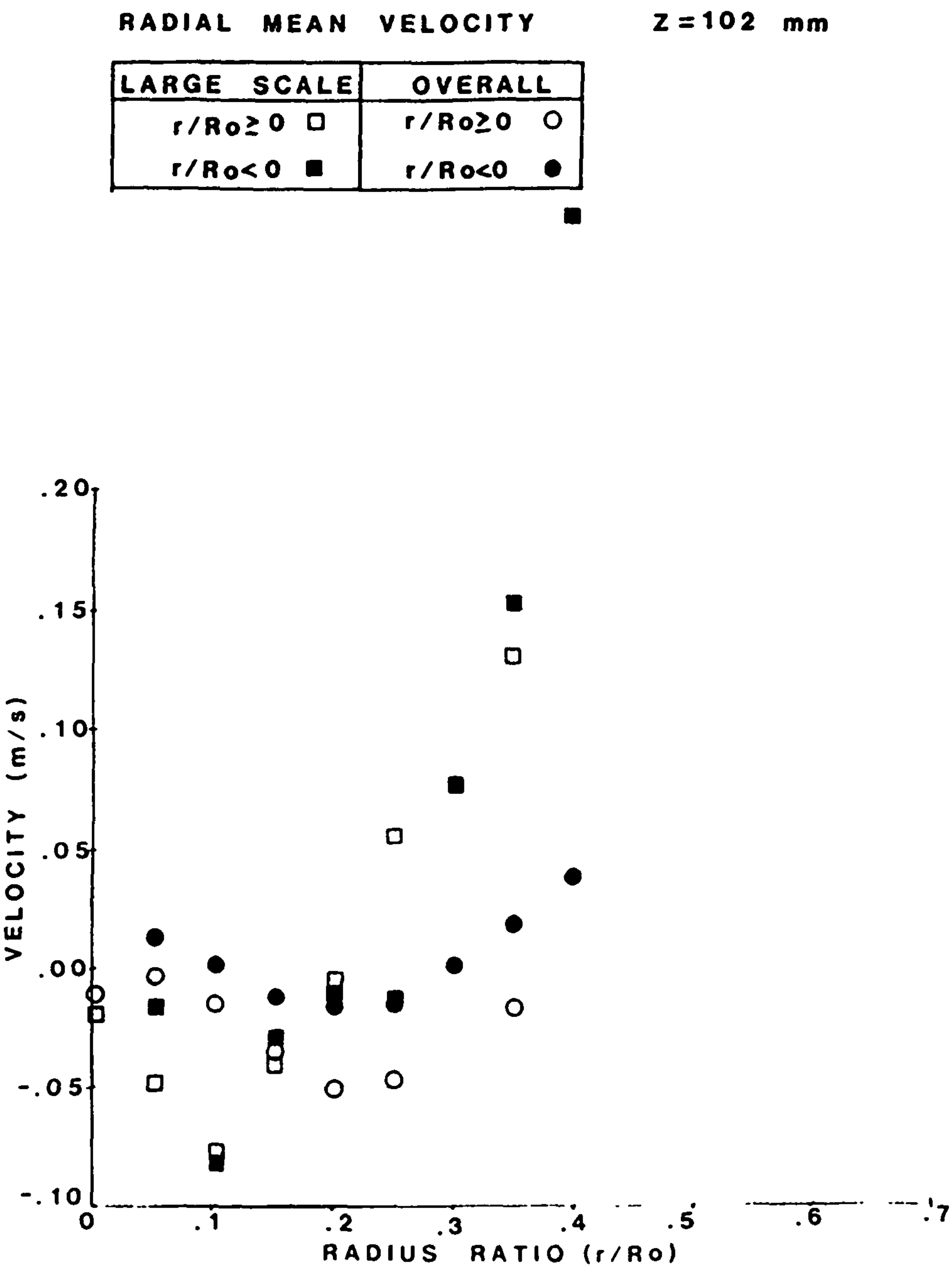

RADIAL MEAN VELOCITY
Z = 102 mm
LARGE SCALE
OVERALL
r/Ro ≥ 0
r/Ro < 0
r/Ro ≥ 0
r/Ro < 0
VELOCITY (m/s)
.20
.15
.10
.05
.00
-.05
-.10
0
.1
.2
.3
.4
.5
.6
.7
RADIUS RATIO (r/Ro)

Fig. 53

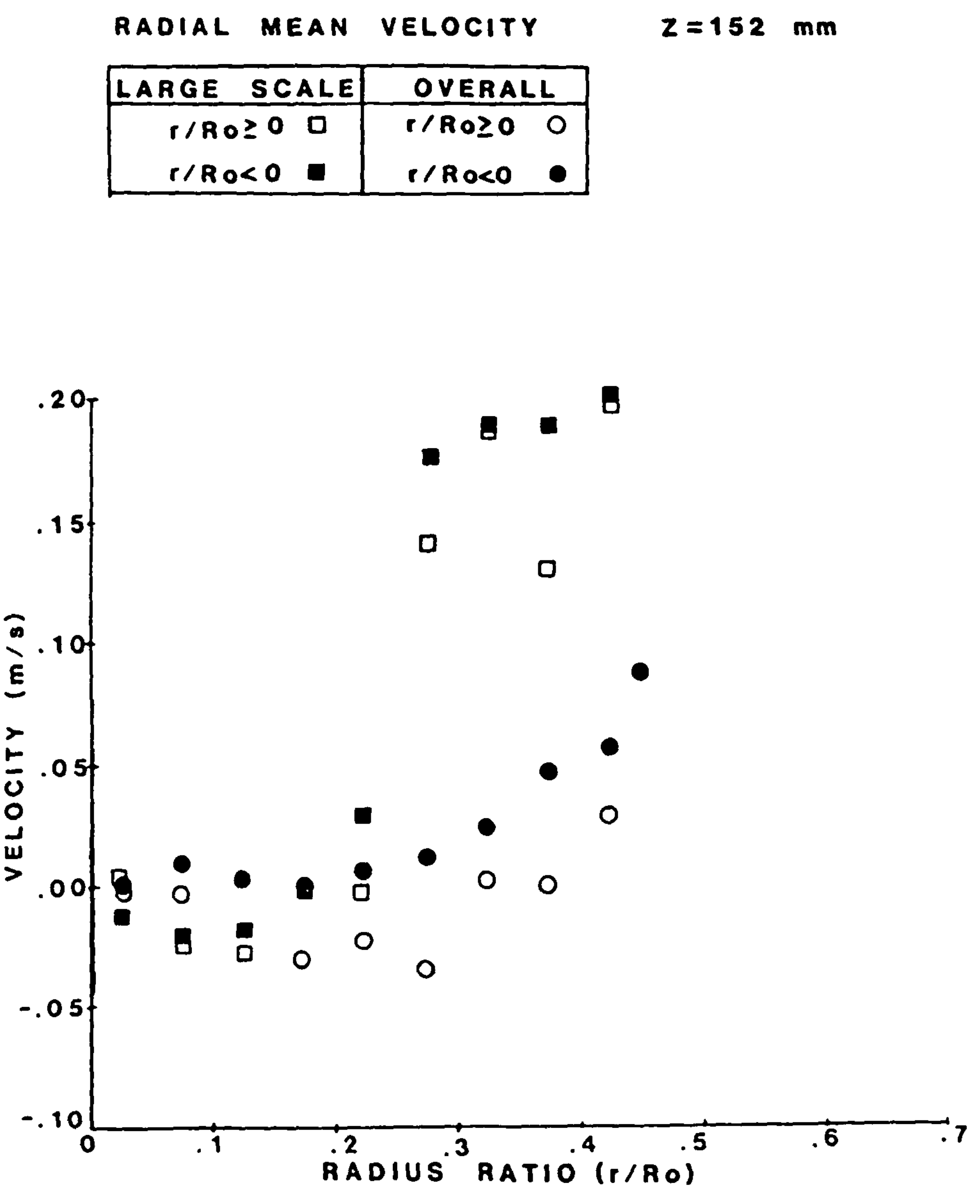

RADIAL MEAN VELOCITY Z=152 mm
LARGE SCALE
r/Ro≥0
r/Ro<0
OVERALL
r/Ro≥0
r/Ro<0
VELOCITY (m/s)
.20
.15
.10
.05
.00
-.05
-.10
0
.1
.2
.3
.4
.5
.6
.7
RADIUS RATIO (r/Ro)

Fig. 54

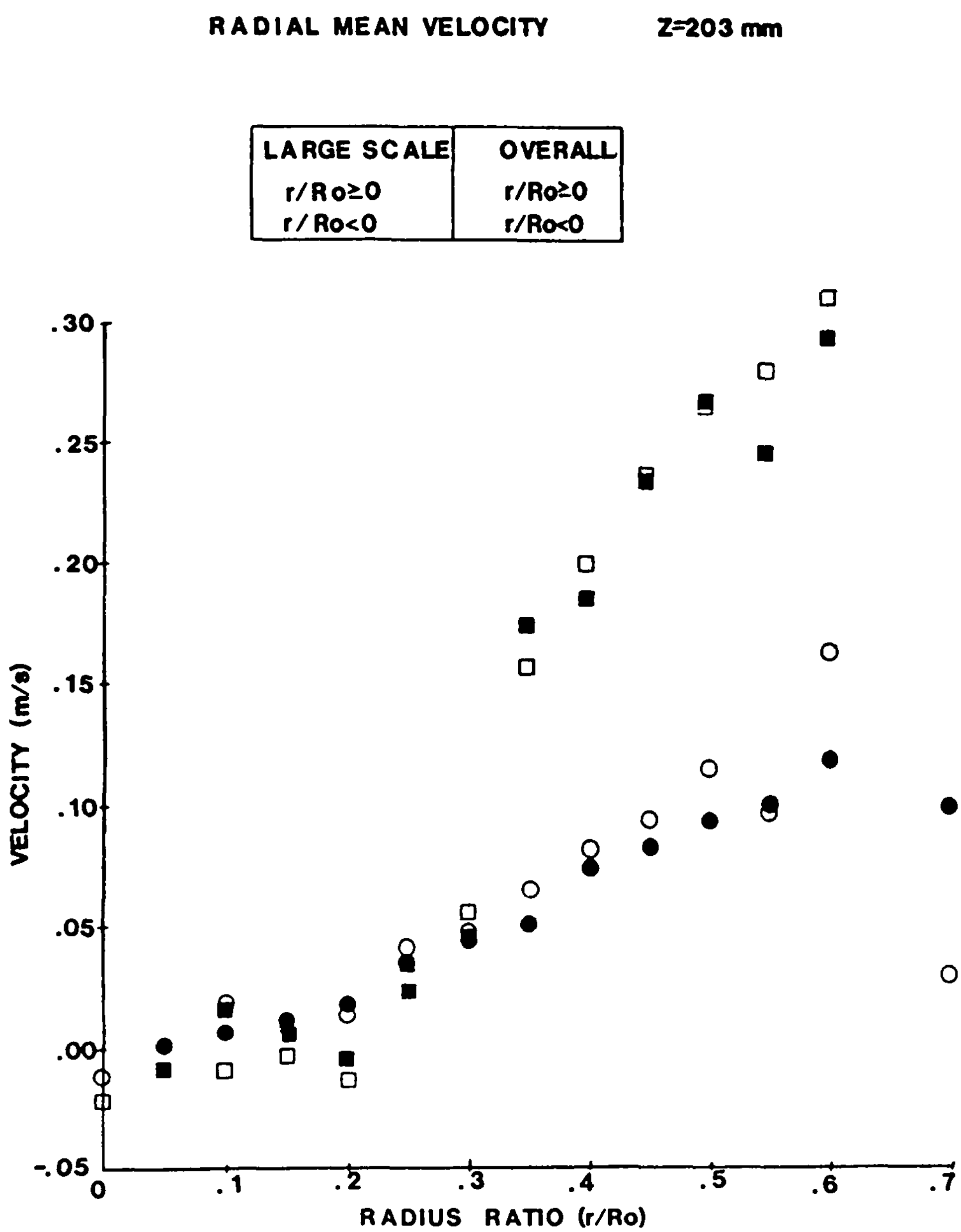

RADIAL MEAN VELOCITY
Z=203 mm
LARGE SCALE
r/Ro≥0
r/Ro<0
OVERALL
r/Ro≥0
r/Ro<0
VELOCITY (m/s)
.30
.25
.20
.15
.10
.05
.00
-.05
0
.1
.2
.3
.4
.5
.6
.7
RADIUS RATIO (r/Ro)

Fig. 55

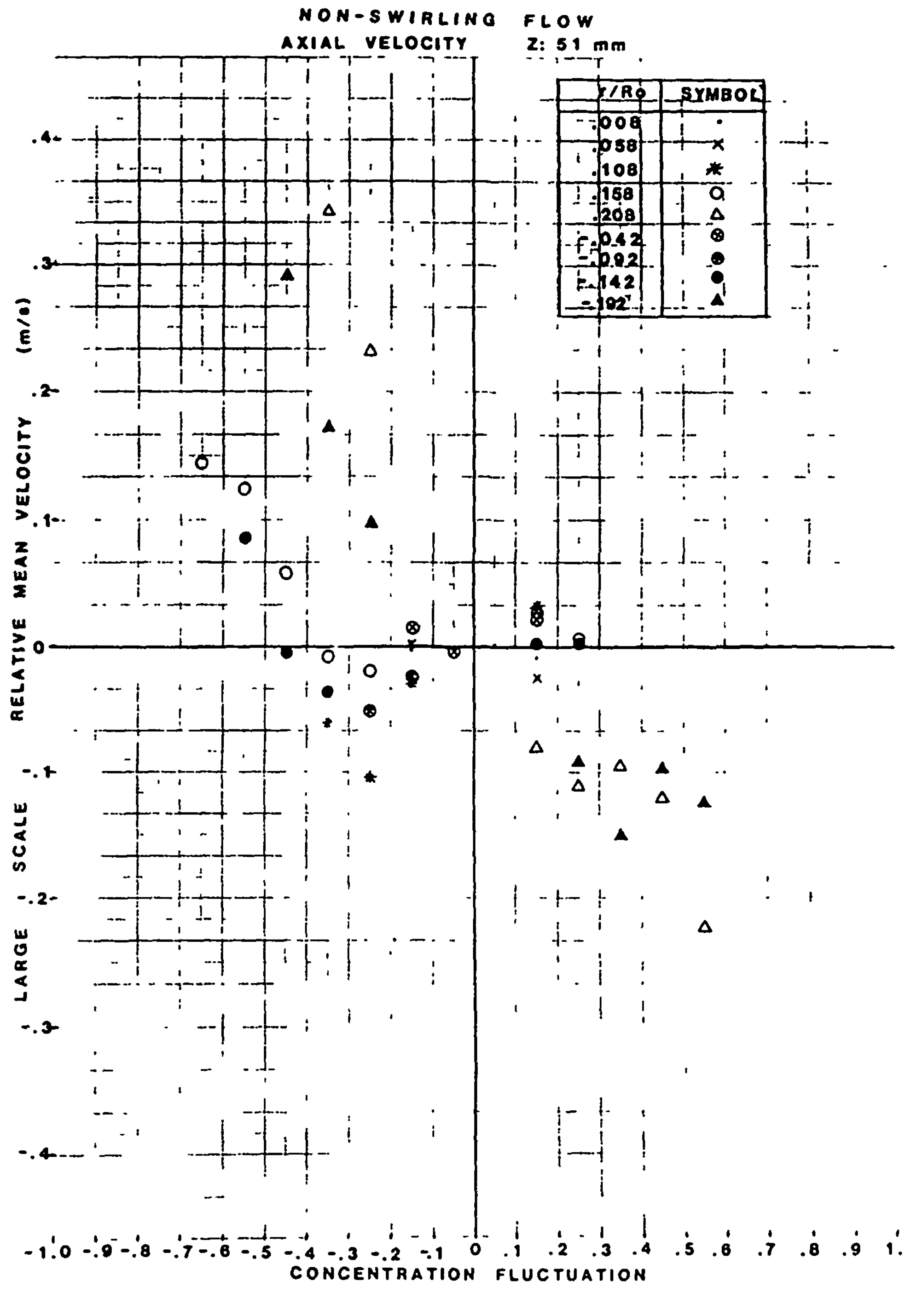
NON-SWIRLING FLOW
AXIAL VELOCITY Z: 51 mm
r/Ro SYMBOL
.008
.058
.108
.158
.208
-.042
-.092
-.142
-.192
LARGE SCALE RELATIVE MEAN VELOCITY (m/s)
.4
.3
.2
.1
0
-.1
-.2
-.3
-.4
-1.0 -.9 -.8 -.7 -.6 -.5 -.4 -.3 -.2 -.1 0 .1 .2 .3 .4 .5 .6 .7 .8 .9 1.
CONCENTRATION FLUCTUATION

Fig. 56

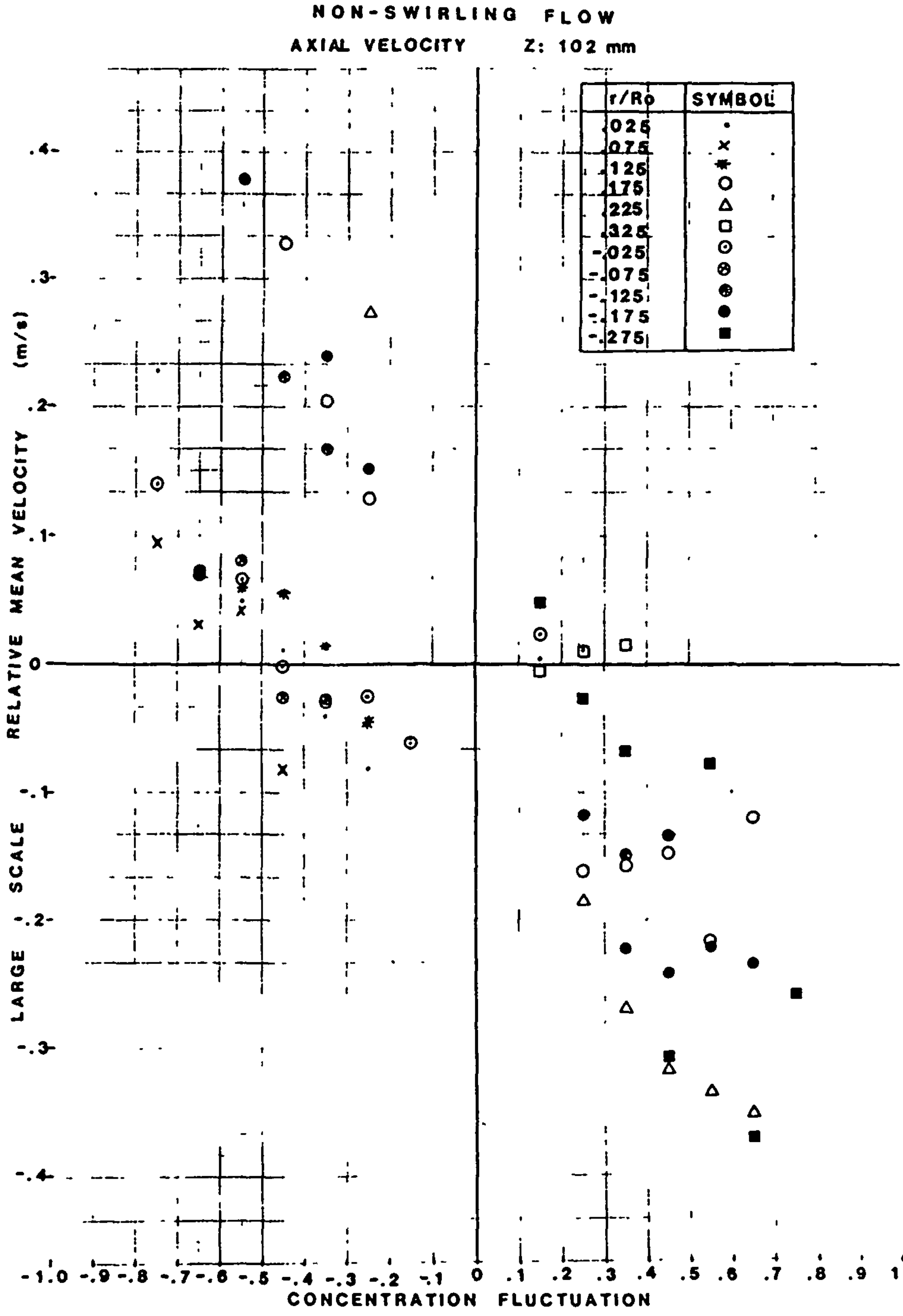
NON-SWIRLING FLOW
AXIAL VELOCITY Z: 102 mm
r/Ro
SYMBOL
.025
.075
.125
.175
.225
.325
-.025
-.075
-.125
-.175
-.275
LARGE SCALE RELATIVE MEAN VELOCITY (m/s)
.4
.3
.2
.1
0
-.1
-.2
-.3
-.4
-1.0 -.9 -.8 -.7 -.6 -.5 -.4 -.3 -.2 -.1 0 .1 .2 .3 .4 .5 .6 .7 .8 .9 1.
CONCENTRATION FLUCTUATION

ORIGINAL PAGE IS
OF POOR QUALITY

Fig. 57

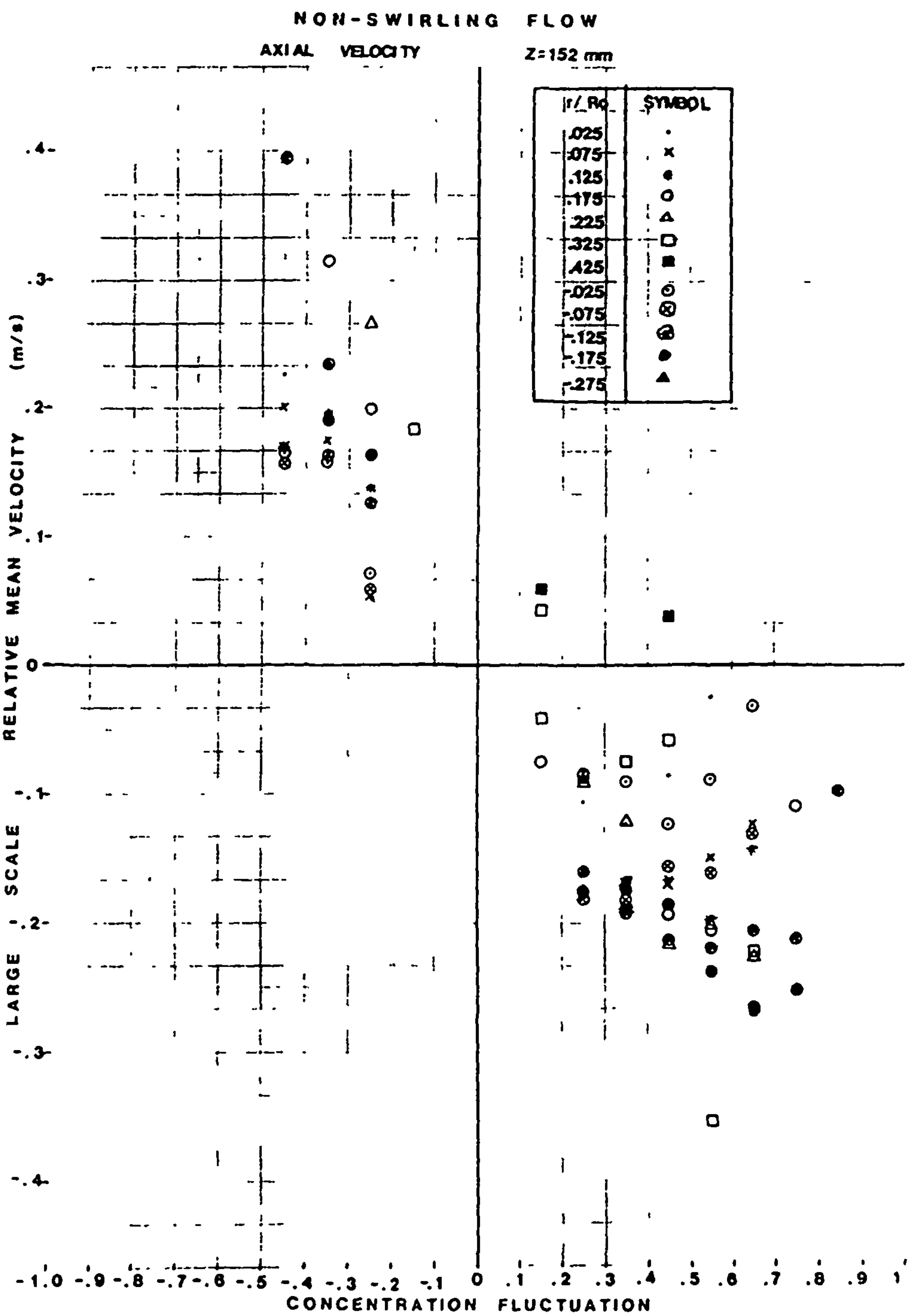

REFERENCES

1. Gerstein, M. (Ed.), "Fundamentals of Gas turbine Combustion". NASA Conference Publication 2087, 1979.

2. Hudson, D.W., "Combustion Modelling Needs for the 80's". AIAA Preprint, 80-1288.

3. Mellor, A.M., "Turbulent Combustion Interaction Models for PrActical High Intensity Combustors". Seventeenth Symposium on Combustion, pg. 377, Combustion Institute, 1979.

4. Johnson, B.V., and Bennett, J.C., "Mass and Momentum Turbulent Transport Experiments with Confined Coaxial Jet". Fourth Symposium on Turbulent Shear Flows, Karlsruhe, Germany, September, 1983.

5. Morganthaler, J.H., "Turbulent Mixing and Reacting flow Characterization". Fluid Mechanics of Combustion, pp. 21-34, ASME, N.Y., 1974.

6. Johnson, B.V., and Bennett, J.C., "Velocity and Concentration Characteristics and Their Cross Correlations for Coaxial Jets in a Confined Sudden Expansion, Part I: Experiments". Proceedings of ASME Symposium on the Fluid Mechanicas of Combustions Systems, Boulder, CO, June, 1981.

7. Syed, S.A., and Sturgess, G.J., "Velocity and Concentration Characteristics and Their Correlations for Coaxial Jets in a Confined Sudden Expansion, Part II: Predictions". Proceedings of ASME Symposium on the Fluid Mechanics of Combustion Systems, Boulder, CO, June, 1981.

8. Habib, M.A., and Whitelaw, J.H., "Velocity Characteristics of a Confined Coaxial Jet". ASME Journal of Fluids Engineering, Vol. 101 (December 1979), pg. 521-529.

9. Habib, M.A., and Whitelaw, J.H., "Velocity Characteristics of Confined Coaxial Jets With and Without Swirl". ASME Journal of Fluids Engineering, Vol. 102 (March 1980), pg. 47-53.

10. Johnson, B.V., and Bennett, J.C., "Statistical Characteristics of Velocity, Concentration, Mass Transport, and Momentum Transport for Coaxial Jet Mixing in a Confined Duct". Journal of Engineering for Gas Turbines and Power, Vol. 106 (January 1984), pg. 121-127.

11. Johnson, B.V., and Bennett, J.C., "Mass and Momentum Turbulent Transport Experiments with Confined Coaxial Jets", NASA Contractor Report NASA CR-165574, UTCR Report R81-915540-9, November, 1981.

12. Roback, R. and Johnson, B.V., "Mass and Momentum Turbulent Transport Experiments with Confined Coaxial Swirling Jets", NASA Contractor Report CR-168252, UTRC Report R83-915540-26, August, 1983.

13. Schetz, J.A., "Injection and Mixing in Turbulent Flow", Progress in Astronautics and Aeronautics (Vol. 68), Edited by M. Summerfield. New York: AIAA, 1980.

14. Mathieu, J., and Jeandel, D., "Pathological Cases in Turbulent Field and Spectral Approach", Prediction Methods for Turbulent Flows, Edited by W. Kollmann. Washington: Hemisphere Publishing, 1980.

15. Launder, B.E., and Schiestel, R., On the Use of Multiple Time Scales in Modelling Turbulent Flow. C.R.A.S., A, 1978.

16. Borghi, R., "Models of Turbulent Combustion for Numerical Predictions", Prediction Methods for Turbulent Flows, Edited by W. Kollmann. Washington: Hemisphere Publishing, 1980.

17. Roshko, A., "Structures of Turbulent Shear Flows: A New Look". A.I.A.A. Journal, Vol. 14 (October 1976), pg. 1349-1357.

18. Cantwell, B.J., "Organized Motion in Turbulent Flow", Annual Review of Fluid Mehchanics, Edited by M. Van Dyke, J.V. Wehausen, and J.L. Lumley, Vol. 13, pg. 457-515. Palo Alto, CA: Annual Reviews, Inc., 1981.

19. Davies, P.O.A.L., and Yule, A.J., "Coherent Structures in Turbulence". Journal of fluid Mechanics, Vol. 69 (1975), pg. 513-537.

20. Yule, A.J., "Investigations of Eddy Coherence in Jet Flows", in The Role of Cherent Structures in Modelling Turbulence and Mixing, Lecture Notes in Physics, Edited by J. Jiminez, Vol. 136, pg. 188-207. Springer Verlag, Berlin/Heidelberg/New York, 1980.

21. Brown, G.L., and Roshko, A., "On Density Effects and Large Structure in Turbulent Mixing Layers", Journal of Fluid Mechanics, Vol. 64 (1974), pg. 775-816.

22. Winant, C., and Browand, F., "Vortex Pairing: The Mechanism of Turbulent Mixing - Layer Growth at Moderate Reynolds Number". Journal of Fluid Mechanics, Vol. 63 (1974), pg. 237-255.

23. Dimotakis, P., and Brown, G.L., "The Mixing Layer at High Reynolds Number: Large-Structure Dynamics and Entrainment". Journal of Fluid Mechanics, Vol. 78 (1976), pg. 535-560.

24. Blackwelder, R.F., and Kaplan, R.E., "On the Wall Structure of the Turbulent Boundary Layer". Journal of Fluid Mechanics, Vol. 76 (1976), pg. 89-112

25. Lu, S.S., and Willmarth, W.W., "Measurements of the Structure of the Reynolds Stress in a Turbulent Boundary Layer". Journal of Fluid Mechanics, Vol. 60 (1973), pg. 481-511.

26. Corino, E.R., and Brodkey, R.S., "A Visual Investigation of the Wall Region in Turbulent flow". Journal of Fluid Mechanics, Vol. 37 (1969), pg. 1-30.

27. Kovasznay, L.S.G., Kibens, V., and Blackwelder, R., "Large-Scale Motion in the Intermittent Region of a Turbulent Boundary Layer". Journal of Fluid Mechanics, Vol. 41 (1970), pg. 283-325.

28. Mathieu, J., and Charnay, G., "Experimental Methods in Turbulent Structure Research", in The Role of Coherent Structures in Modelling Turbulence and Mixing, Lecture Notes in Physics, Edited by J. Jiminez, Vol. 103, pg. 146-187. Springer Verlag, Berlin/Heidelberg/New York, 1980.

29. Schlicting, H., Boundary Layer Theory, Trans. by J. Kestin (New York: McGraw Hill, 1979), seventh edition, Ch. 24.

30. Riley, J.J., and Metcalfe, R.W., "Direct Simulations of Chemically Reacting Turbulent Mixing Layers", NASA Contractor Report 174640, March 1984.

APPENDIX A

HOLD.CV

```
      DIMENSION V(1000),C(1000),VN(1000)
      REAL*8 VEL
      REAL NEWBAR,NEWRMS
      INTEGER RUN,POINT,Z
      VBAR=0.
      VRMS=0.
      N4=0
C  THIS PROGRAM PERFORMS CONDITIONAL SAMPLING ON RUNS OF CONCENTRATION-
C  VELOCITY DATA(METRIC UNITS)'
C   READ INFO FROM HEADER
      READ(11,10)RUN,POINT
   10 FORMAT(26X,I2,10X,I2)
      READ(11,15)NO
   15 FORMAT(41X,I3)
      NFIRST=NO
      READ(11,20)Z,RRO
   20 FORMAT(27X,I3,12X,F6.3)
      READ(11,25)
      READ(11,25)
   25 FORMAT(5X)
      READ(11,30)VEL
   30 FORMAT(34X,1A8)
      DO 40 N=1,4
      READ(11,25)
   40 CONTINUE
C  READ ALL DATA; CALCULATE INITIAL MEAN & RMS
      DO 50 I=1,NO
      READ(11,45)V(I),C(I)
   45 FORMAT(33X,F6.3,7X,F6.3)
      VBAR=VBAR+V(I)
      VRMS=VRMS+V(I)**2
   50 CONTINUE
      VBAR=VBAR/FLOAT(NO)
      VRMS=VRMS/FLOAT(NO)-VBAR**2
      VRMS=SQRT(VRMS)
C  THROW OUT DATA FARTHER THAN 3*VRMS AWAY FROM VBAR & CALCULATE
C  NEW MEAN & RMS WITH DATA LEFT OVER.
      DO 200 N=1,5
      IF((FLOAT(N4)/FLOAT(NO)).GT.0.99)GO TO 200
      IF(N.GT.1)NO=N4
      NEWBAR=0.
      NEWRMS=0.
      N4=0
      DO 100 I=1,NO
      IF(ABS(V(I)-VBAR).GT.(3.0*VRMS))GO TO 100
      N4=N4+1
      NEWBAR=NEWBAR+V(I)
      NEWRMS=NEWRMS+V(I)**2
      V(N4)=V(I)
      C(N4)=C(I)
  100 CONTINUE
      VBAR=NEWBAR/FLOAT(N4)
      VRMS=NEWRMS/FLOAT(N4)-VBAR**2
      VRMS=SQRT(VRMS)
  200 CONTINUE
      V1=0.
      V2=0.
      U3=0.
      U4=0.
      Q1=0.
      Q2=0.
      G1=0.
C  CALCULATE ASSORTED STATISTICAL PARAMETERS(MEAN,RMS,MOMENTS,ETC.)
      DO 500 I=1,N4
      V1=V1+V(I)
      V2=V2+V(I)**2
      U3=U3+V(I)**3
      U4=U4+V(I)**4
      Q1=Q1+C(I)
      Q2=Q2+C(I)**2
      G1=G1+V(I)*C(I)
  500 CONTINUE
      V1=V1/FLOAT(N4)
      U4=U4/FLOAT(N4)-4.*V1*U3/FLOAT(N4)+6.*V1**2*V2/FLOAT(N4)-3.*V1**4
      U3=U3/FLOAT(N4)-3.*V1*V2/FLOAT(N4)+2.*V1**3
      V2=V2/FLOAT(N4)-V1**2
      U2=SQRT(V2)
      Q1=Q1/FLOAT(N4)
      Q2=Q2/FLOAT(N4)-Q1**2
      Q2=SQRT(Q2)
```

```
      G1=G1/FLOAT(N4)-Q1*V1
      N6=0
      P8=0.
      R9=0.
      N7=0
      R8=0.
  809 WRITE(7,810)
  810 FORMAT(/)
      WRITE(7,815)RUN,POINT
  815 FORMAT(5X,'DATA OUTPUT FOR RUN',I3,' POINT',I3)
      WRITE(7,820)
  820 FORMAT(/)
      WRITE(7,822)VEL
  822 FORMAT(1X,1A7,' VELOCITY VS CONCENTRATION')
      WRITE(7,823)Z,RRO
  823 FORMAT(1X,'Z=',I3,' MM AND R/RO=',F6.3)
      WRITE(7,825)NFIRST,N4
  825 FORMAT(1X,'NO='I4,' AND N4=',I3)
      WRITE(7,830)V1
  830 FORMAT(1X,'VBAR=',F9.4,' MPS')
      WRITE(7,840)U2
  840 FORMAT(1X,'VRMS=',F9.4,' MPS')
      WRITE(7,850)U3
  850 FORMAT(1X,'THIRD MOMENT OF TURBULENCE=',E12.5,' MPS**3')
      R3=U3/U2**3
      WRITE(7,860)R3
  860 FORMAT(1X,'THIRD CORRELATION COEFFICIENT=',F9.4)
      WRITE(7,870)U4
  870 FORMAT(1X,'FOURTH MOMENT OF TURBULENCE=',E12.5,' MPS**4')
      R4=U4/U2**4
      WRITE(7,880)R4
  880 FORMAT(1X,'FOURTH CORRELATION COEFFICIENT=',F9.4)
      WRITE(7,881)Q1
  881 FORMAT(1X,'CBAR=',F8.3,'%')
      WRITE(7,882)Q2
  882 FORMAT(1X,'CRMS=',F8.3,'%')
      WRITE(7,883)G1
  883 FORMAT(1X,'CPVPBAR=',F10.6)
      TT=G1/Q2/U2
      WRITE(7,884)TT
  884 FORMAT(1X,'OVERALL TRANSPORT COEFFICIENT=',F10.6)
      WRITE(7,810)
C CONDITIONAL SAMPLING SECTION BEGINS HERE!
      WRITE(7,890)
  890 FORMAT(29X,'CONDITIONAL SAMPLING RESULTS')
      WRITE(7,900)
  900 FORMAT(/)
      WRITE(7,910)
  910 FORMAT(1X,'CONCENTRATION',4X,'NUMBER OF',15X,'RELATIVE',19X,'TRANSPORT',6X,'TRANSPORT')
      WRITE(7,920)
  920 FORMAT(2X,'FLUCTUATION',5X,'OCCURANCES',4X,'MEAN',8X,'MEAN',
     !10X,'RMS' 7X,'COEFFICIENT',7X,'RATIO')
      DO 975 K=1,20
      A1=-1.0+(K-1)*0.1
      A2=A1+.0999
      W1=0.
      NCOND=0
      V3=0.
      V4=0.
      VR=0.
      DO 925 N=1,N4
C TEST TO MAKE SURE C' IS IN THE DESIRED RANGE.
      IF(V(N).EQ.-100.) GO TO 925
      IF((C(N)-Q1).LT.A1) GO TO 925
      IF((C(N)-Q1).GT.(A2)) GO TO 925
      V3=V3+V(N)
      V4=V4+V(N)**2
      NCOND=NCOND+1
      W1=W1+(C(N)-Q1)*(V(N)-V1)
  925 CONTINUE
  927 IF(NCOND.EQ.0) GO TO 950
C V3 IS CONDITIONAL MEAN VELOCITY.
      V3=V3/FLOAT(NCOND)
C V4 IS CONDITIONAL RMS VELOCITY FLUCTUATION.
      V4=V4/FLOAT(NCOND)-V3**2
      V4=SQRT(V4)
C W1 IS CONDITIONAL MASS TRANSPORT COEFFICIENT.
      W1=W1/FLOAT(NCOND)/U2/Q2
C VR IS RELATIVE MEAN VELOCITY(CONDITIONAL MEAN-OVERALL MEAN).
      VR=V3-V1
```

```
C Y IS THE MASS TRANSPORT COEFFICIENT RATIO(CONDITIONAL/OVERALL).
      Y=W1/TT
      WRITE(7,930)A1,A2,NCOND,V3,VR,V4,W1,Y
  930 FORMAT(1X,F4.1,' - ',F7.4,6X,I3,5X,F8.4,4X,F9.5,4X,F9.5,4X,F10.5,5X,F10.3)
      GO TO 974
  950 WRITE(7,960)A1,A2,NCOND
  960 FORMAT(1X,F4.1,' - ',F7.4,6X,I3)
C X IS THE CENTER OF THE C' INTERVAL.
  974 X=A1+.05
C 928 IS THE FORMAT STATEMENT USED FOR WRITING PLOT FILES.
  928 FORMAT(F5.2,F10.3)
  975 CONTINUE
      WRITE(7,820)
  965 WRITE(7,970)RUN,POINT
  970 FORMAT(1X,'END OF RUN',I3,' -POINT',I3)
      STOP
      END
```

HOLD.COND3

```
      DIMENSION N1(1000),N2(1000)
      DIMENSION V(1000),C(1000),VN(1000)
      REAL*8 VEL
      REAL NEWBAR,NEWRMS
      INTEGER RUN,POINT,Z
      VBAR=0.
      VRMS=0.
      N4=0
C  THIS PROGRAM PERFORMS CONDITIONAL SAMPLING ON RUNS OF CONCENTRATION-
C  VELOCITY DATA(METRIC UNITS) AND CALCULATES PROBABILITY DENSITY DISTRIBUTIONS
C   READ INFO FROM HEADER
      READ(11,10)RUN,POINT
   10 FORMAT(26X,I2,10X,I2)
      READ(11,15)NO
   15 FORMAT(41X,I3)
      NFIRST=NO
      READ(11,20)Z,RRO
   20 FORMAT(27X,I3,12X,F6.3)
      READ(11,25)
      READ(11,25)
   25 FORMAT(5X)
      READ(11,30)VEL
   30 FORMAT(34X,1A8)
      DO 40 N=1,4
      READ(11,25)
   40 CONTINUE
C  READ ALL DATA; CALCULATE INITIAL MEAN & RMS
      DO 50 I=1,NO
      READ(11,45)V(I),C(I)
   45 FORMAT(33X,F6.3,7X,F6.3)
      VBAR=VBAR+V(I)
      VRMS=VRMS+V(I)**2
   50 CONTINUE
      VBAR=VBAR/FLOAT(NO)
      VRMS=VRMS/FLOAT(NO)-VBAR**2
      VRMS=SQRT(VRMS)
C  THROW OUT DATA FARTHER THAN 3*VRMS AWAY FROM VBAR & CALCULATE
C  NEW MEAN & RMS WITH DATA LEFT OVER.
      DO 200 N=1,5
      IF((FLOAT(N4)/FLOAT(NO)).GT.0.99)GO TO 200
      IF(N.GT.1)NO=N4
      NEWBAR=0.
      NEWRMS=0.
      N4=0
      DO 100 I=1,NO
      IF(ABS(V(I)-VBAR).GT.(3.0*VRMS))GO TO 100
      N4=N4+1
      NEWBAR=NEWBAR+V(I)
      NEWRMS=NEWRMS+V(I)**2
      V(N4)=V(I)
      C(N4)=C(I)
  100 CONTINUE
      VBAR=NEWBAR/FLOAT(N4)
      VRMS=NEWRMS/FLOAT(N4)-VBAR**2
      VRMS=SQRT(VRMS)
  200 CONTINUE
      DO 500 I=1,N4
      V1=V1+V(I)
      V2=V2+V(I)**2
      Q1=Q1+C(I)
  500 CONTINUE
      V1=V1/FLOAT(N4)
      V2=V2/FLOAT(N4)-V1**2
      U2=SQRT(V2)
      Q1=Q1/FLOAT(N4)
  809 WRITE(7,810)
  810 FORMAT(/)
      WRITE(7,815)RUN,POINT
  815 FORMAT(5X,'DATA OUTPUT FOR RUN',I3,' POINT',I3)
      WRITE(7,820)
  820 FORMAT(/)
      WRITE(7,822)VEL
  822 FORMAT(1X,1A7,' VELOCITY VS CONCENTRATION')
      WRITE(7,823)Z,RRO
  823 FORMAT(1X,'Z=',I3,' MM AND R/RO=',F6.3)
      WRITE(7,25)
      WRITE(7,980)
  980 FORMAT(3X,'SELECT MINIMUM POSITIVE AND NEGATIVE CONCENTRATION FLUCTUATION')
      WRITE(7,981)
  981 FORMAT(1X,'TO BE INCLUDED IN LARGE SCALE STRUCTURE USING F4.1 FORMAT')
```


C-2

```
      WRITE(7,982)
  982 FORMAT(2X,'CPPOS=')
      READ(7,983)CPPOS
  983 FORMAT(F4.1)
      WRITE(7,984)
  984 FORMAT(2X,'CPNEG=')
      READ(7,983)CPNEG
      N5=0
      UBAR=0.
      URMS=0.
      DO 999 I=1,N4
      N1(I)=0
      N2(I)=0
  999 CONTINUE
      VMIN=VBAR-3.0*VRMS
      VMAX=VBAR+3.0*VRMS
      DO 1000 N=1,N4
      IF(((C(N)-Q1).LT.CPPOS).AND.((C(N)-Q1).GE.CPNEG)) GO TO 950
      N5=N5+1
      UBAR=UBAR+V(N)
      URMS=URMS+V(N)**2
      I=INT(((V(N)-VMIN)/(VMAX-VMIN))*50)+1
      IF(I.EQ.51)I=50
C     N1 IS THE NUMBER OF CONDITIONAL SAMPLES
      N1(I)=N1(I)+1
  950 I=INT(((V(N)-VMIN)/(VMAX-VMIN))*50)+1
      IF (I.EQ.51)I=50
C     N2 IS THE NUMBER OF TOTAL SAMPLES
      N2(I)=N2(I)+1
 1000 CONTINUE
C   UBAR & URMS ARE CONDITIONAL(LARGE SCALE) MEAN &RMS VELOCITIES
      UBAR=UBAR/FLOAT(N5)
      URMS=(URMS/FLOAT(N5)-UBAR**2)**.5
      WRITE(7,25)
      WRITE(7,1010)NFIRST,N4,N5
 1010 FORMAT(1X,'NUMBER OF SAMPLES; ORIGINAL=',I3,' GOOD DATA=',I3,'  LARGE SCALE=',I3)
      WRITE(7,25)
      WRITE(7,1025)
 1025 FORMAT(25X,'NUMBER OF SAMPLES')
      WRITE(7,1050)
 1050 FORMAT(5X,'I',5X,'VMID(M/S)',5X,'L.S.',5X,'OVERALL')
      WRITE(7,25)
      DO 1100 I=1,50
      VMID=VMIN+(VMAX-VMIN)/50.*(I-.5)
      WRITE(7,1075)I,VMID,N1(I),N2(I)
 1075 FORMAT(4X,I2,6X,F6.3,7X,I3,7X,I3)
 1100 CONTINUE
      WRITE(7,25)
      WRITE(7,1500)VBAR,UBAR
 1500 FORMAT(1X,'MEAN VELOCITY(M/S); OVERALL=',F6.3,' & LARGE SCALE=',F6.3)
      WRITE(7,1600)VRMS,URMS
 1600 FORMAT(1X,'RMS VELOCITY(M/S); OVERALL=',F6.3,' & LARGE SCALE=',F6.3)
      WRITE(7,1700)Q1,CPPOS,CPNEG
 1700 FORMAT(1X,'CBAR=',F6.3,'  CPPOS=',F6.3,'  CPNEG=',F6.3)
      STOP
      END
```

APPENDIX B

```
SAMPLE 63,17
 SUCCESSFUL (TEMP) RESTORE RUN63P17 AS (TP17)
 CANCELLED: DDNAME RMDS     UNKNOWN

    DATA OUTPUT FOR RUN 63 POINT 17

AXIAL   VELOCITY VS CONCENTRATION
Z=152 MM AND R/RO= 0.025
NO= 999 AND N4=995
VBAR=   0.9244 MPS
VRMS=   0.1916 MPS
THIRD MOMENT OF TURBULENCE= 0.19140E-02 MPS**3
THIRD CORRELATION COEFFICIENT=   0.2721
FOURTH MOMENT OF TURBULENCE= 0.37374E-02 MPS**4
FOURTH CORRELATION COEFFICIENT=   2.7726
CBAR=   0.504%
CRMS=   0.263%
CPVPBAR= -0.022902
OVERALL TRANSPORT COEFFICIENT= -0.454270
```

CONDITIONAL SAMPLING RESULTS

CONCENTRATION FLUCTUATION	NUMBER OF OCCURANCES	MEAN	RELATIVE MEAN	RMS	TRANSPORT COEFFICIENT	TRANSPORT RATIO
-1.0 - -0.9001	0					
-0.9 - -0.8001	0					
-0.8 - -0.7001	0					
0.7 - -0.6001	0					
-0.6 - -0.5001	1	1.4450	0.52056	0.00000	-5.18168	11.407
-0.5 - -0.4001	43	1.1458	0.22137	0.17740	1.72815	4.244
-0.4 - -0.3001	85	1.0816	0.15712	0.19224	-1.09566	2.412
-0.3 - -0.2001	137	1.0153	0.09081	0.18916	-0.45393	0.999
-0.2 - -0.1001	126	0.9327	0.00823	0.18489	-0.04148	0.071
-0.1 - -0.0001	148	0.9411	0.01666	0.16404	-0.02478	0.055
-0.0 - 0.0999	115	0.8689	-0.05559	0.17576	-0.04960	0.109
0.1 - 0.1999	94	0.8373	-0.08713	0.15552	-0.27027	0.595
0.2 - 0.2999	77	0.8142	-0.11025	0.14164	-0.54529	1.200
0.3 - 0.3999	72	0.7975	-0.12693	0.09456	-0.88232	1.942
0.4 - 0.4999	71	0.8356	0.00883	0.12068	-0.77370	1.747
0.5 - 0.5999	26	0.8961	-0.02833	0.11139	-0.29574	0.651
0.6 - 0.6999	0					
0.7 - 0.7999	0					
0.8 - 0.8999	0					
0.9 - 0.9999	0					

```
END OF RUN 63 -POINT 17
 TERMINATED: STOP
```

SAMPLE 63,18
SUCCESSFUL (TEMP) RESTORE RUN63P18 AS (TF18)
CANCELLED: DDNAME RMDS UNKNOWN

DATA OUTPUT FOR RUN 63 POINT 18

AXIAL VELOCITY VS CONCENTRATION
Z=152 MM AND R/RO=-0.025
NO= 999 AND N4=997
VBAR= 0.9180 MPS
VRMS= 0.1948 MPS
THIRD MOMENT OF TURBULENCE= 0.14629E-02 MPS**3
THIRD CORRELATION COEFFICIENT= 0.1980
FOURTH MOMENT OF TURBULENCE= 0.41790E-02 MPS**4
FOURTH CORRELATION COEFFICIENT= 2.9033
CBAR= 0.508%
CRMS= 0.267%
CPVPBAR= -0.021049
OVERALL TRANSPORT COEFFICIENT= -0.405335

CONDITIONAL SAMPLING RESULTS

CONCENTRATION FLUCTUATION	NUMBER OF OCCURANCES	MEAN	RELATIVE MEAN	RMS	TRANSPORT COEFFICIENT	TRANSPORT RATIO
-1.0 - -0.9001	0					
-0.9 - -0.8001	0					
-0.8 - -0.7001	0					
-0.7 - -0.6001	0					
-0.6 - -0.5001	0					
-0.5 - -0.4001	32	1.0863	0.16832	0.20598	-1.45983	3.602
-0.4 - -0.3001	102	1.0801	0.16209	0.18968	1.09105	2.592
-0.3 - -0.2001	128	0.9937	0.07569	0.20108	-0.39880	0.984
-0.2 - -0.1001	160	0.9354	0.01733	0.20236	-0.05051	0.125
-0.1 - -0.0001	121	0.9030	-0.01498	0.18455	-0.00481	0.012
-0.0 - 0.0999	112	0.8861	-0.03191	0.17327	-0.03586	0.088
0.1 - 0.1999	92	0.8487	-0.06928	0.15151	-0.19860	0.490
0.2 - 0.2999	70	0.8391	-0.07890	0.14158	-0.39470	0.974
0.3 - 0.3999	90	0.8304	-0.08764	0.14393	0.59399	1.465
0.4 - 0.4999	54	0.7987	-0.11936	0.11972	-1.03118	2.544
0.5 - 0.5999	30	0.8341	0.08393	0.09709	0.87713	2.164
0.6 - 0.6999	6	0.8907	-0.02736	0.10235	-0.32656	0.806
0.7 - 0.7999	0					
0.8 - 0.8999	0					
0.9 - 0.9999	0					

END OF RUN 63 -POINT 18
TERMINATED: STOP

```
SAMPLE 63,19
 SUCCESSFUL (TEMP) RESTORE RUN63F19 AS (TF19)
 CANCELLED: DDNAME RMDS     UNKNOWN

   DATA OUTPUT FOR RUN 63 POINT 19

AXIAL   VELOCITY VS CONCENTRATION
Z=152 MM AND R/RO=-0.075
NO= 999 AND N4=998
VBAR=   0.9728 MPS
VRMS=   0.2004 MPS
THIRD MOMENT OF TURBULENCE= 0.19636E-02 MPS**3
THIRD CORRELATION COEFFICIENT=   0.2440
FOURTH MOMENT OF TURBULENCE= 0.42067E-02 MPS**4
FOURTH CORRELATION COEFFICIENT=   2.6087
CBAR=   0.464%
CRMS=   0.262%
CPVPBAR= -0.024204
OVERALL TRANSPORT COEFFICIENT= -0.461109
```

CONDITIONAL SAMPLING RESULTS

CONCENTRATION FLUCTUATION	NUMBER OF OCCURANCES	MEAN	RELATIVE MEAN	RMS	TRANSPORT COEFFICIENT	TRANSPORT RATIO
-1.0 - -0.9001	0					
-0.9 - -0.8001	0					
-0.8 - -0.7001	0					
-0.7 - -0.6001	0					
-0.6 - -0.5001	0					
-0.5 - -0.4001	31	1.1630	0.19020	0.18501	-1.57263	3.411
-0.4 - -0.3001	86	1.1689	0.19610	0.17428	1.30379	2.828
-0.3 - -0.2001	143	1.0656	0.09285	0.19000	-0.46430	1.007
-0.2 - -0.1001	157	0.9997	0.02690	0.19065	0.09028	0.196
-0.1 - -0.0001	138	0.9452	-0.02762	0.18217	0.01042	-0.023
-0.0 - 0.0999	106	0.9351	-0.03767	0.19978	-0.03806	0.083
0.1 - 0.1999	95	0.9151	0.05772	0.17557	-0.17123	0.371
0.2 - 0.2999	78	0.9094	-0.06342	0.15909	-0.29565	0.641
0.3 - 0.3999	65	0.8238	-0.14903	0.11079	-0.97510	2.138
0.4 - 0.4999	62	0.8497	-0.12308	0.12264	-1.04662	2.270
0.5 - 0.5999	33	0.8445	-0.12832	0.09782	-1.31825	2.859
0.6 - 0.6999	4	0.8752	-0.09755	0.13103	-1.15456	2.504
0.7 - 0.7999	0					
0.8 - 0.8999	0					
0.9 - 0.9999	0					

```
END OF RUN 63 -POINT 19
 TERMINATED: STOP
```

SAMPLE 63.20
SUCCESSFUL (TEMP) RESTORE RUN63P20 AS (TP20)
CANCELLED: DDNAME RMDS UNKNOWN

DATA OUTPUT FOR RUN 63 POINT 20

AXIAL VELOCITY VS CONCENTRATION
Z=152 MM AND R/RO=-0.125
NO= 999 AND N4=998
VBAR= 1.0689 MPS
VRMS= 0.2352 MPS
THIRD MOMENT OF TURBULENCE= 0.22793E-02 MPS**3
THIRD CORRELATION COEFFICIENT= 0.1751
FOURTH MOMENT OF TURBULENCE= 0.76303E-02 MPS**4
FOURTH CORRELATION COEFFICIENT= 2.4927
CBAR= 0.401%
CRMS= 0.253%
CPVPBAR= -0.032587
OVERALL TRANSPORT COEFFICIENT= -0.546930

CONDITIONAL SAMPLING RESULTS

CONCENTRATION FLUCTUATION	NUMBER OF OCCURANCES	MEAN	RELATIVE MEAN	RMS	TRANSPORT COEFFICIENT	TRANSPORT RATIO
-1.0 - -0.9001	0					
-0.9 - -0.8001	0					
-0.8 - -0.7001	0					
-0.7 - -0.6001	0					
-0.6 - -0.5001	0					
-0.5 - -0.4001	7	1.4759	0.40698	0.11547	2.79736	5.115
-0.4 - -0.3001	82	1.3162	0.24728	0.19080	-1.45902	2.668
-0.3 - -0.2001	141	1.2069	0.13804	0.20554	-0.59798	1.093
-0.2 - -0.1001	171	1.1418	0.07296	0.22556	-0.19097	0.349
-0.1 - -0.0001	171	1.0737	0.00481	0.19925	0.00200	-0.004
-0.0 - 0.0999	120	0.9938	-0.07504	0.18982	0.08426	0.134
0.1 - 0.1999	87	0.9622	-0.10671	0.17666	-0.26570	0.485
0.2 - 0.2999	69	0.9213	-0.14761	0.17437	-0.60496	1.106
0.3 - 0.3999	47	0.8876	-0.18129	0.17570	1.05837	1.735
0.4 - 0.4999	46	0.8678	-0.20110	0.13553	-1.48891	2.722
0.5 - 0.5999	26	0.8617	0.20719	0.13159	1.87688	3.432
0.6 - 0.6999	17	0.8739	-0.19494	0.12500	-2.09077	3.823
0.7 - 0.7999	4	0.8685	-0.20038	0.07705	-2.51619	4.601
0.8 - 0.8999	1	0.9830	-0.08580	0.00000	-1.17460	2.148
0.9 0.9999	0					

END OF RUN 63 -POINT 20
TERMINATED: STOP

ORIGINAL PAGE IS
OF POOR QUALITY

```
SAMPLE 63,21
 SUCCESSFUL (TEMP) RESTORE RUN63F21 AS (TP21)
 CANCELLED: DDNAME RMDS     UNKNOWN

    DATA OUTPUT FOR RUN 63 POINT 21

AXIAL   VELOCITY VS CONCENTRATION
Z=152 MM AND R/RO=-0.175
NO= 999 AND N4=998
VBAR=   1.1634 MPS
VRMS=   0.2386 MPS
THIRD MOMENT OF TURBULENCE=-0.14229E-02 MPS**3
THIRD CORRELATION COFFFICIENT=  -0.1048
FOURTH MOMENT OF TURBULENCE= 0.85964E-02 MPS**4
FOURTH CORRELATION COEFFICIENT=    2.6543
CBAR=   0.315%
CRMS=   0.233%
CPVPBAR= -0.029299
OVERALL TRANSPORT COEFFICIENT= -0.527584
```

CONDITIONAL SAMPLING RESULTS

CONCENTRATION FLUCTUATION	NUMBER OF OCCURANCES	MEAN	RELATIVE MEAN	RMS	TRANSPORT COEFFICIENT	TRANSPORT RATIO
-1.0 - -0.9001	0					
-0.9 - -0.8001	0					
-0.8 - -0.7001	0					
-0.7 - -0.6001	0					
-0.6 - -0.5001	0					
-0.5 - -0.4001	0					
-0.4 - -0.3001	40	1.3532	0.18986	0.22904	-1.07672	2.041
-0.3 - -0.2001	175	1.3249	0.16151	0.20354	0.72917	1.382
-0.2 - -0.1001	189	1.2696	0.10622	0.17378	-0.28248	0.535
-0.1 -0.0001	167	1.1640	0.00057	0.24519	0.01400	0.027
-0.0 - 0.0999	143	1.0955	-0.06789	0.19480	-0.05420	0.103
0.1 0.1999	98	1.0617	0.10163	0.20368	-0.25831	0.490
0.2 - 0.2999	75	0.9877	-0.17571	0.17325	-0.78189	1.482
0.3 - 0.3999	37	0.9888	0.17461	0.16513	-1.12599	2.134
0.4 - 0.4999	29	0.9768	-0.10663	0.16281	-1.51163	2.865
0.5 - 0.5999	25	0.9251	0.23827	0.16771	2.36309	4.479
0.6 - 0.6999	14	0.8964	-0.26703	0.11330	-3.17737	6.022
0.7 - 0.7999	6	0.9098	-0.25355	0.11807	-3.31135	6.276
0.8 - 0.8999	0					
0.9 - 0.9999	0					

```
END OF RUN 63 -POINT 21
 TERMINATED: STOP
```

SAMPLE 63,22
SUCCESSFUL (TEMP) RESTORE RUN63P22 AS (TP22)
CANCELLED: DDNAME KMDS UNKNOWN

DATA OUTPUT FOR RUN 63 POINT 22

AXIAL VELOCITY VS CONCENTRATION
Z=152 MM AND R/RO=-0.275
NO= 999 AND N4=994
VBAR= 1.3404 MPS
VRMS= 0.2348 MPS
THIRD MOMENT OF TURBULENCE=-0.77915E-02 MPS**3
THIRD CORRELATION COEFFICIENT= -0.6018
FOURTH MOMENT OF TURBULENCE= 0.94004E-02 MPS**4
FOURTH CORRELATION COEFFICIENT= 3.0922
CBAR= 0.136%
CRMS= 0.153%
CPVPBAR= -0.011062
OVERALL TRANSPORT COEFFICIENT= -0.308312

CONDITIONAL SAMPLING RESULTS

CONCENTRATION FLUCTUATION	NUMBER OF OCCURANCES	MEAN	RELATIVE MEAN	RMS	TRANSPORT COEFFICIENT	TRANSPORT RATIO
-1.0 - -0.9001	0					
-0.9 - -0.8001	0					
-0.8 - -0.7001	0					
-0.7 - -0.6001	0					
-0.6 - -0.5001	0					
-0.5 - -0.4001	0					
-0.4 - -0.3001	0					
-0.3 - -0.2001	0					
-0.2 - -0.1001	350	1.3996	0.05925	0.23583	-0.22204	0.720
-0.1 - -0.0001	268	1.3730	0.03258	0.20309	0.05678	0.184
-0.0 - 0.0999	154	1.3087	-0.03171	0.22686	-0.07870	0.255
0.1 - 0.1999	110	1.2733	0.04703	0.21056	0.28768	0.933
0.2 - 0.2999	59	1.2181	-0.12224	0.25093	0.92278	2.991
0.3 - 0.3999	31	1.1369	-0.20345	0.23616	-2.01097	6.523
0.4 0.4999	11	1.2433	0.07711	0.20968	1.24042	4.023
0.5 - 0.5999	9	1.0910	-0.24930	0.20791	-3.78054	12.262
0.6 - 0.6999	1	1.1610	-0.17938	0.00000	3.02255	9.004
0.7 - 0.7999	1	1.2060	-0.13430	0.00000	-2.76619	8.972
0.8 - 0.8999	0					
0.9 - 0.9999	0					

END OF RUN 63 -POINT 22
TERMINATED: STOP

```
SAMPLE 63,26
 SUCCESSFUL (TEMP) RESTORE RUN63P26 AS (TP26)
 CANCELLED: DDNAME RMDS     UNKNOWN

    DATA OUTPUT FOR RUN 63 POINT 26

AXIAL   VELOCITY VS CONCENTRATION
Z=152 MM AND R/RO=-0.674
NO= 499 AND N4=498
VBAR=   0.1676 MPS
VRMS=   0.3987 MPS
THIRD MOMENT OF TURBULENCE= 0.16914E-01 MPS**3
THIRD CORRELATION COEFFICIENT=    0.2669
FOURTH MOMENT OF TURBULENCE= 0.64401E-01 MPS**4
FOURTH CORRELATION COEFFICIENT=    2.5488
CBAR=   0.017%
CRMS=   0.020%
CPVPBAR= -0.001629
OVERALL TRANSPORT COEFFICIENT= -0.207616
```

CONDITIONAL SAMPLING RESULTS

CONCENTRATION FLUCTUATION	NUMBER OF OCCURANCES	MEAN	RELATIVE MEAN	RMS	TRANSPORT COEFFICIENT	TRANSPORT RATIO
-1.0 - -0.9001	0					
-0.9 - -0.8001	0					
-0.8 - -0.7001	0					
-0.7 - -0.6001	0					
-0.6 - -0.5001	0					
-0.5 - -0.4001	0					
-0.4 - -0.3001	0					
-0.3 - -0.2001	0					
-0.2 - -0.1001	0					
-0.1 - -0.0001	268	0.2332	0.06565	0.40282	-0.16239	0.782
-0.0 - 0.0999	230	0.0911	0.07650	0.37978	0.26034	1.254
0.1 - 0.1999	0					
0.2 - 0.2999	0					
0.3 - 0.3999	0					
0.4 - 0.4999	0					
0.5 - 0.5999	0					
0.6 - 0.6999	0					
0.7 - 0.7999	0					
0.8 - 0.8999	0					
0.9 - 0.9999	0					

```
END OF RUN 63 -POINT 26
 TERMINATED: STOP
```

SAMPLE 63,27
SUCCESSFUL (TEMP) RESTORE RUN63P27 AS (TP27)
CANCELLED: DDNAME RMDS UNKNOWN

DATA OUTPUT FOR RUN 63 POINT 27

AXIAL VELOCITY VS CONCENTRATION
Z=152 MM AND R/RO= 0.025
NO= 999 AND N4=996
VBAR= 0.9195 MPS
VRMS= 0.1969 MPS
THIRD MOMENT OF TURBULENCE= 0.29316E-02 MPS**3
THIRD CORRELATION COEFFICIENT= 0.3840
FOURTH MOMENT OF TURBULENCE= 0.42467E-02 MPS**4
FOURTH CORRELATION COEFFICIENT= 2.8231
CBAR= 0.537%
CRMS= 0.267%
CPVPBAR= -0.022243
OVERALL TRANSPORT COEFFICIENT= -0.423246

CONDITIONAL SAMPLING RESULTS

CONCENTRATION FLUCTUATION	NUMBER OF OCCURANCES	MEAN	RELATIVE MEAN	RMS	TRANSPORT COEFFICIENT	TRANSPORT RATIO
-1.0 - -0.9001	0					
-0.9 - -0.8001	0					
-0.8 - -0.7001	0					
-0.7 - -0.6001	0					
-0.6 - -0.5001	6	1.2780	0.35852	0.09241	-3.57417	8.327
-0.5 - -0.4001	40	1.2007	0.20124	0.16525	2.18064	5.625
-0.4 - -0.3001	90	1.0528	0.13334	0.19419	-0.86785	2.050
-0.3 - -0.2001	127	0.9982	0.07876	0.21224	-0.37539	0.887
-0.2 - -0.1001	150	0.9576	0.03814	0.18466	-0.11254	0.266
-0.1 - -0.0001	134	0.8786	-0.04085	0.17856	0.03930	-0.093
-0.0 - 0.0999	95	0.8544	0.06511	0.16338	-0.05538	0.131
0.1 - 0.1999	95	0.8453	-0.07413	0.16232	-0.21722	0.513
0.2 - 0.2999	87	0.8035	-0.11595	0.13633	-0.56315	1.331
0.3 - 0.3999	74	0.8326	-0.08690	0.13035	-0.56210	1.128
0.4 - 0.4999	74	0.8605	-0.05901	0.11445	-0.50259	1.187
0.5 - 0.5999	23	0.8590	0.06048	0.10770	-0.61866	1.462
0.6 - 0.6999	1	0.8500	-0.06947	0.00000	-0.80356	1.899
0.7 - 0.7999	0					
0.8 - 0.8999	0					
0.9 - 0.9999	0					

END OF RUN 63 -POINT 27
TERMINATED: STOP

SAMPLE 63,28
SUCCESSFUL (TEMP) RESTORE RUN63P28 AS (TF28)
CANCELLED: DDNAME RMDS UNKNOWN

DATA OUTPUT FOR RUN 63 POINT 28

AXIAL VELOCITY VS CONCENTRATION
Z=152 MM AND R/RO= 0.075
NO= 999 AND N4=996
VBAR= 0.9769 MPS
VRMS= 0.2154 MPS
THIRD MOMENT OF TURBULENCE= 0.37899E-02 MPS**3
THIRD CORRELATION COEFFICIENT= 0.3791
FOURTH MOMENT OF TURBULENCE= 0.62628E-02 MPS**4
FOURTH CORRELATION COEFFICIENT= 2.9082
CBAR= 0.466%
CRMS= 0.266%
CPVPBAR= -0.027163
OVERALL TRANSPORT COEFFICIENT= -0.473547

CONDITIONAL SAMPLING RESULTS

CONCENTRATION FLUCTUATION	NUMBER OF OCCURANCES	MEAN	RELATIVE MEAN	RMS	TRANSPORT COEFFICIENT	TRANSPORT RATIO
-1.0 - -0.9001	0					
-0.9 - -0.8001	0					
-0.8 - -0.7001	0					
-0.7 - -0.6001	0					
-0.6 - -0.5001	0					
-0.5 - -0.4001	31	1.2321	0.25525	0.23829	-1.94549	4.108
-0.4 - -0.3001	95	1.2052	0.22830	0.21101	1.40306	2.963
-0.3 - -0.2001	127	1.0866	0.10971	0.20262	-0.49345	1.042
-0.2 - -0.1001	180	0.9931	0.01624	0.19245	-0.06144	0.130
-0.1 - -0.0001	118	0.9546	-0.02222	0.19422	0.01847	-0.039
-0.0 - 0.0999	117	0.9058	0.07108	0.18028	-0.07063	0.149
0.1 - 0.1999	87	0.8655	-0.11134	0.18644	-0.28664	0.605
0.2 - 0.2999	61	0.8830	-0.09386	0.13054	-0.40863	0.863
0.3 - 0.3999	69	0.8606	-0.11631	0.12400	-0.70546	1.490
0.4 0.4999	74	0.8598	-0.11712	0.12584	-0.72789	1.939
0.5 - 0.5999	31	0.8831	-0.09378	0.14141	-0.88245	1.863
0.6 - 0.6999	6	0.9062	-0.07070	0.08127	-0.75330	1.591
0.7 - 0.7999	0					
0.8 - 0.8999	0					
0.9 - 0.9999	0					

END OF RUN 63 -POINT 28
TERMINATED: STOP

```
SAMPLE 63,29
 SUCCESSFUL (TEMP) RESTORE RUN63P29 AS (TP29)
 CANCELLED: DDNAME RMDS     UNKNOWN

    DATA OUTPUT FOR RUN 63 POINT 29

AXIAL    VELOCITY VS CONCENTRATION
Z=152 MM AND R/RO= 0.125
NO= 999 AND N4=998
VBAR=    1.0449 MPS
VRMS=    0.2190 MPS
THIRD MOMENT OF TURBULENCE= 0.22058E-02 MPS**3
THIRD CORRELATION COEFFICIENT=    0.2099
FOURTH MOMENT OF TURBULENCE= 0.57974E-02 MPS**4
FOURTH CORRELATION COEFFICIENT=    2.5181
CBAR=    0.417%
CRMS=    0.255%
CPVPBAR= -0.028794
OVERALL TRANSPORT COEFFICIENT= -0.515516
```

CONDITIONAL SAMPLING RESULTS

CONCENTRATION FLUCTUATION	NUMBER OF OCCURANCES	MEAN	RELATIVE MEAN	RMS	TRANSPORT COEFFICIENT	TRANSPORT RATIO
-1.0 - -0.9001	0					
-0.9 - -0.8001	0					
-0.8 - -0.7001	0					
-0.7 - -0.6001	0					
-0.6 - -0.5001	0					
-0.5 - -0.4001	3	1.2290	0.18411	0.19559	-1.38565	2.688
-0.4 - -0.3001	99	1.2580	0.21313	0.18172	1.29885	2.520
-0.3 - -0.2001	134	1.2016	0.15668	0.18996	-0.72187	1.400
-0.2 - -0.1001	191	1.1037	0.05877	0.19858	-0.16814	0.326
-0.1 - -0.0001	140	0.9928	-0.05212	0.19457	0.04397	-0.085
-0.0 - 0.0999	129	0.9971	-0.04777	0.19840	-0.03937	0.076
0.1 - 0.1999	81	0.9592	0.00571	0.17666	0.24324	0.472
0.2 - 0.2999	69	0.8880	-0.15686	0.14674	-0.73269	1.421
0.3 - 0.3999	60	0.9064	-0.13847	0.16569	-0.86407	1.676
0.4 - 0.4999	37	0.8974	-0.14746	0.13298	-1.19425	2.317
0.5 - 0.5999	40	0.8704	-0.17446	0.09376	-1.69724	3.292
0.6 - 0.6999	15	0.9235	-0.12135	0.07988	-1.36790	2.653
0.7 - 0.7999	0					
0.8 - 0.8999	0					
0.9 - 0.9999	0					

```
END OF RUN 63 -POINT 29
 TERMINATED: STOP
```

SAMPLE 63,30
SUCCESSFUL (TEMP) RESTORE RUN63F30 AS (TF30)
CANCELLED: DDNAME RMDS UNKNOWN

DATA OUTPUT FOR RUN 63 POINT 30

AXIAL VELOCITY VS CONCENTRATION
Z=152 MM AND R/RO= 0.175
NO= 999 AND N4=998
VBAR= 1.1652 MPS
VRMS= 0.2307 MPS
THIRD MOMENT OF TURBULENCE=-0.14648E-02 MPS**3
THIRD CORRELATION COEFFICIENT= -0.1192
FOURTH MOMENT OF TURBULENCE= 0.71564E-02 MPS**4
FOURTH CORRELATION COEFFICIENT= 2.5246
CBAR= 0.276%
CRMS= 0.197%
CPVPBAR= -0.024480
OVERALL TRANSPORT COEFFICIENT= -0.537532

CONDITIONAL SAMPLING RESULTS

CONCENTRATION FLUCTUATION	NUMBER OF OCCURANCES	MEAN	RELATIVE MEAN	RMS	TRANSPORT COEFFICIENT	TRANSPORT RATIO
-1.0 - -0.9001	0					
-0.9 - -0.8001	0					
-0.8 - -0.7001	0					
-0.7 - -0.6001	0					
-0.6 - -0.5001	0					
-0.5 - -0.4001	0					
-0.4 - -0.3001	2	1.4635	0.29832	0.06851	-2.01486	3.748
-0.3 - -0.2001	140	1.3500	0.18487	0.20949	-1.02391	1.905
-0.2 - -0.1001	196	1.2780	0.11278	0.16765	-0.37885	0.705
-0.1 - -0.0001	224	1.1847	0.01953	0.21010	-0.04897	0.091
-0.0 - 0.0999	179	1.1180	-0.04715	0.18819	-0.06301	0.117
0.1 - 0.1999	106	1.0331	-0.13211	0.21002	-0.43830	0.815
0.2 - 0.2999	70	0.9728	-0.19237	0.19492	-1.04965	1.953
0.3 - 0.3999	37	0.9789	0.18623	0.16566	1.42606	2.653
0.4 - 0.4999	18	0.9613	-0.20384	0.13920	-1.99683	3.715
0.5 - 0.5999	11	0.9483	0.21690	0.10704	2.49833	4.648
0.6 - 0.6999	14	0.8874	-0.27775	0.13630	-3.93111	7.313
0.7 - 0.7999	1	1.0430	0.12218	0.00000	1.93742	3.604
0.8 - 0.8999	0					
0.9 - 0.9999	0					

END OF RUN 63 -POINT 30
TERMINATED: STOP

```
SAMPLE 63,31
 SUCCESSFUL (TEMP) RESTORE RUN63P31 AS (TF31)
 CANCELLED: DDNAME RMDS      UNKNOWN


    DATA OUTPUT FOR RUN 63 POINT 31


AXIAL    VELOCITY VS CONCENTRATION
Z=152 MM AND R/RO= 0.225
NO= 999 AND N4=997
VBAR=   1.2683 MPS
VRMS=   0.2422 MPS
THIRD MOMENT OF TURBULENCE=-0.52404E-02 MPS**3
THIRD CORRELATION COEFFICIENT=  -0.3690
FOURTH MOMENT OF TURBULENCE= 0.90446E-02 MPS**4
FOURTH CORRELATION COEFFICIENT=   2.6300
CBAR=   0.197%
CRMS=   0.171%
CPVPBAR= -0.021122
OVERALL TRANSPORT COEFFICIENT= -0.510441
```

CONDITIONAL SAMPLING RESULTS

CONCENTRATION FLUCTUATION	NUMBER OF OCCURANCES	MEAN	RELATIVE MEAN	RMS	TRANSPORT COEFFICIENT	TRANSPORT RATIO
-1.0 - -0.9001	0					
-0.9 - -0.8001	0					
-0.8 - -0.7001	0					
-0.7 - -0.6001	0					
-0.6 - -0.5001	0					
-0.5 - -0.4001	0					
-0.4 - -0.3001	0					
-0.3 - -0.2001	60	1.4328	0.16446	0.21294	-0.82973	1.626
-0.2 - -0.1001	280	1.3884	0.12014	0.21635	0.43350	0.849
-0.1 - -0.0001	225	1.3185	0.05024	0.19989	-0.08231	0.161
-0.0 - 0.0999	192	1.2157	-0.05265	0.21256	0.07853	0.134
0.1 - 0.1999	111	1.1282	-0.14007	0.20359	-0.51467	1.008
0.2 - 0.2999	64	1.0785	0.18976	0.18299	-1.10108	2.157
0.3 - 0.3999	36	1.0466	-0.22173	0.22466	-1.81961	3.565
0.4 0.4999	13	0.9562	0.31215	0.15726	3.46937	6.797
0.5 - 0.5999	13	0.9677	-0.30061	0.11614	-3.96355	7.765
0.6 - 0.6999	3	0.9413	0.32697	0.03797	-4.97792	9.752
0.7 - 0.7999	0					
0.8 - 0.8999	0					
0.9 - 0.9999	0					

```
END OF RUN 63 -POINT 31
 TERMINATED: STOP
-
```

SAMPLE 63.32
SUCCESSFUL (TEMP) RESTORE RUN63P32 AS (TF32)
CANCELLED: DDNAME RMDS UNKNOWN

DATA OUTPUT FOR RUN 63 POINT 32

AXIAL VELOCITY VS CONCENTRATION
Z=152 MM AND R/RO= 0.325
NO= 999 AND N4=974
VBAR= 1.3713 MPS
VRMS= 0.2231 MPS
THIRD MOMENT OF TURBULENCE=-0.86908E-02 MPS**3
THIRD CORRELATION COEFFICIENT= -0.7329
FOURTH MOMENT OF TURBULENCE= 0.80614E-02 MPS**4
FOURTH CORRELATION COEFFICIENT= 3.2355
CBAR= 0.073%
CRMS= 0.116%
CPVPBAR= -0.005959
OVERALL TRANSPORT COEFFICIENT= -0.230130

CONDITIONAL SAMPLING RESULTS

CONCENTRATION FLUCTUATION	NUMBER OF OCCURANCES	MEAN	RELATIVE MEAN	RMS	TRANSPORT COEFFICIENT	TRANSPORT RATIO
-1.0 - -0.9001	0					
-0.9 - -0.8001	0					
-0.8 - -0.7001	0					
-0.7 - -0.6001	0					
-0.6 - -0.5001	0					
-0.5 - -0.4001	0					
-0.4 - -0.3001	0					
-0.3 - -0.2001	0					
-0.2 - -0.1001	19	1.4574	0.08602	0.19955	-0.34965	1.519
-0.1 - -0.0001	646	1.3856	0.01424	0.22648	0.02969	0.129
-0.0 - 0.0999	160	1.4143	0.04300	0.17252	0.04505	-0.196
0.1 - 0.1999	76	1.3165	-0.05481	0.17902	-0.35660	1.550
0.2 - 0.2999	34	1.1926	-0.17870	0.24405	-1.78822	7.770
0.3 - 0.3999	24	1.2007	-0.17060	0.23666	-2.28260	9.919
0.4 - 0.4999	11	1.2186	-0.15271	0.17507	2.58150	11.218
0.5 - 0.5999	3	0.9260	-0.44534	0.13437	-9.00262	39.120
0.6 - 0.6999	1	1.0550	0.31634	0.00000	-7.80620	33.921
0.7 - 0.7999	0					
0.8 - 0.8999	0					
0.9 - 0.9999	0					

END OF RUN 63 -POINT 32
TERMINATED: STOP

SAMPLE 63,33
SUCCESSFUL (TEMP) RESTORE RUN63P33 AS (TP33)
CANCELLED: DDNAME RMDS UNKNOWN

DATA OUTPUT FOR RUN 63 POINT 33

AXIAL VELOCITY VS CONCENTRATION
Z=152 MM AND R/RO= 0.425
NO= 999 AND N4=982
VBAR= 1.2108 MPS
VRMS= 0.2943 MPS
THIRD MOMENT OF TURBULENCE=-0.18863E-01 MPS**3
THIRD CORRELATION COEFFICIENT= -0.7398
FOURTH MOMENT OF TURBULENCE= 0.24559E-01 MPS**4
FOURTH CORRELATION COEFFICIENT= 3.2725
CBAR= 0.017%
CRMS= 0.053%
CPVPBAR= 0.000444
OVERALL TRANSPORT COEFFICIENT= 0.028279

CONDITIONAL SAMPLING RESULTS

CONCENTRATION FLUCTUATION	NUMBER OF OCCURANCES	MEAN	RELATIVE MEAN	RMS	TRANSPORT COEFFICIENT	TRANSPORT RATIO
-1.0 - -0.9001	0					
-0.9 - -0.8001	0					
-0.8 - -0.7001	0					
-0.7 - -0.6001	0					
-0.6 - -0.5001	0					
-0.5 - -0.4001	0					
-0.4 - -0.3001	0					
-0.3 - -0.2001	0					
-0.2 - -0.1001	0					
-0.1 - -0.0001	685	1.2133	0.00245	0.29197	-0.02270	-0.803
-0.0 - 0.0999	234	1.1993	-0.01152	0.30915	0.06888	2.436
0.1 - 0.1999	28	1.3410	0.11018	0.19807	1.20554	42.430
0.2 - 0.2999	10	1.1928	-0.01802	0.16546	-0.42700	-15.099
0.3 - 0.3999	5	1.1140	0.09682	0.17651	2.34077	-82.773
0.4 - 0.4999	1	1.3190	0.10818	0.00000	3.06063	108.228
0.5 - 0.5999	0					
0.6 - 0.6999	0					
0.7 - 0.7999	0					
0.8 - 0.8999	0					
0.9 - 0.9999	0					

END OF RUN 63 -POINT 33
TERMINATED: STOP

SAMPLE 63.34
SUCCESSFUL (TEMP) RESTORE RUN63P34 AS (TF34)
CANCELLED: DDNAME RMDS UNKNOWN

DATA OUTPUT FOR RUN 63 POINT 34

AXIAL VELOCITY VS CONCENTRATION
Z=152 MM AND R/RO= 0.025
NO= 999 AND N4=996
VBAR= 0.9075 MPS
VRMS= 0.1888 MPS
THIRD MOMENT OF TURBULENCE= 0.22869E-02 MPS**3
THIRD CORRELATION COEFFICIENT= 0.3396
FOURTH MOMENT OF TURBULENCE= 0.37632E-02 MPS**4
FOURTH CORRELATION COEFFICIENT= 2.9575
CBAR= 0.550%
CRMS= 0.273%
CPVPBAR= -0.021361
OVERALL TRANSPORT COEFFICIENT= -0.414777

CONDITIONAL SAMPLING RESULTS

CONCENTRATION FLUCTUATION	NUMBER OF OCCURANCES	MEAN	RELATIVE MEAN	RMS	TRANSPORT COEFFICIENT	TRANSPORT RATIO
-1.0 - -0.9001	0					
-0.9 - -0.8001	0					
-0.8 - -0.7001	0					
-0.7 - -0.6001	0					
-0.6 - -0.5001	5	1.1706	0.26312	0.15440	-2.70662	6.525
-0.5 - -0.4001	34	1.1185	0.21104	0.15158	-1.84638	4.452
-0.4 - -0.3001	105	1.0790	0.17150	0.19885	1.20077	2.895
-0.3 - -0.2001	143	0.9634	0.05587	0.19596	-0.28276	0.682
-0.2 - -0.1001	127	0.9331	0.02564	0.17618	-0.08198	0.198
-0.1 - -0.0001	106	0.8734	-0.03411	0.19100	0.02660	-0.064
-0.0 - 0.0999	127	0.8455	-0.06194	0.16067	-0.04809	0.116
0.1 - 0.1999	89	0.8442	-0.06328	0.16521	-0.18760	0.452
0.2 - 0.2999	79	0.8001	-0.10734	0.11691	-0.51699	1.246
0.3 - 0.3999	72	0.8425	-0.06507	0.11705	-0.44230	1.066
0.4 - 0.4999	86	0.8433	-0.06418	0.10371	-0.56038	1.351
0.5 - 0.5999	20	0.9228	0.00468	0.10318	-0.89086	2.148
0.6 - 0.6999	3	0.8490	-0.05848	0.06067	-0.70457	1.699
0.7 - 0.7999	0					
0.8 - 0.8999	0					
0.9 - 0.9999	0					

END OF RUN 63 -POINT 34
TERMINATED: STOP

```
SAMPLE 51,8
 SUCCESSFUL (TEMP) RESTORE RUN51P8 AS (TF8)
 CANCELLED: DDNAME RMDS     UNKNOWN

    DATA OUTPUT FOR RUN 51 POINT  8

RADIAL  VELOCITY VS CONCENTRATION
Z=152 MM AND R/RO= 0.025
NO= 999 AND N4=982
VBAR=  -0.0012 MPS
VRMS=   0.1325 MPS
THIRD MOMENT OF TURBULENCE= 0.20624E-03 MPS**3
THIRD CORRELATION COEFFICIENT=   0.0886
FOURTH MOMENT OF TURBULENCE= 0.98762E-03 MPS**4
FOURTH CORRELATION COEFFICIENT=    3.2010
CBAR=   0.548%
CRMS=   0.265%
CPVPBAR= -0.001080
OVERALL TRANSPORT COEFFICIENT= -0.030756
```

CONDITIONAL SAMPLING RESULTS

CONCENTRATION FLUCTUATION	NUMBER OF OCCURANCES	MEAN	RELATIVE MEAN	RMS	TRANSPORT COEFFICIENT	TRANSPORT RATIO
-1.0 - -0.9001	0					
-0.9 - -0.8001	0					
-0.8 - -0.7001	0					
-0.7 - -0.6001	0					
-0.6 - -0.5001	6	0.0467	0.04785	0.18330	-0.62957	20.469
-0.5 - -0.4001	39	-0.0282	-0.02700	0.18836	0.38850	-12.631
-0.4 - -0.3001	78	0.0345	0.03566	0.18482	-0.36367	11.424
-0.3 - -0.2001	140	-0.0023	-0.00110	0.16783	-0.00516	0.168
-0.2 - -0.1001	133	0.0084	0.00958	0.13447	-0.04415	1.436
-0.1 - -0.0001	138	-0.0121	-0.01088	0.12704	0.01861	-0.605
-0.0 - 0.0999	118	-0.0119	-0.01076	0.12464	-0.01405	0.457
0.1 - 0.1999	82	0.0123	0.01344	0.09079	0.06097	-1.982
0.2 - 0.2999	72	-0.0051	-0.00396	0.08590	-0.02749	0.894
0.3 - 0.3999	81	-0.0145	-0.01334	0.07768	-0.13071	4.250
0.4 - 0.4999	73	-0.0079	-0.00669	0.08937	-0.08344	2.713
0.5 - 0.5999	20	0.0133	0.01453	0.06337	0.22293	-7.248
0.6 - 0.6999	2	0.0470	0.04818	0.02100	0.83476	-27.141
0.7 - 0.7999	0					
0.8 - 0.8999	0					
0.9 - 0.9999	0					

```
END OF RUN 51 -POINT  8
 TERMINATED: STOP
```

```
SAMPLE 51,9
 SUCCESSFUL (TEMP) RESTORE RUN51F9 AS (TF9)
 CANCELLED: DDNAME RMDS     UNKNOWN


    DATA OUTPUT FOR RUN 51 POINT  9


RADIAL  VELOCITY VS CONCENTRATION
Z=152 MM AND R/RO= 0.075
NO= 999 AND N4=990
VBAR=  -0.0129 MPS
VRMS=   0.1360 MPS
THIRD MOMENT OF TURBULENCE=-0.87412E-03 MPS**3
THIRD CORRELATION COEFFICIENT=  -0.3473
FOURTH MOMENT OF TURBULENCE= 0.11120E-02 MPS**4
FOURTH CORRELATION COEFFICIENT=   3.2484
CBAR=   0.510%
CRMS=   0.256%
CPVPBAR=  0.011591
OVERALL TRANSPORT COEFFICIENT=  0.332705
```

CONDITIONAL SAMPLING RESULTS

CONCENTRATION FLUCTUATION	NUMBER OF OCCURANCES	MEAN	RELATIVE MEAN	RMS	TRANSPORT COEFFICIENT	TRANSPORT RATIO
-1.0 - -0.9001	0					
-0.9 - -0.8001	0					
-0.8 - -0.7001	0					
-0.7 - -0.6001	0					
-0.6 - -0.5001	3	-0.3003	-0.28744	0.04229	4.20971	12.653
-0.5 - -0.4001	37	-0.1336	-0.12076	0.17973	1.57153	4.723
-0.4 - -0.3001	83	-0.0924	-0.07952	0.19612	0.76825	2.309
-0.3 - -0.2001	127	-0.0643	-0.05145	0.14166	0.37102	1.115
-0.2 - -0.1001	147	-0.0198	-0.00693	0.13609	0.03440	0.103
-0.1 - -0.0001	137	-0.0093	-0.00359	0.11738	-0.00784	-0.024
-0.0 - 0.0999	106	0.0195	0.03244	0.10833	0.05193	0.156
0.1 - 0.1999	109	0.0083	0.02115	0.11133	0.09511	0.286
0.2 - 0.2999	83	0.0522	0.06508	0.08491	0.45506	1.368
0.3 - 0.3999	77	0.0439	0.05676	0.07209	0.56326	1.693
0.4 - 0.4999	55	0.0289	0.04182	0.09190	0.52975	1.592
0.5 - 0.5999	26	0.0323	0.04523	0.07382	0.67765	2.037
0.6 - 0.6999	0					
0.7 - 0.7999	0					
0.8 - 0.8999	0					
0.9 - 0.9999	0					

```
END OF RUN 51 -POINT  9
 TERMINATED: STOP
```

SAMPLE 51,10
SUCCESSFUL (TEMP) RESTORE RUN51F10 AS (TF10)
CANCELLED: DDNAME RMDS UNKNOWN

DATA OUTPUT FOR RUN 51 POINT 10

RADIAL VELOCITY VS CONCENTRATION
Z=152 MM AND R/RO= 0.125
NO= 999 AND N4=991
VBAR= -0.0215 MPS
VRMS= 0.1509 MPS
THIRD MOMENT OF TURBULENCE=-0.98048E-03 MPS**3
THIRD CORRELATION COEFFICIENT= -0.2853
FOURTH MOMENT OF TURBULENCE= 0.16024E-02 MPS**4
FOURTH CORRELATION COEFFICIENT= 3.0901
CBAR= 0.401%
CRMS= 0.236%
CPVPBAR= 0.016350
OVERALL TRANSPORT COEFFICIENT= 0.458312

CONDITIONAL SAMPLING RESULTS

CONCENTRATION FLUCTUATION	NUMBER OF OCCURANCES	MEAN	RELATIVE MEAN	RMS	TRANSPORT COEFFICIENT	TRANSPORT RATIO
-1.0 - -0.9001	0					
-0.9 - -0.8001	0					
-0.8 - -0.7001	0					
-0.7 - -0.6001	0					
-0.6 - -0.5001	0					
-0.5 - -0.4001	7	-0.1844	-0.16289	0.14217	1.87018	4.081
-0.4 - -0.3001	62	-0.1698	0.14830	0.17977	1.43485	3.174
-0.3 - -0.2001	128	-0.1013	-0.07974	0.17016	0.57672	1.258
-0.2 - -0.1001	209	-0.0708	-0.04575	0.13847	0.22689	0.495
-0.1 - -0.0001	169	-0.0126	0.00891	0.13698	-0.00087	-0.002
-0.0 - 0.0999	126	0.0155	0.03704	0.12841	0.06687	0.146
0.1 - 0.1999	83	0.0521	0.07367	0.10364	0.29254	0.638
0.2 - 0.2999	62	0.0644	0.08596	0.08374	0.59441	1.297
0.3 - 0.3999	68	0.0626	0.08413	0.09015	0.82475	1.800
0.4 - 0.4999	46	0.0707	0.07219	0.06815	1.18191	2.579
0.5 - 0.5999	26	0.0869	0.10847	0.08139	1.62240	3.540
0.6 - 0.6999	5	0.0656	0.08714	0.05642	1.53452	3.348
0.7 - 0.7999	0					
0.8 - 0.8999	0					
0.9 - 0.9999	0					

END OF RUN 51 -POINT 10
TERMINATED: STOP

```
SAMPLE 61,11
 SUCCESSFUL (TEMP) RESTORE RUN51F11 AS (TF11)
 CANCELLED: DDNAME RMDS      UNKNOWN

    DATA OUTPUT FOR RUN 51 POINT 11

RADIAL  VELOCITY VS CONCENTRATION
Z=152 MM AND R/RO= 0.175
NO= 999 AND N4=993
VBAR=  -0.0371 MPS
VRMS=   0.1608 MPS
THIRD MOMENT OF TURBULENCE=-0.67203E-03 MPS**3
THIRD CORRELATION COEFFICIENT=  -0.1617
FOURTH MOMENT OF TURBULENCE= 0.18304E-02 MPS**4
FOURTH CORRELATION COEFFICIENT=   2.7404
CBAR=   0.321%
CRMS=   0.216%
CPVPBAR=  0.017106
OVERALL TRANSPORT COEFFICIENT=  0.492046
```

CONDITIONAL SAMPLING RESULTS

CONCENTRATION FLUCTUATION	NUMBER OF OCCURANCES	MEAN	RELATIVE MEAN	RMS	TRANSPORT COEFFICIENT	TRANSPORT RATIO
-1.0 - -0.9001	0					
-0.9 - -0.8001	0					
-0.8 - -0.7001	0					
-0.7 - -0.6001	0					
-0.6 - -0.5001	0					
-0.5 - -0.4001	0					
-0.4 - -0.3001	31	-0.1651	-0.12801	0.12936	1.18328	2.405
-0.3 - -0.2001	152	-0.1439	-0.10680	0.14701	0.77300	1.571
-0.2 - -0.1001	197	-0.0958	-0.05869	0.16571	0.25234	0.513
-0.1 -0.0001	187	-0.0556	-0.01854	0.14607	0.03399	0.069
-0.0 - 0.0999	141	-0.0014	0.03571	0.13051	0.05761	0.117
0.1 - 0.1999	111	0.0421	0.07919	0.12418	0.34489	0.701
0.2 - 0.2999	69	0.0643	0.10144	0.10283	0.70436	1.431
0.3 - 0.3999	47	0.1001	0.13719	0.09931	1.35553	2.755
0.4 - 0.4999	30	0.0862	0.12325	0.09846	1.59463	3.241
0.5 - 0.5999	14	0.1384	0.17552	0.11674	2.74419	5.577
0.6 - 0.6999	13	0.0922	0.12924	0.08843	2.38544	4.848
0.7 - 0.7999	1	0.0830	0.12009	0.00000	2.44864	4.976
0.8 - 0.8999	0					
0.9 - 0.9999	0					

```
END OF RUN 51 -POINT 11
 TERMINATED: STOP
```

ORIGINAL PAGE IS
OF POOR QUALITY

SAMPLE 51.12
SUCCESSFUL (TEMP) RESTORE RUN51P12 AS (TF12)
CANCELLED: DDNAME RMDS UNKNOWN

DATA OUTPUT FOR RUN 51 POINT 12

RADIAL VELOCITY VS CONCENTRATION
Z=152 MM AND R/RO= 0.225
NO= 999 AND N4=993
VBAR= -0.0143 MPS
VRMS= 0.1679 MPS
THIRD MOMENT OF TURBULENCE=-0.92308E-03 MPS**3
THIRD CORRELATION COEFFICIENT= -0.1950
FOURTH MOMENT OF TURBULENCE= 0.22956E-02 MPS**4
FOURTH CORRELATION COEFFICIENT= 2.8885
CBAR= 0.250%
CRMS= 0.209%
CPVPBAR= 0.016107
OVERALL TRANSPORT COEFFICIENT= 0.458471

CONDITIONAL SAMPLING RESULTS

CONCENTRATION FLUCTUATION	NUMBER OF OCCURANCES	MEAN	RELATIVE MEAN	RMS	TRANSPORT COEFFICIENT	TRANSPORT RATIO
-1.0 - -0.9001	0					
-0.9 - -0.8001	0					
-0.8 - -0.7001	0					
-0.7 - -0.6001	0					
-0.6 - -0.5001	0					
-0.5 - -0.4001	0					
-0.4 - -0.3001	0					
-0.3 - -0.2001	189	-0.1058	-0.09153	0.15423	0.59511	1.298
-0.2 - -0.1001	177	-0.0727	-0.05841	0.16311	0.25980	0.567
-0.1 - -0.0001	212	-0.0346	-0.02030	0.15859	0.03441	0.075
-0.0 - 0.0999	170	0.0048	0.01909	0.14367	0.02541	0.055
0.1 - 0.1999	91	0.0604	0.07470	0.14014	0.32057	0.699
0.2 - 0.2999	53	0.1032	0.11747	0.13470	0.84002	1.832
0.3 - 0.3999	45	0.1290	0.14328	0.10903	1.40861	3.072
0.4 - 0.4999	25	0.1487	0.16296	0.10326	2.08685	4.552
0.5 - 0.5999	15	0.1409	0.15515	0.10452	2.47207	5.392
0.6 - 0.6999	10	0.1264	0.14068	0.05536	2.59859	5.668
0.7 - 0.7999	3	0.1743	0.18861	0.02073	3.94406	8.603
0.8 - 0.8999	3	0.2697	0.28395	0.07759	7.01706	15.305
0.9 - 0.9999	0					

END OF RUN 51 -POINT 12
TERMINATED: STOP

SAMPLE 51,14
SUCCESSFUL (TEMP) RESTORE RUN51P14 AS (TF14)
CANCELLED: DDNAME RMDS UNKNOWN

DATA OUTPUT FOR RUN 51 POINT 14

RADIAL VELOCITY VS CONCENTRATION
Z=152 MM AND R/RO= 0.275
NO= 999 AND N4=990
VBAR= -0.0134 MPS
VRMS= 0.1768 MPS
THIRD MOMENT OF TURBULENCE=-0.17353E 02 MPS**3
THIRD CORRELATION COEFFICIENT= -0.3138
FOURTH MOMENT OF TURBULENCE= 0.30041E-02 MPS**4
FOURTH CORRELATION COEFFICIENT= 3.0715
CBAR= 0.169%
CRMS= 0.173%
CPVPBAR= 0.012604
OVERALL TRANSPORT COEFFICIENT= 0.412194

CONDITIONAL SAMPLING RESULTS

CONCENTRATION FLUCTUATION	NUMBER OF OCCURANCES	MEAN	RELATIVE MEAN	RMS	TRANSPORT COEFFICIENT	TRANSPORT RATIO
-1.0 - -0.9001	0					
-0.9 - -0.8001	0					
-0.8 - -0.7001	0					
-0.7 - -0.6001	0					
-0.6 - -0.5001	0					
-0.5 - -0.4001	0					
-0.4 - -0.3001	0					
-0.3 - -0.2001	2	-0.0050	0.00840	0.04200	-0.05513	-0.134
-0.2 - -0.1001	378	-0.0837	0.07029	0.18107	0.34857	0.846
-0.1 - -0.0001	213	-0.0314	-0.01797	0.16066	0.02661	0.065
-0.0 0.0999	160	0.0236	0.01700	0.15339	0.07001	0.170
0.1 - 0.1999	120	0.0376	0.05098	0.12868	0.26512	0.643
0.2 - 0.2999	53	0.1205	0.11387	0.13512	1.09814	2.664
0.3 - 0.3999	28	0.1421	0.15547	0.14350	1.78440	4.329
0.4 - 0.4999	16	0.1922	0.20559	0.10523	2.99292	7.261
0.5 - 0.5999	12	0.1481	0.16148	0.08884	2.91831	7.080
0.6 - 0.6999	4	0.2650	0.27840	0.04467	5.75303	13.957
0.7 - 0.7999	3	0.1190	0.13240	0.08916	3.08397	7.482
0.8 - 0.8999	1	0.1460	0.15940	0.00000	4.41731	10.717
0.9 - 0.9999	0					

END OF RUN 51 -POINT 14
TERMINATED: STOP

SAMPLE 51,15
SUCCESSFUL (TEMP) RESTORE RUN51P15 AS (TF15)
CANCELLED: DDNAME RMDS UNKNOWN

DATA OUTPUT FOR RUN 51 POINT 15

RADIAL VELOCITY VS CONCENTRATION
Z=152 MM AND R/RO= 0.324
NO= 999 AND N4=984
VBAR= 0.0177 MPS
VRMS= 0.1837 MPS
THIRD MOMENT OF TURBULENCE=-0.11389E-02 MPS**3
THIRD CORRELATION COEFFICIENT= -0.1838
FOURTH MOMENT OF TURBULENCE= 0.34364E-02 MPS**4
FOURTH CORRELATION COEFFICIENT= 3.0175
CBAR= 0.086%
CRMS= 0.127%
CPVPBAR= 0.007435
OVERALL TRANSPORT COEFFICIENT= 0.317890

CONDITIONAL SAMPLING RESULTS

CONCENTRATION FLUCTUATION	NUMBER OF OCCURANCES	MEAN	RELATIVE MEAN	RMS	TRANSPORT COEFFICIENT	TRANSPORT RATIO
-1.0 - -0.9001	0					
-0.9 - -0.8001	0					
-0.8 - -0.7001	0					
-0.7 - -0.6001	0					
-0.6 - -0.5001	0					
-0.5 - -0.4001	0					
-0.4 - -0.3001	0					
-0.3 - -0.2001	0					
-0.2 - -0.1001	70	-0.0308	-0.04852	0.13920	0.21957	0.691
-0.1 - -0.0001	587	-0.0147	-0.03234	0.18553	0.10116	0.110
-0.0 - 0.0999	166	0.0519	0.03424	0.15823	0.08644	0.272
0.1 0.1999	85	0.0621	0.04446	0.16496	0.30277	0.752
0.2 - 0.2999	36	0.1730	0.15535	0.16782	1.67483	5.269
0.3 - 0.3999	21	0.1800	0.16232	0.14754	2.44363	7.687
0.4 - 0.4999	8	0.2357	0.21807	0.07744	4.13511	13.008
0.5 - 0.5999	8	0.2014	0.13370	0.10173	4.29196	13.501
0.6 - 0.6999	3	0.2530	0.23532	0.03476	6.31431	19.863
0.7 - 0.7999	0					
0.8 - 0.8999	0					
0.9 - 0.9999	0					

END OF RUN 51 -POINT 15
TERMINATED: STOP

```
SAMPLE 51.16
 SUCCESSFUL (TEMP) RESTORE RUN51P16 AS (TP16)
 CANCELLED: DDNAME RMDS      UNKNOWN

   DATA OUTPUT FOR RUN 51 POINT 16

RADIAL  VELOCITY VS CONCENTRATION
Z=152 MM AND R/RO= 0.375
NO= 999 AND N4=991
VBAR=   0.0141 MPS
VRMS=   0.2063 MPS
THIRD MOMENT OF TURBULENCE=-0.24825E-02 MPS**3
THIRD CORRELATION COEFFICIENT=  -0.2827
FOURTH MOMENT OF TURBULENCE= 0.59804E-02 MPS**4
FOURTH CORRELATION COEFFICIENT=   3.3015
CBAR=   0.045%
CRMS=   0.091%
CPVPBAR=  0.004325
OVERALL TRANSPORT COEFFICIENT=  0.231336
```

CONDITIONAL SAMPLING RESULTS

CONCENTRATION FLUCTUATION	NUMBER OF OCCURANCES	MEAN	RELATIVE MEAN	RMS	TRANSPORT COEFFICIENT	TRANSPORT RATIO
-1.0 - -0.9001	0					
-0.9 - -0.8001	0					
-0.8 - -0.7001	0					
-0.7 - -0.6001	0					
-0.6 - -0.5001	0					
-0.5 - -0.4001	0					
-0.4 - -0.3001	0					
-0.3 - -0.2001	0					
-0.2 - -0.1001	0					
-0.1 - -0.0001	718	-0.0104	-0.02454	0.20708	0.05304	0.229
-0.0 - 0.0999	175	0.0485	0.03434	0.20017	0.14858	0.642
0.1 - 0.1999	60	0.1020	0.08787	0.14338	0.65101	2.814
0.2 - 0.2999	15	0.1249	0.11079	0.14966	1.35809	5.071
0.3 - 0.3999	10	0.1665	0.15236	0.12214	2.81257	12.158
0.4 - 0.4999	10	0.2609	0.24676	0.19204	5.49601	24.622
0.5 - 0.5999	2	0.2760	0.26186	0.00201	7.64486	33.047
0.6 - 0.6999	1	0.1740	0.15986	0.00000	5.37428	23.[illegible]32
0.7 - 0.7999	0					
0.8 - 0.8999	0					
0.9 - 0.9999	0					

```
END OF RUN 51 -POINT 16
 TERMINATED: STOP
```

SAMPLE 51,17
SUCCESSFUL (TEMP) RESTORE RUN51F17 AS (TF17)
CANCELLED: DDNAME RMDS UNKNOWN

DATA OUTPUT FOR RUN 51 POINT 17

RADIAL VELOCITY VS CONCENTRATION
Z=152 MM AND R/RO= 0.425
NO= 999 AND N4=990
VBAR= 0.0401 MPS
VRMS= 0.2194 MPS
THIRD MOMENT OF TURBULENCE=-0.42006E-02 MPS**3
THIRD CORRELATION COEFFICIENT= -0.3979
FOURTH MOMENT OF TURBULENCE= 0.74492E-02 MPS**4
FOURTH CORRELATION COEFFICIENT= 3.2166
CBAR= 0.023%
CRMS= 0.056%
CPVPBAR= 0.002122
OVERALL TRANSPORT COEFFICIENT= 0.171592

CONDITIONAL SAMPLING RESULTS

CONCENTRATION FLUCTUATION	NUMBER OF OCCURANCES	MEAN	RELATIVE MEAN	RMS	TRANSPORT COEFFICIENT	TRANSPORT RATIO
-1.0 - -0.9001	0					
-0.9 - -0.8001	0					
-0.8 - -0.7001	0					
-0.7 - -0.6001	0					
-0.6 - -0.5001	0					
-0.5 - -0.4001	0					
-0.4 - -0.3001	0					
-0.3 - -0.2001	0					
-0.2 - -0.1001	0					
-0.1 - -0.0001	692	0.0267	-0.01335	0.21606	0.00440	0.026
-0.0 - 0.0999	240	0.0403	0.00023	0.22886	0.05017	0.292
0.1 - 0.1999	40	0.1752	0.13511	0.15020	1.65402	9.639
0.2 - 0.2999	15	0.2375	0.19747	0.11400	3.88145	22.520
0.3 - 0.3999	1	0.2610	0.22093	0.00000	6.50590	37.915
0.4 - 0.4999	2	0.3395	0.29943	0.04850	11.95493	69.670
0.5 - 0.5999	0					
0.6 - 0.6999	0					
0.7 - 0.7999	0					
0.8 - 0.8999	0					
0.9 - 0.9999	0					

END OF RUN 51 -POINT 17
TERMINATED: STOP

SAMPLE 51,21
SUCCESSFUL (TEMP) RESTORE RUN51F21 AS (TF21)
CANCELLED: DDNAME RMDS UNKNOWN

DATA OUTPUT FOR RUN 51 POINT 21

RADIAL VELOCITY VS CONCENTRATION
Z=152 MM AND R/RO= 0.624
NO= 999 AND N4=991
VBAR= 0.0405 MPS
VRMS= 0.2339 MPS
THIRD MOMENT OF TURBULENCE= 0.16932E-02 MPS**3
THIRD CORRELATION COEFFICIENT= 0.1324
FOURTH MOMENT OF TURBULENCE= 0.10379E-01 MPS**4
FOURTH CORRELATION COEFFICIENT= 3.4689
CBAR= 0.013%
CRMS= 0.022%
CPVPBAR= -0.000354
OVERALL TRANSPORT COEFFICIENT= -0.068616

CONDITIONAL SAMPLING RESULTS

CONCENTRATION FLUCTUATION	NUMBER OF OCCURANCES	MEAN	RELATIVE MEAN	RMS	TRANSPORT COEFFICIENT	TRANSPORT RATIO
-1.0 - -0.9001	0					
-0.9 - -0.8001	0					
-0.8 - -0.7001	0					
-0.7 - -0.6001	0					
-0.6 - -0.5001	0					
-0.5 - -0.4001	0					
-0.4 - -0.3001	0					
-0.3 - -0.2001	0					
-0.2 - -0.1001	0					
-0.1 - -0.0001	522	0.0576	0.01710	0.22337	-0.07901	1.151
-0.0 - 0.0999	469	0.0215	-0.01903	0.24366	-0.05707	0.832
0.1 - 0.1999	0					
0.2 - 0.2999	0					
0.3 - 0.3999	0					
0.4 - 0.4999	0					
0.5 - 0.5999	0					
0.6 - 0.6999	0					
0.7 - 0.7999	0					
0.8 - 0.8999	0					
0.9 - 0.9999	0					

END OF RUN 51 -POINT 21
TERMINATED: STOP

```
SAMPLE 51,27
 SUCCESSFUL (TEMP) RESTORE RUN51P27 AS (TF 7)
 CANCELLED: DDNAME RMDS      UNKNOWN

    DATA OUTPUT FOR RUN 51 POINT 27

RADIAL  VELOCITY VS CONCENTRATION
Z=152 MM AND R/RO= 0.025
NO= 999 AND N4=991
VBAR=  -0.0126 MPS
VRMS=   0.1430 MPS
THIRD MOMENT OF TURBULENCE=-0.40891E-03 M S**3
THIRD CORRELATION COEFFICIENT=  -0.1397
FOURTH MOMENT OF TURBULENCE= 0.14709E-02 M S**4
FOURTH CORRELATION COEFFICIENT=   3.5145
CBAR=   0.550%
CRMS=   0.275%
CPVPBAR=  0.004816
OVERALL TRANSPORT COEFFICIENT=  0.122495
```

CONDITIONAL SAMPLING RESULTS

CONCENTRATION FLUCTUATION	NUMBER OF OCCURANCES	MEAN	RELATIVE MEAN	RMS	TRANSPORT COEFFICIENT	TRANSPORT RATIO
-1.0 - -0.9001	0					
-0.9 - -0.8001	0					
-0.8 - -0.7001	0					
-0.7 - -0.6001	0					
-0.6 - -0.5001	11	-0.0353	-0.02263	0.28142	0.31005	2.531
-0.5 - -0.4001	54	-0.0401	0.02746	0.21717	0.32881	2.684
-0.4 - -0.3001	75	-0.0335	-0.02086	0.18454	0.18580	1.517
-0.3 -0.2001	123	-0.0386	-0.02598	0.16912	0.17968	1.467
-0.2 - -0.1001	133	-0.0244	-0.01177	0.15898	0.05197	0.424
-0.1 - -0.0001	136	0.0029	0.01554	0.11980	-0.02128	-0.174
-0.0 - 0.0999	99	-0.0154	-0.00278	0.12126	-0.00789	-0.064
0.1 - 0.1999	95	-0.0080	0.00461	0.11021	0.01739	0.142
0.2 - 0.2999	83	0.0073	0.01994	0.10624	0.12593	1.028
0.3 - 0.3999	75	0.0075	0.02017	0.08644	0.17825	1.455
0.4 - 0.4999	65	0.0213	0.03394	0.07392	0.40442	3.302
0.5 - 0.5999	33	0.0023	0.01492	0.08903	0.20286	1.656
0.6 - 0.6999	2	-0.0545	-0.04185	0.03250	-0.67197	-5.486
0.7 - 0.7999	0					
0.8 - 0.8999	0					
0.9 - 0.9999	0					

```
END OF RUN 51 -POINT 27
 TERMINATED: STOP
```

ORIGINAL PAGE IS OF POOR QUALITY

SAMPLE 51.28
SUCCESSFUL (TEMP) RESTORE RUN51P28 AS (TF28)
CANCELLED: DDNAME RMD UNKNOWN

DATA OUTPUT FOR RUN 51 POINT 28

RADIAL VELOCITY VS CONCENTRATION
Z=152 MM AND R/RO=-0.025
NO= 999 AND N4=986
VBAR= -0.0033 MPS
VRMS= 0.1440 MPS
THIRD MOMENT OF TURBULENCE=-0.63230E-03 MPS**3
THIRD CORRELATION COEFFICIENT= -0.2117
FOURTH MOMENT OF TURBULENCE= 0.13094E-02 MPS**4
FOURTH CORRELATION COEFFICIENT= 3.0439
CBAR= 0.578%
CRMS= 0.288%
CPVPBAR= 0.010838
OVERALL TRANSPORT COEFFICIENT= 0.261394

CONDITIONAL SAMPLING RESULTS

CONCENTRATION FLUCTUATION	NUMBER OF OCCURANCES	MEAN	RELATIVE MEAN	RMS	TRANSPORT COEFFICIENT	TRANSPORT RATIO
-1.0 - -0.9001	0					
-0.9 - -0.8001	0					
-0.8 - -0.7001	0					
-0.7 - -0.6001	0					
-0.6 - -0.5001	9	-0.1730	-0.16974	0.18176	2.17482	8.320
-0.5 -0.4001	44	0.0845	0.08124	0.20060	0.85176	3.259
-0.4 - -0.3001	109	-0.0616	-0.05832	0.19559	0.48301	1.848
-0.3 - -0.2001	136	-0.0260	-0.02272	0.16002	0.15482	0.592
-0.2 - -0.1001	121	-0.0379	-0.03461	0.15017	0.11689	0.447
-0.1 - -0.0001	114	0.0189	0.02214	0.11763	0.02017	-0.077
-0.0 - 0.0999	102	0.0315	0.03475	0.11180	0.04810	0.184
0.1 - 0.1999	78	0.0096	0.01286	0.12191	0.04198	0.161
0.2 - 0.2999	84	0.0363	0.03958	0.10218	0.22963	0.878
0.3 - 0.3999	57	0.0412	0.04444	0.06902	0.38079	1.457
0.4 - 0.4999	92	0.0476	0.05088	0.08786	0.55434	2.121
0.5 - 0.5999	40	0.0248	0.02811	0.08539	0.37441	1.432
0.6 - 0.6999	0					
0.7 - 0.7999	0					
0.8 - 0.8999	0					
0.9 - 0.9999	0					

END OF RUN 51 -POINT 28
TERMINATED: STOP

SAMPLE 51,29
SUCCESSFUL (TEMP) RESTORE RUN51P29 AS (TF29)
CANCELLED: DDNAME RMDS UNKNOWN

DATA OUTPUT FOR RUN 51 POINT 29

RADIAL VELOCITY VS CONCENTRATION
Z=152 MM AND R/RO=-0.075
NO= 999 AND N4=980
VBAR= -0.0074 MPS
VRMS= 0.1460 MPS
THIRD MOMENT OF TURBULENCE=-0.11105E-02 MPS**3
THIRD CORRELATION COEFFICIENT= -0.3569
FOURTH MOMENT OF TURBULENCE= 0.14492E-02 MPS**4
FOURTH CORRELATION COEFFICIENT= 3.1909
CBAR= 0.510%
CRMS= 0.288%
CPVPBAR= 0.016242
OVERALL TRANSPORT COEFFICIENT= 0.386500

CONDITIONAL SAMPLING RESULTS

CONCENTRATION FLUCTUATION	NUMBER OF OCCURANCES	MEAN	RELATIVE MEAN	RMS	TRANSPORT COEFFICIENT	TRANSPORT RATIO
-1.0 - -0.9001	0					
-0.9 - -0.8001	0					
-0.8 - -0.7001	0					
-0.7 - -0.6001	0					
-0.6 - -0.5001	5	-0.1952	-0.18775	0.09425	2.29057	5.926
-0.5 - -0.4001	57	-0.1481	-0.14066	0.13368	1.48452	3.841
-0.4 - -0.3001	91	-0.0992	-0.09173	0.16993	0.75201	1.946
-0.3 -0.2001	129	-0.0549	-0.04742	0.16459	0.29357	0.760
-0.2 - -0.1001	135	-0.0265	-0.01900	0.14487	0.07027	0.182
-0.1 - -0.0001	120	0.0090	0.01645	0.15040	-0.01064	-0.028
-0.0 - 0.0999	98	0.0466	0.05406	0.10974	0.06969	0.180
0.1 - 0.1999	95	0.0256	0.03306	0.11737	0.10677	0.276
0.2 0.2999	72	0.0464	0.05384	0.08684	0.31413	0.465
0.3 - 0.3999	62	0.0525	0.06000	0.10360	0.52177	1.350
0.4 - 0.4999	53	0.0797	0.08719	0.06854	0.93474	2.418
0.5 - 0.5999	49	0.0453	0.05280	0.08075	0.68717	1.778
0.6 0.6999	14	0.0474	0.05488	0.03592	0.82968	2.147
0.7 - 0.7999	0					
0.8 - 0.8999	0					
0.9 - 0.9999	0					

END OF RUN 51 -POINT 29
TERMINATED: STOP

SAMPLE 51,30
SUCCESSFUL (TEMP) RESTORE RUN51F30 AS (TF30)
CANCELLED: DDNAME RMDS UNKNOWN

DATA OUTPUT FOR RUN 51 POINT 30

RADIAL VELOCITY VS CONCENTRATION
Z=152 MM AND R/RO=-0.125
NO= 999 AND N4=993
VBAR= -0.0059 MPS
VRMS= 0.1526 MPS
THIRD MOMENT OF TURBULENCE=-0.63993E-03 MPS**3
THIRD CORRELATION COEFFICIENT= -0.1800
FOURTH MOMENT OF TURBULENCE= 0.15618E-02 MPS**4
FOURTH CORRELATION COEFFICIENT= 2.8777
CBAR= 0.410%
CRMS= 0.258%
CPVPBAR= 0.016842
OVERALL TRANSPORT COEFFICIENT= 0.427718

CONDITIONAL SAMPLING RESULTS

CONCENTRATION FLUCTUATION	NUMBER OF OCCURANCES	MEAN	RELATIVE MEAN	RMS	TRANSPORT COEFFICIENT	TRANSPORT RATIO
-1.0 - -0.9001	0					
-0.9 - -0.8001	0					
-0.8 - -0.7001	0					
-0.7 - -0.6001	0					
-0.6 - -0.5001	0					
-0.5 - -0.4001	17	-0.1455	-0.13962	0.14079	1.46858	3.434
-0.4 - -0.3001	83	-0.0936	0.08767	0.15426	0.73554	1.766
-0.3 - -0.2001	138	-0.0903	-0.08441	0.16386	0.53749	1.257
-0.2 - -0.1001	164	-0.0378	0.03187	0.14871	0.10998	0.257
-0.1 - -0.0001	171	-0.0199	-0.01402	0.13552	0.02015	0.047
-0.0 - 0.0999	127	0.0309	0.03679	0.14561	0.07540	0.176
0.1 - 0.1999	77	0.0540	0.05994	0.11775	0.25478	0.596
0.2 - 0.2999	68	0.0537	0.05965	0.10855	0.37089	0.867
0.3 - 0.3999	59	0.0809	0.08681	0.09484	0.77300	1.807
0.4 0.4999	39	0.1217	0.12763	0.09669	1.46247	3.419
0.5 - 0.5999	27	0.1044	0.11036	0.09560	1.55321	3.631
0.5 0.6999	18	0.1124	0.11836	0.05730	1.96129	4.335
0.7 - 0.7999	5	0.0680	0.07391	0.10726	1.42281	3.327
0.8 - 0.8999	0					
0.9 - 0.9999	0					

END OF RUN 51 -POINT 30
TERMINATED: STOP
-

SAMPLE 51,31
SUCCESSFUL (TEMP) RESTORE RUN51P31 AS (TF31)
CANCELLED: DDNAME RMDS UNKNOWN

DATA OUTPUT FOR RUN 51 POINT 31

RADIAL VELOCITY VS CONCENTRATION
Z=152 MM AND R/RO=-0.175
NO= 999 AND N4=992
VBAR= 0.0003 MPS
VRMS= 0.1558 MPS
THIRD MOMENT OF TURBULENCE=-0.97946E-03 MPS**3
THIRD CORRELATION COEFFICIENT= -0.2[illegible]89
FOURTH MOMENT OF TURBULENCE= 0.17766E-02 MPS**4
FOURTH CORRELATION COEFFICIENT= 3.0139
CBAR= 0.329%
CRMS= 0.239%
CPVPBAR= 0.016425
OVERALL TRANSPORT COEFFICIENT= 0.440394

CONDITIONAL SAMPLING RESULTS

CONCENTRATION FLUCTUATION	NUMBER OF OCCURANCES	MEAN	RELATIVE MEAN	RMS	TRANSPORT COEFFICIENT	TRANSPORT RATIO
-1.0 - -0.9001	0					
-0.9 - -0.8001	0					
-0.8 - -0.7001	0					
-0.7 - -0.6001	0					
-0.6 - -0.5001	0					
-0.5 - -0.4001	0					
-0.4 - -0.3001	63	-0.0998	-0.10009	0.14419	0.86180	1.957
-0.3 - -0.2001	159	-0.0892	-0.08954	0.17458	0.60622	1.377
-0.2 - -0.1001	174	-0.0338	-0.03412	0.14848	0.15194	0.345
-0.1 - -0.0001	162	-0.0165	0.01680	0.13329	0.03614	0.082
-0.0 - 0.0999	151	0.0298	0.02947	0.14549	0.04386	0.100
0.1 - 0.1999	99	0.0463	0.04596	0.10797	0.18710	0.425
0.2 - 0.2999	64	0.1003	0.10000	0.12770	0.69159	1.570
0.3 - 0.3999	53	0.0889	0.08854	0.10224	0.83705	1.901
0.4 - 0.4999	29	0.1146	0.11426	0.10233	1.33801	3.038
0.5 - 0.5999	15	0.1595	0.15914	0.06916	2.35268	5.342
0.6 - 0.6999	13	0.1453	0.14498	0.06086	2.50372	5.685
0.7 - 0.7999	4	0.1510	0.15068	0.07156	2.95614	6.712
0.8 - 0.8999	5	0.1478	0.14748	0.04726	3.43323	7.796
0.9 - 0.9999	1	0.1830	0.18268	0.00000	4.50817	10.237

END OF RUN 51 -POINT 31
TERMINATED: STOP

```
SAMPLE 51,32
 SUCCESSFUL (TEMP) RESTORE RUN51P32 AS (TF32)
 CANCELLED: DDNAME RMDS     UNKNOWN

    DATA OUTPUT FOR RUN 51 POINT 32

RADIAL  VELOCITY VS CONCENTRATION
Z=152 MM AND R/RO=-0.225
NO= 999 AND N4=991
VBAR=   0.0151 MPS
VRMS=   0.1795 MPS
THIRD MOMENT OF TURBULENCE=-0.68932E-03 MPS**3
THIRD CORRELATION COEFFICIENT=  -0.1192
FOURTH MOMENT OF TURBULENCE= 0.32729E-02 MPS**4
FOURTH CORRELATION COEFFICIENT=   3.1532
CBAR=   0.237%
CRMS=   0.214%
CPVPBAR=  0.016870
OVERALL TRANSPORT COEFFICIENT=  0.439960
```

CONDITIONAL SAMPLING RESULTS

CONCENTRATION FLUCTUATION	NUMBER OF OCCURANCES	MEAN	RELATIVE MEAN	RMS	TRANSPORT COEFFICIENT	TRANSPORT RATIO
-1.0 - -0.9001	0					
-0.9 - -0.8001	0					
-0.8 - -0.7001	0					
-0.7 - -0.6001	0					
-0.6 - -0.5001	0					
-0.5 - -0.4001	0					
-0.4 - -0.3001	0					
-0.3 - -0.2001	184	-0.0768	-0.09197	0.19744	0.53364	1.213
-0.2 - -0.1001	208	-0.0450	-0.06010	0.17019	0.24565	0.558
-0.1 - -0.0001	186	-0.0028	-0.01798	0.15219	0.03985	0.091
-0.0 - 0.0999	135	0.0459	0.03072	0.13672	0.05778	0.131
0.1 - 0.1999	125	0.0694	0.05430	0.14685	0.21981	0.500
0.2 - 0.2999	65	0.1229	0.10771	0.13376	0.71971	1.636
0.3 - 0.3999	30	0.1521	0.13692	0.11788	1.25570	2.854
0.4 - 0.4999	21	0.1887	0.17357	0.12958	1.93297	4.394
0.5 - 0.5999	18	0.1960	0.18085	0.08210	2.58491	5.875
0.6 - 0.6999	11	0.1965	0.18131	0.12100	3.12991	7.114
0.7 - 0.7999	5	0.2424	0.22725	0.05032	4.40830	10.020
0.8 - 0.8999	1	0.2800	0.26485	0.00000	5.61926	12.772
0.9 - 0.9999	2	0.2300	0.21485	0.03100	5.20261	11.825

```
END OF RUN 51 -POINT 32
 TERMINATED: STOP
```

SAMPLE 51,33
SUCCESSFUL (TEMP) RESTORE RUN51P33 AS (TF33)
CANCELLED: DDNAME RMDS UNKNOWN

DATA OUTPUT FOR RUN 51 POINT 33

RADIAL VELOCITY VS CONCENTRATION
Z=152 MM AND R/RO=-0.275
NO= 999 AND N4=990
VBAR= 0.0343 MPS
VRMS= 0.1776 MPS
THIRD MOMENT OF TURBULENCE=-0.54516E-03 MPS**3
THIRD CORRELATION COEFFICIENT= -0.0973
FOURTH MOMENT OF TURBULENCE= 0.31653E-02 MPS**4
FOURTH CORRELATION COEFFICIENT= 3.1803
CBAR= 0.159%
CRMS= 0.185%
CPVPBAR= 0.012373
OVERALL TRANSPORT COEFFICIENT= 0.376874

CONDITIONAL SAMPLING RESULTS

CONCENTRATION FLUCTUATION	NUMBER OF OCCURANCES	MEAN	RELATIVE MEAN	RMS	TRANSPORT COEFFICIENT	TRANSPORT RATIO
-1.0 - -0.9001	0					
-0.9 - -0.8001	0					
-0.8 - -0.7001	0					
-0.7 - -0.6001	0					
-0.6 - -0.5001	0					
-0.5 - -0.4001	0					
-0.4 - -0.3001	0					
-0.3 - -0.2001	0					
-0.2 - -0.1001	411	-0.0197	-0.05399	0.17267	0.23771	0.631
-0.1 - -0.0001	199	0.0079	-0.02639	0.16243	0.04646	0.123
-0.0 - 0.0999	154	0.0558	0.02144	0.15291	0.03033	0.080
0.1 - 0.1999	95	0.0905	0.05616	0.16972	0.25726	0.683
0.2 - 0.2999	50	0.1477	0.11335	0.14813	0.91348	2.424
0.3 - 0.3999	36	0.1564	0.12209	0.13704	1.24971	3.316
0.4 - 0.4999	22	0.2300	0.19567	0.12846	2.69590	7.153
0.5 - 0.5999	12	0.2206	0.18625	0.13035	3.13865	8.328
0.6 - 0.6999	5	0.2412	0.20687	0.14030	4.14299	10.993
0.7 - 0.7999	2	0.3230	0.28867	0.04900	6.65189	17.650
0.8 - 0.8999	3	0.1707	0.13634	0.08387	3.44102	9.130
0.9 - 0.9999	1	0.2190	0.18467	0.00000	5.06840	13.449

END OF RUN 51 -POINT 33
TERMINATED: STOP

```
SAMPLE 51,34
 SUCCESSFUL (TEMP) RESTORE RUN51F34 AS (TF34)
 CANCELLED: DDNAME RMDS     UNKNOWN

    DATA OUTPUT FOR RUN 51 POINT 34

RADIAL  VELOCITY VS CONCENTRATION
Z=152 MM AND R/RO=-0.325
NO= 999 AND N4=994
VBAR=   0.0410 MPS
VRMS=   0.2030 MPS
THIRD MOMENT OF TURBULENCE=-0.19230E-02 MPS**3
THIRD CORRELATION COEFFICIENT=  -0.2299
FOURTH MOMENT OF TURBULENCE= 0.51567E-02 MPS**4
FOURTH CORRELATION COEFFICIENT=    3.0379
CBAR=   0.101%
CRMS=   0.146%
CPVPBAR=  0.008284
OVERALL TRANSPORT COEFFICIENT=  0.280485
```

CONDITIONAL SAMPLING RESULTS

CONCENTRATION FLUCTUATION	NUMBER OF OCCURANCES	MEAN	RELATIVE MEAN	RMS	TRANSPORT COEFFICIENT	TRANSPORT RATIO
-1.0 - -0.9001	0					
-0.9 - -0.8001	0					
-0.8 - -0.7001	0					
-0.7 - -0.6001	0					
-0.6 - -0.5001	0					
-0.5 - -0.4001	0					
-0.4 - -0.3001	0					
-0.3 - -0.2001	0					
-0.2 - -0.1001	162	0.0383	-0.00273	0.17407	0.00887	0.032
-0.1 - -0.0001	526	-0.0002	0.04125	0.21527	0.11573	0.413
-0.0 - 0.0999	124	0.0623	0.02127	0.16709	0.03163	0.113
0.1 - 0.1999	86	0.1036	0.06758	0.16616	0.34618	1.234
0.2 - 0.2999	41	0.1883	0.14727	0.15694	1.24473	4.438
0.3 - 0.3999	35	0.1528	0.11178	0.17292	1.36348	4.861
0.4 - 0.4999	8	0.1954	0.15433	0.12990	2.29087	8.168
0.5 - 0.5999	3	0.3380	0.29695	0.10591	5.64098	20.112
0.6 - 0.6999	5	0.2712	0.23015	0.06351	4.98682	17.779
0.7 - 0.7999	4	0.2662	0.22520	0.11280	5.96094	21.252
0.8 - 0.8999	0					
0.9 - 0.9999	0					

```
END OF RUN 51 -POINT 34
 TERMINATED: STOP
```

```
SAMPLE 51,35
 SUCCESSFUL (TEMP) RESTORE RUN51F35 AS (1F35)
 CANCELLED: DDNAME RMDS     UNKNOWN

    DATA OUTPUT FOR RUN 51 POINT 35

RADIAL  VELOCITY VS CONCENTRATION
Z=152 MM AND R/RO=-0.375
NO= 999 AND N4=994
VBAR=   0.0633 MPS
VRMS=   0.2114 MPS
THIRD MOMENT OF TURBULENCE=-0.12811E-02 MPS**3
THIRD CORRELATION COEFFICIENT=  -0.1357
FOURTH MOMENT OF TURBULENCE= 0.63522E-02 MPS**4
FOURTH CORRELATION COEFFICIENT=   3.1830
CBAR=   0.045%
CRMS=   0.091%
CPVPBAR= 0.003890
OVERALL TRANSPORT COEFFICIENT=  0.202920
```

CONDITIONAL SAMPLING RESULTS

CONCENTRATION FLUCTUATION	NUMBER OF OCCURANCES	MEAN	RELATIVE MEAN	RMS	TRANSPORT COEFFICIENT	TRANSPORT RATIO
-1.0 - -0.9001	0					
-0.9 - -0.8001	0					
-0.8 - -0.7001	0					
-0.7 - -0.6001	0					
-0.6 - -0.5001	0					
-0.5 - -0.4001	0					
-0.4 - -0.3001	0					
-0.3 - -0.2001	0					
-0.2 - -0.1001	0					
-0.1 - -0.0001	742	0.0399	-0.02334	0.20536	0.03489	0.172
-0.0 - 0.0999	149	0.0932	0.02989	0.21901	0.13623	0.571
0.1 - 0.1999	58	0.1958	0.13249	0.20798	0.96715	4.766
0.2 - 0.2999	24	0.1389	0.07563	0.18007	1.00235	4.740
0.3 - 0.3999	13	0.2378	0.17456	0.16155	3.16566	15.600
0.4 - 0.4999	4	0.1322	0.06896	0.10879	1.61432	7.955
0.5 - 0.5999	3	0.2360	0.17271	0.03544	4.59791	22.659
0.6 - 0.6999	0					
0.7 - 0.7999	0					
0.8 - 0.8999	1	0.3660	0.30271	0.00000	13.95503	68.771
0.9 - 0.9999	0					

```
END OF RUN 51 -POINT 35
 TERMINATED: STOP
```

SAMPLE 51,36
SUCCESSFUL (TEMP) RESTORE RUN51P36 AS (TF36)
CANCELLED: DDNAME RMDS UNKNOWN

DATA OUTPUT FOR RUN 51 POINT 36

RADIAL VELOCITY VS CONCENTRATION
Z=152 MM AND R/RO=-0.425
NO= 999 AND N4-995
VBAR= 0.0678 MPS
VRMS= 0.2325 MPS
THIRD MOMENT OF TURBULENCE=-0.34786E-02 MPS**3
THIRD CORRELATION COEFFICIENT= -0.2767
FOURTH MOMENT OF TURBULENCE= 0.84200E-02 MPS**4
FOURTH CORRELATION COEFFICIENT= 2.8797
CBAR= 0.028%
CRMS= 0.067%
CPVPBAR= 0.002330
OVERALL TRANSPORT COEFFICIENT= 0.150439

CONDITIONAL SAMPLING RESULTS

CONCENTRATION FLUCTUATION	NUMBER OF OCCURANCES	MEAN	RELATIVE MEAN	RMS	TRANSPORT COEFFICIENT	TRANSPORT RATIO
-1.0 - -0.9001	0					
-0.9 - -0.8001	0					
-0.8 - -0.7001	0					
-0.7 - -0.6001	0					
-0.6 - -0.5001	0					
-0.5 - -0.4001	0					
-0.4 - -0.3001	0					
-0.3 - -0.2001	0					
-0.2 - -0.1001	0					
-0.1 - -0.0001	726	0.0538	-0.01397	0.22602	0.01159	0.07.
-0.0 - 0.0999	206	0.0758	0.00800	0.23293	0.08273	0.550
0.1 - 0.1999	38	0.1849	0.11710	0.19293	1.09573	7.284
0.2 - 0.2999	14	0.2060	0.13820	0.20051	1.88663	12.541
0.3 - 0.3999	6	0.2677	0.19987	0.18156	4.24673	28.229
0.4 - 0.4999	2	0.2380	0.17020	0.04700	5.11706	34.014
0.5 - 0.5999	2	0.2960	0.22820	0.00600	7.73012	52.713
0.6 - 0.6999	1	0.1860	0.11870	0.00000	4.59792	30.564
0.7 - 0.7999	0					
0.8 - 0.8999	0					
0.9 - 0.9999	0					

END OF RUN 51 -POINT 36
TERMINATED: STOP

*U.S. GOVERNMENT PRINTING OFFICE 1986/646-114/20423

1 Report No	2 Government Accession No	3 Recipient's Catalog No
NASA CR-175035		

4 Title and Subtitle	5 Report Date
Influence of Large-Scale Motion on Turbulent Transport for Confined Coaxial Jets. Volume I - Analytical Analysis of the Experimental Data Using Conditional Sampling	January 1986
	6 Performing Organization Code
7 Author(s)	8 Performing Organization Report No
David C. Brondum and John C. Bennett	None
	10 Work Unit No
9 Performing Organization Name and Address	11 Contract or Grant No
The University of Connecticut P.O. Box U-139 Storrs, Connecticut 06268	NAG 3-350
	13 Type of Report and Period Covered
12 Sponsoring Agency Name and Address	Contractor Report
National Aeronautics and Space Administration Washington, D.C. 20546	14 Sponsoring Agency Code 505-31-42

15 Supplementary Notes

Final report. Project Manager, C. John Marek, Altitude Wind Tunnel Project Office, NASA Lewis Research Center, Cleveland, Ohio 44135.

16 Abstract

The existence of large-scale coherent structures in turbulent shear flows has been well documented. Discrepancies between experimental and computational data suggest a necessity to understand the roles they play in mass and momentum transport. Using conditional sampling and averaging on coincident two-component velocity and concentration-velocity experimental data for swirling and nonswirling coaxial jets, triggers for identifying the structures were examined. Concentration fluctuation was found to be an adequate trigger or indicator for the concentration-velocity data, but no suitable detector was located for the two-component velocity data. The large-scale structures are found in the region where the largest discrepancies exist between model and experiment. The traditional gradient transport model does not fit in this region as a result of these structures. The large-scale motion was found to be responsible for a large percentage of the axial mass transport. The large-scale structures were found to convect downstream at approximately the mean velocity of the overall flow in the axial direction. The radial mean velocity of the structures was found to be substantially greater than that of the overall flow.

17 Key Words (Suggested by Author(s))	18 Distribution Statement
Shear layers; Coaxial jets; Large scale coherent structures	Unclassified - unlimited STAR Category 07

19 Security Classif (of this report)	20 Security Classif (of this page)	21 No of pages	22 Price*
Unclassified	Unclassified	133	A07

*For sale by the National Technical Information Service, Springfield, Virginia 22161